Biotransformation of *trans*-1-chloro-3,3,3-trifluoropropene and 2,3,3,3-tetrafluoropropene

Dissertation zur Erlangung des
naturwissenschaftlichen Doktorgrades der
Julius-Maximilians-Universität Würzburg

Vorgelegt von

Tobias Schmidt

aus

Bad Kissingen

Würzburg 2013

Eingereicht am: _____

Bei der Fakultät für Chemie und Pharmazie

1. Gutachter: Prof. Dr. W. Dekant
2. Gutachter: Prof. Dr. U. Holzgrabe

der Dissertation

1. Prüfer: Prof. Dr. Dr. W. Dekant
2. Prüfer: Prof. Dr. U. Holzgrabe
3. Prüfer: PD Dr. A. Mally

der mündlichen Prüfung

Tag der mündlichen Prüfung: _____

Doktorurkunde ausgehändigt am: _____

Parts of this thesis have already been published as follows:

Publications

Schmidt, T., Bertermann, R., Rusch, G. M., Hoffman, G. M. and Dekant, W. (2012). Biotransformation of 2,3,3,3-tetrafluoropropene (HFO-1234yf) in male, pregnant and non-pregnant female rabbits after single high dose inhalation exposure. *Toxicology and Applied Pharmacology*, 263, p. 32-38.

Schmidt, T., Bertermann, R., Rusch, G. M., Tveit, A. and Dekant, W. (2013). Biotransformation of *trans*-1-chloro-3,3,3-trifluoropropene (*trans*-HCFO-1233zd). *Toxicology and Applied Pharmacology*, 268, p. 343-351.

According to Elvesier's copyright policy, an author can use a published article in full or in part in a dissertation without asking permission:

http://libraryconnect.elsevier.com/newsletters/supporting-usersorganizations/2011-04/ways-use-journal-articles-published-elsevier (last accessed 26 September 2012)

http://libraryconnect.elsevier.com/sites/default/files/lcp0404.pdf (last accessed 26 September 2012)

Presentations at international meetings

Schmidt, T., Bertermann, R., Rusch, G. M., Hoffman, G. M. and Dekant, W. (2011). Acute toxicity and biotransformation of 2,3,3,3-tetrafluoropropene (HFO-1234yf) in pregnant and non-pregnant rabbits. Poster presentation at SOT 50th Annual Meeting, Washington, USA, 6-10th March, 2011.

Schmidt, T., Bertermann, R., Rusch, G. M. and Dekant, W. (2012). Biotransformation of *trans*-1-chloro-3,3,3-trifluoropropene (*trans*-HCFO-1233zd). Poster presentation at SOT 51th Annual Meeting, San Francisco, USA, 11-15th March, 2012. Abstract published in: The Toxicologist, Supplement to Toxicological Sciences, p. 331, 2012.

Table of contents

Abbreviations

ASHRAE	American Society of Heating, Refrigerating and Air Conditioning Engineers
BSA	bovine serum albumin
CAD	collisionally activated dissociation
CFC	chlorofluorocarbon
CK	creatine kinase
CK-MB	creatine kinase, heart muscle isoform
CK-MM	creatine kinase, skeletal muscle isoform
Cys	*L*-cysteine
CNL	constant neutral loss
CYP	cytochrome
d	doublet
dq	doublet of quartet
DCHA	dicyclohexylamine
EC	European Commission
EMS	enhanced mass spectrometry
EPI	enhanced product ion
F	female
FABPs	fatty-acid-binding proteins
GC	gas chromatography
GD	gestation day
GWP	global warming potential
GLP	good laboratory practice
Glu	*L*-glutamic acid
Gly	*L*-glycin

HCFC	hydrochlorofluorocarbon
HCFO	hydrochlorofluoroolefin
trans-HCFO-1233zd	*trans*-1-chloro-3,3,3-trifluoropropene
HFC	hydrofluorocarbon
HFC-134a	tetrafluoroethane
HFO	hydrofluoroolefin
HFO-1234yf	2,3,3,3-tetrafluoropropene
HPLC	high pressure liquid chromatography
IDA	information dependent acquisition
IUPAC	International Union Of Pure And Applied Chemistry
LC	liquid chromatography
LC_{50}	median lethal concentration
LIT	linear ion trap
LOD	limit of detection
LOQ	limit of quantification
m	multiplet
M	male
MRM	multiple reaction monitoring
MS	mass spectrometry
M_w	molecular weight
MYG	myoglobin
NADP	nicotinamide adenine dinucleotide phosphate
NADPH	reduced nicotinamide adenine dinucleotide phosphate
NOAEL	no observed adverse effect level
NOEL	no observed effect level
NZW	New Zealand White

ODP	ozone depletion potential
OECD	Organisation for Economic Co-operation and Development
ppm	parts per million
Q	quadrupole
q	quartet
R^2	coefficient of determination
s	singlet
SD	Sprague Dawley
t	triplet
TISAB	total ionic strength adjustment buffer
TMS	tetramethylsilane

1 Introduction

1.1 Chlorofluorocarbons (CFCs) and their replacement substances

1.1.1 Applications and regulations

Chlorofluorocarbons (CFCs) have been used since the early twentieth century in a wide field of applications such as refrigerants, blowing agents, propellants in medicinal applications and as degreasing solvents. The chemical structures contain only carbon, chlorine and fluorine atoms and derive mostly from methane or ethane. Their excellent physiochemical properties (boiling point, specific heat, heat of vaporization, high insulating value, low surface tension and viscosity, high vapor density) as well as their low toxicity, chemical reactivity and flammability made them suitable for many consumer applications. By 1988, the total world consumption of CFCs had grown to over 10^6 tonnes (Manzer, 1990) or approximately 9 x 10^5 Ozone Depletion Potential tonnes respectively (ODP tonnes; tonnes multiplied with the ozone depletion potential of the considered gas). Due to regulatory restriction by the Montreal Protocol in 1987, the production of CFCs massively declined and reached less than 10^3 ODP tonnes worldwide in 2008 (EPA, 2007; UNEP, 2009).

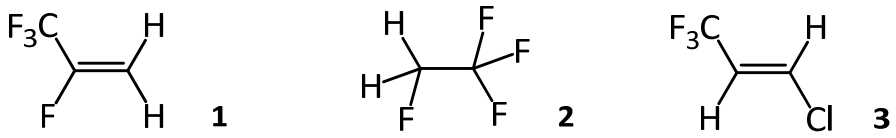

Fig. 1. Structural formula of (**1**) 2,3,3,3-tetrafluoropropene (HFO-1234yf), (**2**) 1,1,1,2-tetrafluoroethane (HFC-134a), (**3**) *trans*-1-chloro-3,3,3-trifluoropropene (*trans*-HCFO-1233zd).

The hydrochlorofluorocarbons (HCFCs) were introduced as the first alternatives for CFCs by the late 1970s and were still produced to an extent of about 3 x 10^4 ODP tonnes in 2008 (mainly China) (UNEP, 2009). HCFCs also feature many of the beneficial properties of CFCs including low flammability, volatility and stability and are still mainly used as refrigerants (e.g. chlorodifluoromethane [HCFC-22]). Hydrofluorocarbons (HFCs) were then introduced as the second generation of replacement substances. Lacking ozone depleting chlorine atoms, they were developed to cope with stricter regulations (e.g. Clean Air Act 1990, US; Regulation (EC) No 1005/2009). The third generation of CFC replacements, the hydrofluoroolefins (HFOs) were recently established with *trans*-2,3,3,3-tetrafluoropropene (HFO-1234yf) (**1**, Fig. 1) as a new refrigerant in mobile air-conditioning systems, replacing 1,1,1,2-tetrafluoroethane (HFC-134a) (**2**, Fig. 1). The latter was banned from newly manufactured cars by the European Union effective January 2011 (EP, 2006). Nevertheless,

HFC-134a is still used in car manufacturing due to the flammability of HFO-1234yf. According to the Montreal Protocol, all remaining ozone depleting substances must be phased-out worldwide by 2040. New replacement compounds with enhanced environmental properties but low remaining ODP, such as the hydrochlorofluoroolefin (HCFO) *trans*-1-chloro-3,3,3-trifluoropropene (*trans*-HCFO-1233zd) (**3**, Fig. 1), will be promoted as temporary alternatives for older compounds.

1.1.2 Environmental effects

The ozone depleting potential (ODP) of CFCs was reported for the first time in 1974 (Molina and Rowland, 1974). It was discovered that CFCs disturb the natural dynamic steady state of ozone formation and cleavage (Fig. 2). CFCs are not degraded in the troposphere and reach the stratosphere, where they are photolytically cleaved under intensive UV-light, releasing chlorine radicals (Fig. 3). These chlorine radicals can react with ozone molecules to give molecular oxygen and chlorine monoxide. Beside this degradation process, formed chlorine monoxide can also interfere with the ozone formation by reacting with atomic oxygen to form molecular oxygen and again chlorine radicals. This catalytic ozone degradation cycle is responsible for the massive loss of stratospheric ozone mainly in the southern hemisphere (Anderson et al., 1991). A second environmental aspect is the contribution of CFCs to the global greenhouse effect (Ramanathan, 1975) that was estimated to be about 25% of the total man-made contribution (Lashof and Ahuja, 1990) during the 1980s.

To cope with these problems, new compounds with improved structural characteristics were designed. HCFCs compounds have a less stable molecule structure due to the introduction of C-H bonds, which are easily degradable by atmospheric hydroxyl radicals (Trochimowicz, 1993; Wallington et al., 1994). Due to more rapid degradation, HCFCs do not reach the ozone layer in any great extent but still exhibit a low ODP and global warming potential (GWP). HFCs lack an ODP because of the missing chlorine in the molecule structure but still exhibit a relatively high GWP increasing with higher fluorine substitution (Dekant, 1996; Franklin, 1993). The latest generation of CFC replacement substance (HFOs and HCFOs) features C-C double bonds in their molecule structures, facilitating the atmospheric breakdown even more than HCFCs and HFCs (Andersen et al., 2008; Nielsen et al., 2007). A list of exemplary compounds and their characteristics relevant to their behavior in the atmosphere is given in Table 1.

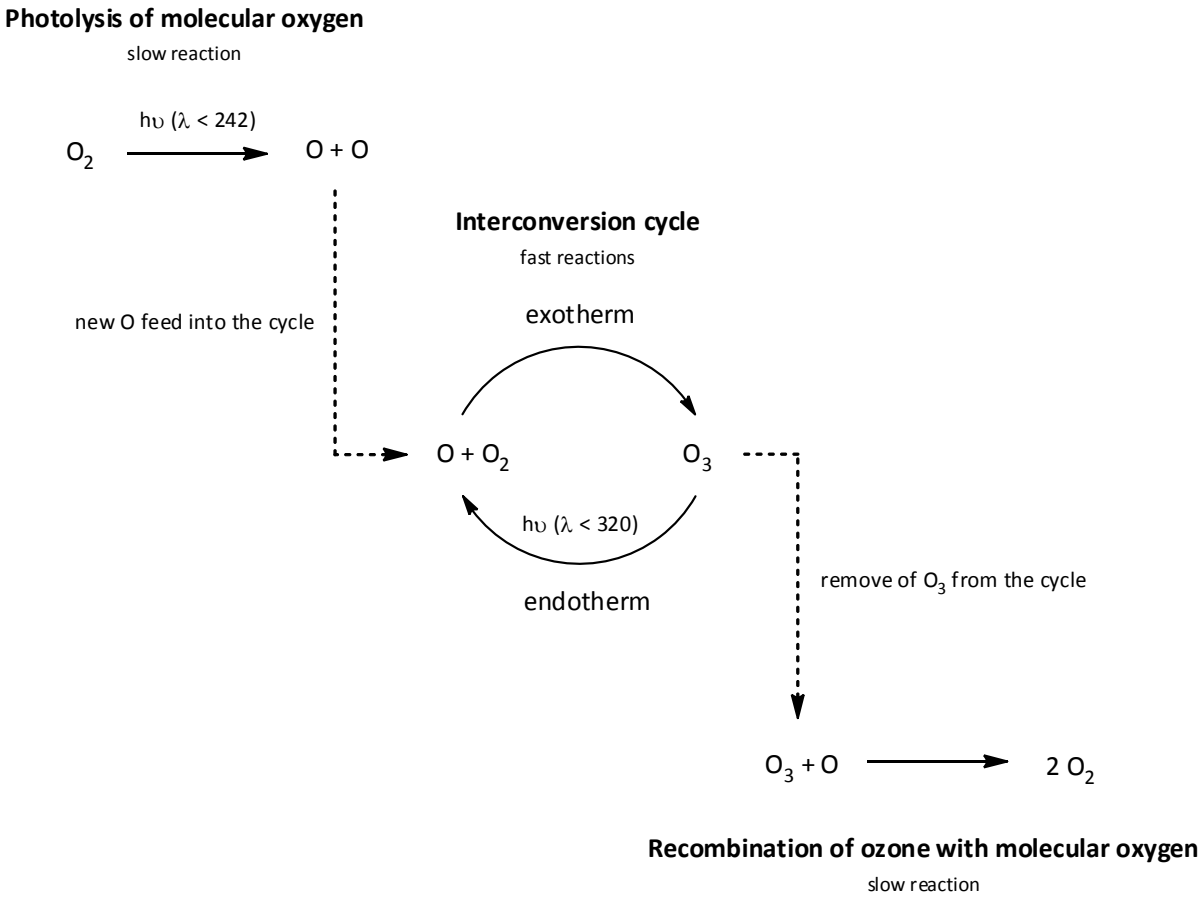

Fig. 2. Stratospheric ozone cycle according to Chapman, 1930.

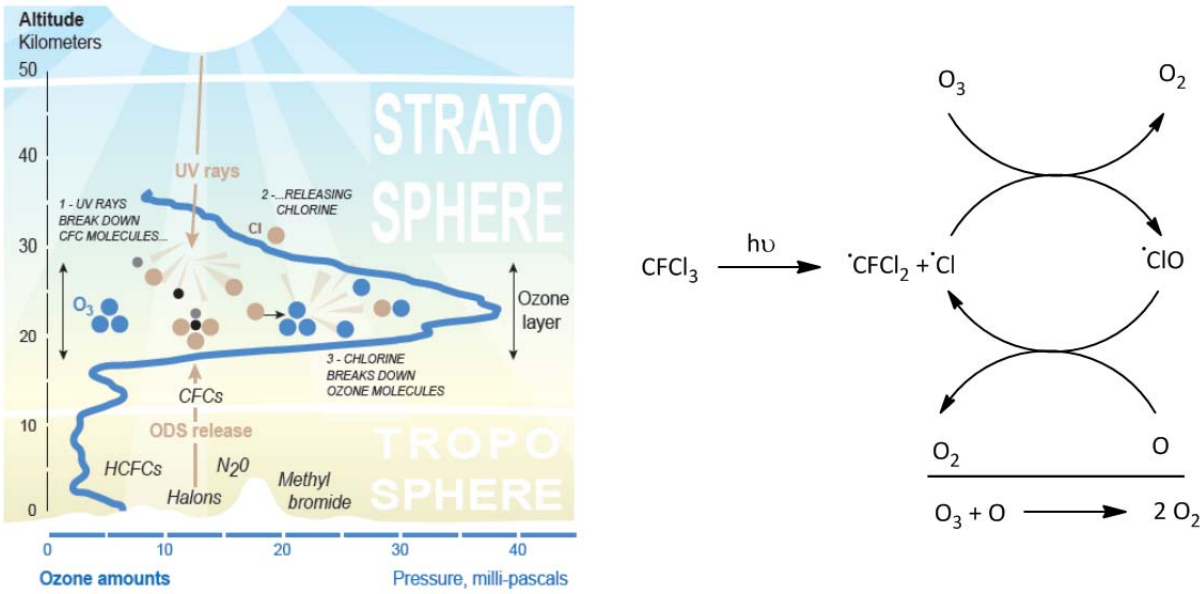

Fig. 3. Chemical ozone destruction process in the stratosphere; Source: United Nation Environment Programme, vital ozone graphics 2.0, 2009 (no copyright protection for non-profit purposes) and Dekant et al., 1996.

Table 1. Examples of compounds* and their atmospheric characteristics.

Use	Generation	Compound	Atmospheric lifetime [years]	ODP relative to CFC-11	GWP for 100 years relative to CO_2	Reference
Refrigerants	1.	**CFC-12** Dichlorodifluoromethane	116	0.95	7,100	(Houghton, 1992) (Wallington et al., 1994)
	2.	**HCFC-22** Chlorodifluoromethane	15.8	0.047	1,600	(Houghton, 1992) (Wallington et al., 1994)
	3.	**HFC-134a** 1,1,1,2-Tetrafluoroethane	14.6	0	1,300	(McCulloch, 1999)
	4.	**HFO-1234yf** 2,3,3,3-Tetrafluoropropene	11 days	0	4	(Nielsen et al., 2007)
Blowing agents	1.	**CFC-11** Trichlorofluoromethane	55	1	3,400	(Houghton, 1992)
	2.	**HCFC-141b** 1,1-Dichloro-1-fluoroethane	10.8	0.085	580	(Wallington et al., 1994) (Houghton, 1992)
	3.	**HFC-245fa** 1,1,1,3,3-Pentafluoropropane	7.4	0	760	(Ko et al., 1999) (Orkin et al., 1996)
	4.	***trans*-HCFO-1233zd** *trans*-1-Chloro-3,3,3-trifluoropropene	26 days	0.003	7	(Andersen et al., 2008)
Solvents for precision cleaning	1.	**CFC-113** 1,1,2-Trichloro-1,2,2-trifluoroethane	85	0.8	5,000	(McCulloch, 1999)
	2.	***trans*-HCFO-1233zd** *trans*-1-Chloro-3,3,3-trifluoropropene	26 days	0.003	7	(Andersen et al., 2008)

*Nomenclature of refrigerants according to ASHRAE standard (American Society of Heating, Refrigerating and Air): for CFCs/HCFCs/HFCs – **1. digit** (the number of carbon atoms minus 1, omitted when digit is zero), **2. digit** (the number of hydrogen atoms plus 1), **3. digit** (the number of fluorine atoms), **lowercase letter** (denotes specific isomer), remaining atoms are chlorine; for HFOs/HCFOs (propenes)– **1. digit** (the number of unsaturated bonds), **2. digit** (the number of carbon atoms minus 1), **3. digit** (the number of hydrogen atoms plus 1), **4. digit** (the number of fluorine atoms), **1. lowercase letter** (substitution on central atom; x = -Cl, y = -F, z = -H), **2. lowercase letter** (substitution on terminal methylene carbon; a = $-CCl_2$, b = CClF, c = CF_2, d= CHCl, e = CHF, f = CH_2).

1.1.3 Mammalian toxicity

1.1.3.1 General metabolism of CFCs and their replacements

The wide range of application for CFCs and their replacement compounds is not only due to their excellent physicochemical properties but also due to their general low potential for toxicity. Regarding acute toxicity, CFCs and their alternates have similar effects as solvents. Their high lipid solubility facilitates their uptake, distribution in the body as well as their distribution into lipid membranes. Thus, acute toxicity is mostly characterized by central nervous system depression and narcosis, with both effects usually being completely reversible if exposure is survived. Potential toxicological cardiovascular effects are manifested as changes in cardiovascular dynamics and the electrical activity of the heart but occur only in specific animal models at very high exposures (e.g. CFC-12, > 200,000 ppm in animals) (Back and Van Stee, 1977; Dekant, 1996). In contrast, chronic CFC exposure does not lead to toxic effects like organ necrosis or cancer observed in such chlorocarbon solvents as trichloromethane (Constan et al., 1999). Their low extent of biotransformation is probably due to C-F bonds, which are much more stable than C-Cl bonds, stabilizing the whole molecule and avoiding metabolic activation (Dekant, 1996; Mclean, 1977).

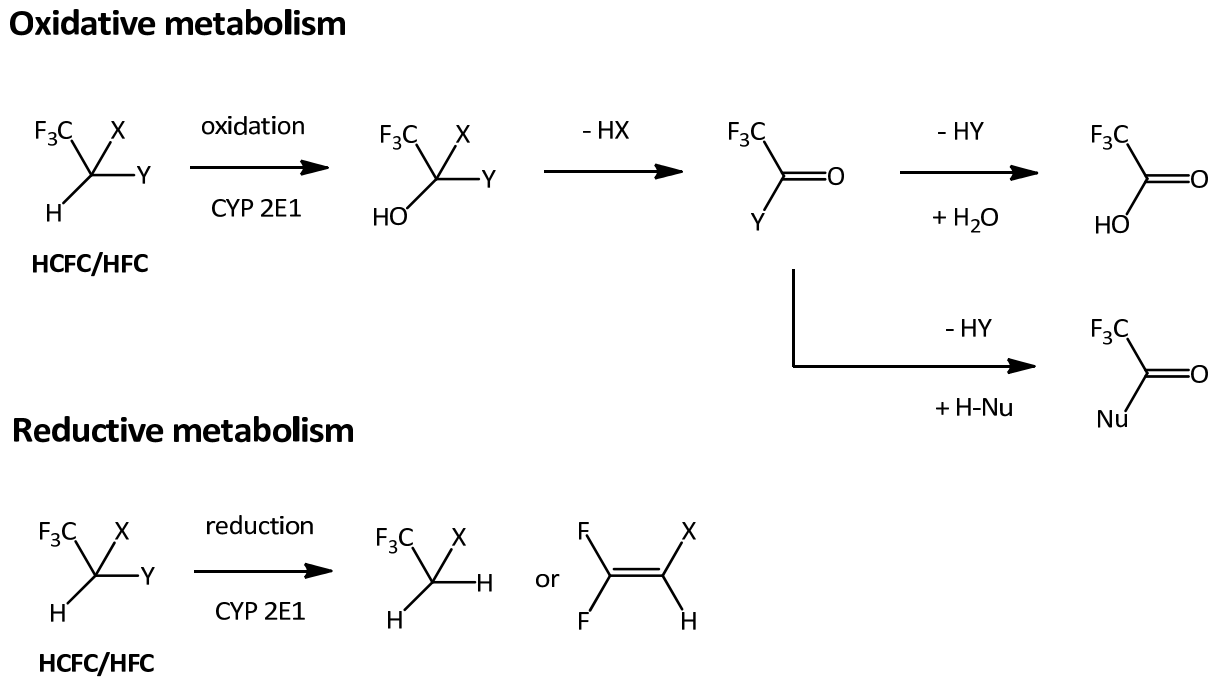

Fig. 4. Examples of oxidative/reductive metabolism of HCFCs or HFCs by cytochrome P-450 2E1 (HCFC-124: X = Cl, Y = F; HFC-125: X = Y = F; Nu, nucleophile), modified from Anders, 1991.

HCFCs and HFCs show an increased potential for mammalian toxicity due to the presence of C-H bonds (Fig. 4). They may undergo C-H σ-bond oxidation or reduction reactions catalyzed by cytochromes P-450, with cytochromes P-450 2E1 being the most important isoform regarding the metabolism of halogenated hydrocarbons (Koop, 1992; Raucy et al., 1993; White and De Matteis, 2001). The oxidative cytochrome P-450 metabolism initially generates geminal halohydrins which may lose HY to form acyl halides or aldehydes. These can further react with either H_2O or nucleophiles (e.g glutathione or proteins). Thus, the metabolism by cytochrome P-450 may serve to detoxify or bioactivate HCFCs/HFCs. The alternative reduction, in absence of oxygen, initially results in haloalkanes lacking one halogen or haloethenes formed by didehalogenation (Anders, 1991).

The latest generation of CFC replacements, the hydrofluoroolefins (HFOs) and hydrochlorofluoroolefins (HCFOs), contain C-C double bonds, facilitating atmospheric breakdown which may also increase the extent of biotransformation. C-C double bonds of halogenated alkenes are subject to nucleophilic attack (Clayton, 1977) as well as cytochrome P-450 metabolism (Guengerich, 2001; Macdonald, 1983) that may both lead to toxification of the parent compound (Fig. 5). Activation by cytochrome P-450 could lead to reactive electrophile epoxides and reactive epoxide cleavage products, responsible for protein and DNA alkylation, shown for example in the hepatotoxic and cancer-causing vinyl chloride (Guengerich et al., 1979; Guengerich et al., 1981). Nucleophilic attack by the endogenous antioxidant glutathione can lead to the formation of toxic metabolites such as halothioketenes, which are responsible for the toxification of trichloroethene (Bruning et al., 1998; Dekant et al., 1991).

Based on their chemical structure, *trans*-HCFO-1233zd and HFO-1234yf are likely subject to biotransformation by cytochrome P-450 2E1 and glutathione *S*-transferase as well. For 2,3,3,3-tetrafluoropropene this was already shown in biotransformation studies with mice, rats and rabbits by Schuster et al. (Schuster et al., 2008; Schuster et al., 2010, 2009). The biotransformation analysis of *trans*-1-chloro-3,3,3-trifluoropropene was one of the subjects of this thesis. Therefore, possible biotransformation processes for this halogenated propene have been evaluated. As the presumed biotransformation reactions for *trans*-HCFO-1233zd (via cytochrome P-450 2E1 and GST) mainly lead to hydrophilic low molecular weight metabolites (< 500 Da) that are easily excreted with the urine, *in vivo* biotransformation studies in this thesis are primarily based on urine analyses (Anders, 1991; Anders and Dekant, 1998; Commandeur et al., 1995; Dekant, 1996; Dekant et al., 1986; Macdonald, 1983; Mitoma et al., 1985; Yllner, 1961).

Cytochrome P-450 mediated bioactivation

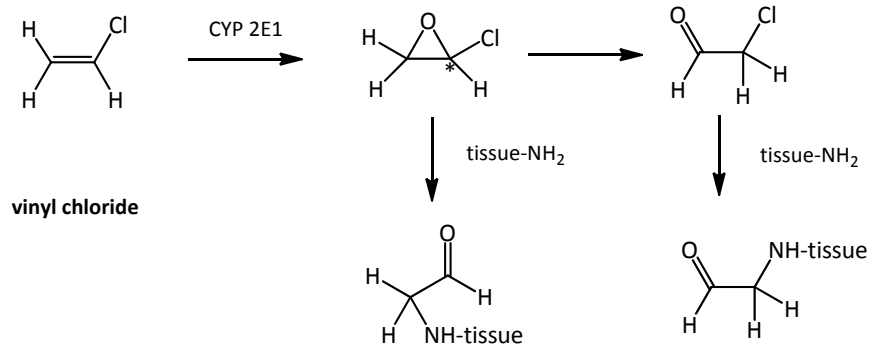

Glutathione S-transferase mediated bioactivation

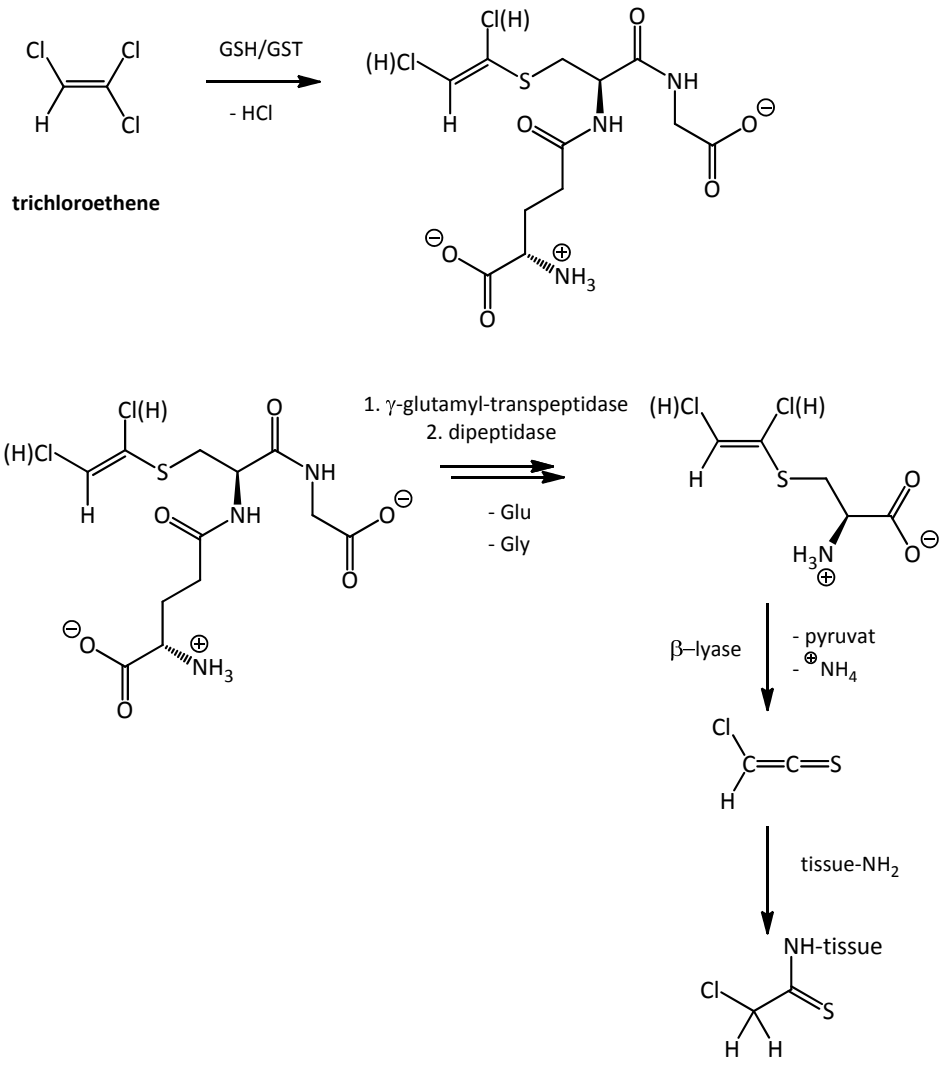

Fig. 5. Metabolic activation of vinyl chloride by cytochrome P-450 2E1 modified from Guengerich et al., 1979; metabolic activation of trichloroethene by glutathione dependent pathway modified from Dekant et al., 1991. GSH, glutathione; GST, glutathione transferase.

1.1.3.2 General metabolism of glutathione *S*-conjugates

The hepatic glutathione *S*-conjugation formation is the first step of the glutathione dependent biotransformation of halocarbons. The conjugation of this tripeptide is an important metabolic pathway for lipophilic xenobiotics and endogenous substances with an electrophilic center (Jakoby, 1978). Depending on the chemical structure of the electrophilic substrate, the reaction may be non-enzymatic or catalyzed by the glutathione *S*-transferase (GST) present in different subcellular fractions of most tissues and blood cells of mammalian organisms (Commandeur et al., 1995). Nevertheless, liver tissue is the primary site of glutathione synthesis and conjugation (Hinchman and Ballatori, 1990, 1994). Thus, glutathione conjugates are usually not excreted in urine or feces, they are further catabolized by the enzymes of the mercapturic acid pathway (Fig. 6). The initial reaction in this degradation process is the y-glutamyltranspeptidase catalyzed cleavage to cysteinylglycine *S*-conjugates followed by the dipeptidase mediated formation of cysteine *S*-conjugates. The latter are acetylated in a final step to mercapturic acids (Hinchman and Ballatori, 1994). Whereas the initial step of GSH conjugation to a xenobiotic occurs in the liver, the following enzymes y-glutamyltranspeptidase and dipeptidase are highly active in the kidney. Resulting cystein *S*-conjugates are then transported back to the liver for acetylation (Orrenius et al., 1983). This inter-organ biosynthesis of mercapturates occurs in the rat. In other species (rabbit, guinea pig, dog) an intrahepatic pathway is more likely, caused by high activities of y-glutamyltranspeptidase and dipeptidase in liver tissue (Hinchman and Ballatori, 1994). Besides the formation of mercapturic acids, the cysteine *S*-conjugate can follow different metabolic routes, including oxidative deamination or transamination to mercaptopyruvic acid *S*-conjugates that can be further reduced to mercaptolactic *S*-conjugates (Commandeur et al., 1995). An alternative biotransformation pathway is mediated by renal β-lyases, cleaving S-C bonds of *S*-cysteine conjugates (step d, Fig. 6). This pyridoxal-phosphate dependent cleavage results in the formation of dehydroalanine that rapidly hydrolyzes in ammonia and pyruvic acid and generally stable thiol compounds (Stevens et al., 1986). Regardless, they may also be transformed to highly reactive and/or mutagenic intermediates as shown for halogenated alkenes (Vamvakas et al., 1987). Stable thiols can be further metabolized to *S*-glucuronides, *S*-methyl conjugates or highly reactive sulfenic acids, reacting with thiol groups to form disulphides or to thiolsulfinates by dimerization (Davis et al., 1986). Sulfoxides of cysteine, mercapturic acids, mercaptolactic acids and mercaptolactic acids *S*-conjugates were identified in *in vivo* and *in vitro* studies of several compounds (Commandeur et al., 1995). These reactions are mainly catalyzed by flavin-monooxygenases (FMOs) (Damani and Houdi, 1988; Sausen and Elfarra, 1990) and cythochrome P-450 (Benoit et al., 1992; Werner et al., 1996) associated with the hepatic and renal microsomal fraction. Due to their possible metabolism by the β–lyase, sulfoxide conjugates may also play a role in *S*-conjugate toxicity. The β–lyase mediated cleavage leads to sulfenic acids, associated with toxic potential as mentioned before

(Tomisawa et al., 1993). The sulfoxide can further act as a direct acting electrophile able to react with tissue nucleophiles, as shown for the sulfoxide of *S*-(1,2-dichlorovinyl)-*L*-cysteine (Sausen and Elfarra, 1991).

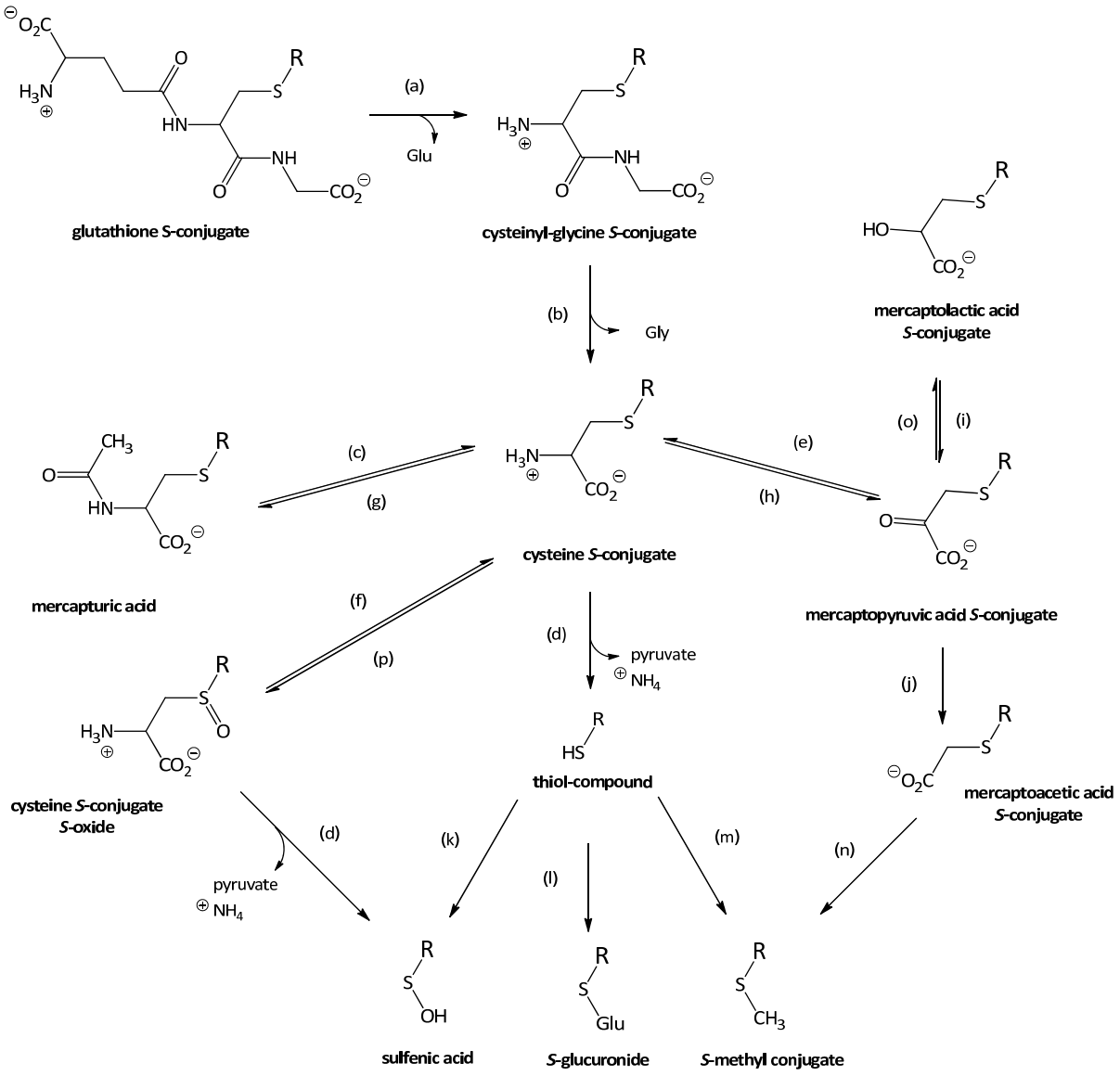

Fig. 6. General metabolism of glutathione *S*-conjugates (modified from Commandeur et al., 1995); (a) γ-glutamyltranspeptidase; (b) dipeptidases: cysteineglycine dipeptidase and aminopeptidase M; (c) cysteine conjugate *N*-acetyltransferase; (d) cysteine conjugate β-lyase; (e) cysteine conjugate transaminase and *L*-amino acid oxidase; (f) cysteine conjugate *S*-oxidase; (g) *N*-deacetylase; (h) transaminases; (i) 3-mercaptopyruvic acid *S*-conjugate reductase; (j) decarboxylase; (k) *S*-oxygenase; (l) uridine diphosphate-glucuronyl transferase; (m) *S*-methyl transferase; (n) decarboxylase; (o) 3-mercaptolactic acid *S*-conjugate oxidase; (p) sulfoxide reductase; Glu, *L*-glutamic acid; Gly, *L*-glycin.

1.1.3.3 Cytochrome P-450 and GSH activated metabolism of propenyl halides

Conjugation of foreign compounds with GSH almost always leads to less reactive products that are easily excreted. In a few instances, however, glutathione conjugates are more reactive than the parent compound (Hayes et al., 2005). Examples of this phenomenon are short-chain alkyl halides. Several of these compounds are nephrotoxic as demonstrated for perfluoropropene or 1,1,2-trichloro-3,3,3-trifluoropropene (Dekant et al., 1990; Monks et al., 1990; Vamvakas et al., 1989).

In general both, addition and addition-elimination reactions are observed in the glutathione *S*-transferase-catalyzed reaction of glutathione with haloalkenes (Anders and Dekant, 1998). Bioactivation is mediated by enzymatic transformation to the corresponding *L*-cysteine *S*-conjugates and further metabolized by the renal β-lyase pathway to α-haloalkenylthiolates (Fig. 7). The latter can generate highly electrophilic thioacylhalides or thioketenes that can further react to covalent bonds with tissue nucleophile structures such as amino groups of proteins-bond lysine, mitochondrial phospholipids or the DNA (Birner et al., 1994; Chen et al., 1990; Schaumann, 1988). Besides the β-lyase pathway, flavoprotein- or cytochrome P-450-dependent sulfoxidation may lead to the formation of activated *S*-(haloalkenyl)-*L*-cysteine sulfoxides, also forming covalent bindings with nucleophilic groups by acting as a Michael-acceptor (Werner et al., 1995). As an example *S*-(1,2-dichlorovinyl)-*L*-cysteine sulfoxide is a potent nephrotoxicant in rats because of its cellular thiol depletion potential (Lash et al., 1994). As described previously, halogenated carbons containing a double bond also serve as cytochrome P-450 substrate and may therefore be transformed to highly activated epoxides (Guengerich, 2001; Macdonald, 1983). The unstable epoxide of this hepatic phase one reaction is further cleaved by nucleophiles such as hydroxide ions or the thiol group of endogenous glutathione. Depending on the chemical structure of the halogen alkene, the latter detoxifying process, may again lead to toxification by transfer to the corresponding *L*-cysteine conjugate and its activation by renal β-lyase to a thioacyl halide (Fig. 7) (Anders and Dekant, 1998; Macdonald, 1983). Regarding the metabolism of *trans*-HCFO-1233zd and HFO-1234yf, previously mentioned activation reactions are not likely to occur, due to the lack of multiple halogen leaving groups.

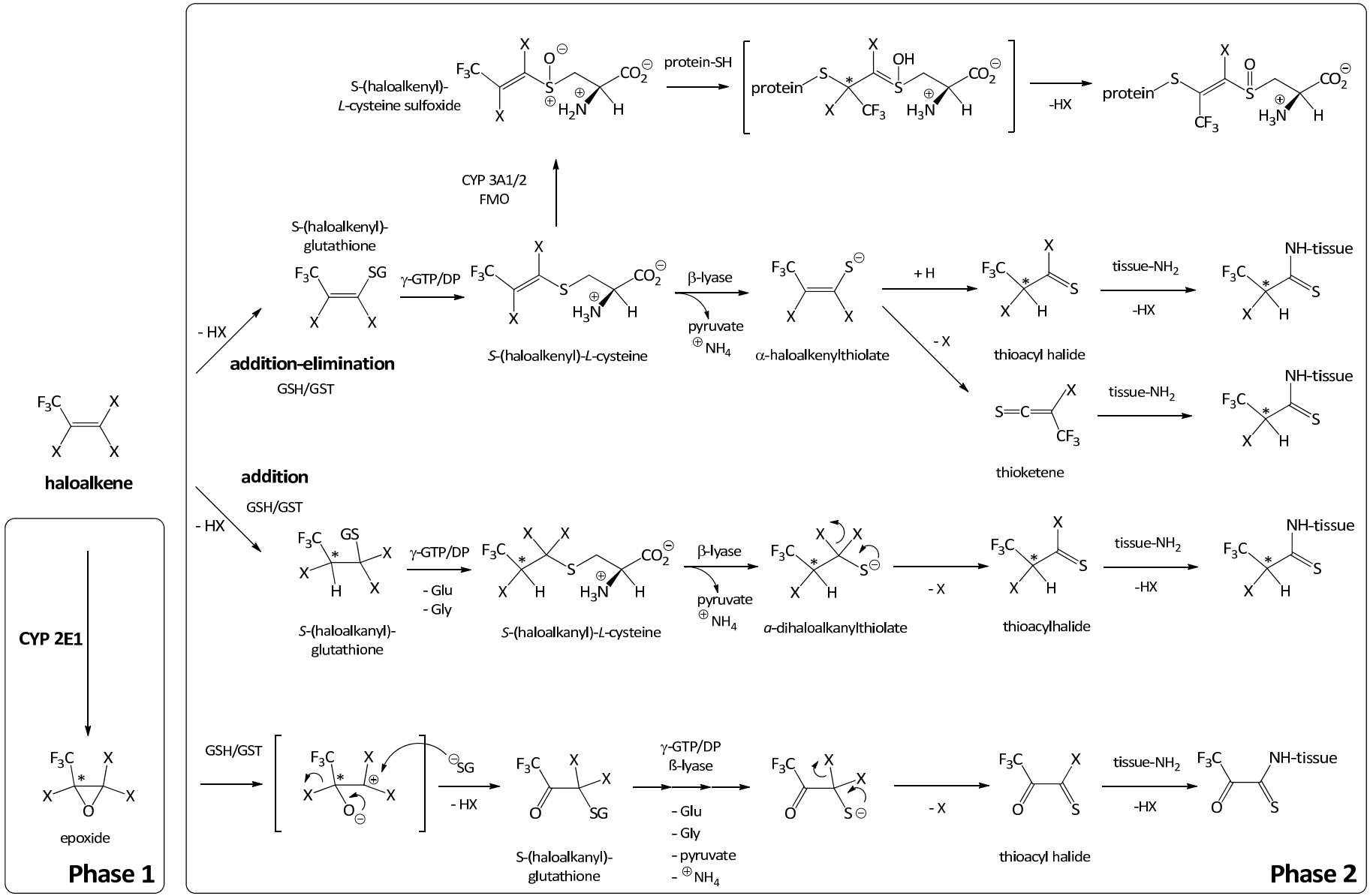

Fig. 7. Metabolic activation of propenyl halides by cytochrome P-450 2E1 and glutathione modified from Schuster P., 2009 and Anders, M. W. and Dekant, W., 1998; γ–GTP, γ-glutamyl transpeptidase; DP, dipeptidase; GSH, glutathione; GST, glutathione *S*-transferase; X = Br, Cl, F.

1.2 2,3,3,3-Tetrafluoropropene (HFO-1234yf)

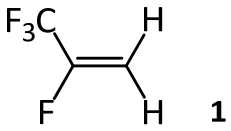

1

1.2.1 Chemical properties and applications

2,3,3,3-Tetrafluoropropene is a novel refrigerant intended for the use in mobile air conditioning systems. It has been developed as a replacement for halocarbons such as HFC-134a, which is currently the most common refrigerant in mobile air conditioning systems (McCulloch, 1999).

HFO-1234yf is a colorless gas with a vapor pressure of 607 kPa at 21 °C and a boiling point of -30 °C (Honeywell, 2007). Blood/air partition coefficients were determined as 0.04 (human), 0.07 (rabbit) and 0.08 (rat) (DuPont, 2008). HFO-1234yf has a slight odor and is of mild flammability (Minor et al., 2010). Its log *P* value of approximately 2.2 is comparable with the lipophilicity of inhalation anesthetics (e.g. halothane, log *P* = 2.1). Its beneficial environmental characteristics such as non-ozone-depleting hydrofluorocarbon with a low global warming potential (GWP, 4 relative to CO_2), absence of capacity for ozone depletion and a short atmospheric life time of only 11 days (Nielsen et al., 2007), designate it as an appropriate replacement substance for HFC-134a.

1.2.2 Toxicity testing results and biotransformation

Acute inhalation toxicity (Organisation for Economic Co-operation and Development [OECD] 403) of HFO-1234yf tested in female and male CD-1 mice and Sprague Dawley (SD) rats for four hours revealed no lethality. All animals survived the exposure of the highest concentration without clinical signs of toxicity (99,830 ppm in mice and 405,800 ppm in rats) (Huntingdon, 2004; TNO, 2006a). In another GLP-compliant (GLP, good laboratory practice) study, groups of 5 male and 5 female SD rats were exposed, nose only to vapors of HFO-1234yf at levels of 0 (control), 5,000, 20,000 or 50,000 ppm 6 h/day, 5 days/week for 2 weeks (TNO, 2006b). In this subacute pretest neither mortality nor other adverse effects were observed. Consequently a no observed adverse effect level (NOAEL) of at least 50,000 ppm was concluded. This value was confirmed in a subchronic toxicity study in SD rats (OECD 412) exposed to concentrations of 5,000, 20,000 or 50,000 ppm 6-hours/day, 5 days/week for 4 weeks (TNO, 2006c). A second subchronic toxicity study (90 days, OECD 413) of HFO-1234yf in F344 rats and B6C3F1 mice, integrating a toxicogenomic assessment,

predicted no carcinogenicity for HFO-1234yf to the target organs liver (evaluated in mice) and kidney (evaluated in rats). Further, no treatment-related histopathological lesions were observed following exposure to HFO-1234yf at 10,000 and 50,000 ppm (no observed effect level, NOEL) (Hamner, 2007). A rat prenatal developmental toxicity study (OECD 414) revealed a NOAEL of 50,000 ppm (Waalkens-Berendsen, 2011). Despite this overall low potential for toxicity of HFO-1234yf in rodents, a prenatal developmental toxicity study in New Zealand White (NZW) rabbits showed mortality at exposure levels of 5,500 ppm and above. In contrast, no lethality was observed at exposure levels of 2,500 and 4,000 ppm of HFO-1234yf (WIL, 2008). Histopathological examination revealed subacute inflammation of the heart as a predominant effect both in surviving and deceased maternal rabbits at all exposure levels. In addition, non dose-dependent mineralization was detected in the heart and liver of a few maternal rabbits. Intrauterine growth and survival were not affected by test substance exposure at any concentration. Based on mortality, moribundity, lower mean body weight gain, mean body weight loss and/or lower food consumption observed at 5,500 and 7,500 ppm (maternally lethal exposure concentrations), an exposure concentration of 4,000 ppm was considered to be the NOAEL for maternal toxicity. Because of test substance-related visceral malformations in the heart and/or great vessels which were also observed in 5,500 and 7,500 ppm exposure groups, the NOAEL for embryo/fetal development was considered to be 4,000 ppm as well (WIL, 2011). Cardiac sensitization potential evaluated in beagle dogs, with concentration levels up to 120,000 ppm, showed no arrhythmic potential nor other signs of toxicity. Thus, the highest exposure concentration was defined as NOEL (120,000 ppm) (WIL, 2006).

Genotoxicity and mutagenicity was tested by several *in vitro* assays. A GLP-compliant Ames assay which involved exposure of Salmonella typhimurium (TA 1535, TA1537, TA 98, and TA 100), E. coli (WP2 uvrA) and chromosome aberration study in human lymphocytes was conducted. A two-fold increase in mutations was seen with TA 100 and WP2 uvr2 in the presence of S-9 at exposure levels of 20%. All other cell lines were inactive both in presence and absence of S-9 metabolic activation (TNO, 2007, 2005a). No genotoxicity was observed *in vivo* or in mammalian cells. In GLP-compliant micronucleus studies in mice with acute exposure levels up to 200,000 ppm and SD rats with repeated exposure levels up to 50,000 ppm, no chromosomal damage or damage to the mitotic spindle apparatus in bone marrow cells were observed (TNO, 2005b, 2006c).

Biotransformation of HFO-1234yf (Fig. 8) was studied by Schuster et al. both *in vivo* in male SD rats, male B6C3F1 mice and female NZW rabbits and *in vitro* in hepatic subcellular incubations experiments (Schuster, 2009; Schuster et al., 2008; Schuster et al., 2010). Based on ^{19}F-NMR analysis *N*-acetyl-*S*-(3,3,3-trifluoro-2-hydroxypropanyl)-*L*-cysteine (**9**, Fig. 8) was the predominant urinary metabolite in the rat (90%), mice (32%) and rabbit (44%). *S*-(3,3,3-trifluoro-2-hydroxypropanyl)-mercaptolactic acid *S*-conjugate (**11**, Fig. 8), its sulfoxide (**12**, Fig. 8) and the sulfoxide of *N*-acetyl-*S*-(3,3,3-trifluoro-2-hydroxypropanyl)-*L*-cysteine (**10**, Fig.

8) as well as 3,3,3-trifluoro-1,2-propanediol (**17**, Fig. 8) were determined as minor metabolites in all species. The only species difference in metabolism was the absence of 3,3,3-trifluoroaceton (**14**, Fig. 8) and 3,3,3-trifluoro-2-propanol in rat urine (**15**, Fig. 8) as well as of 3,3,3-trifluoro-1-hydroxyacetone (**16**, Fig. 8), 3,3,3-trilfluorolactic acid (**18**, Fig. 8) and trifluoroacetic acid (**19**, Fig. 8) in rabbit urine. *In vitro* experiments with rat and human liver microsomes and rabbit subcellular liver fractions supported the metabolic pathways of HFO-1234yf observed *in vivo*.

Quantitation of the predominant metabolite *N*-acetyl-*S*-(3,3,3-trifluoro-2-hydroxypropanyl)-*L*-cysteine revealed a very low biotransformation of less than 1% of the received dose in all three analyzed species. Additionally, more than 90% of the total metabolite excretion was recovered within the first 18 hours after termination of inhalation exposures. The suggested high exhalation of inhaled high volatile HFO-1234yf and the observed very low biotransformation amount supported the assumption of a low toxicity potential. Hepatotoxic metabolites as the highly reactive intermediate 2,3,3,3-tetrafluoroepoxypropane (**5**, Fig. 8) and trifluoroacetic acid (**19**, Fig. 8) (Rosenberg and Wahlstrom, 1971; Stier et al., 1972) are not expected to cause any damage due to the very low amounts formed and an efficient detoxification (GSH conjugation, hydrolysis).

The results revealed that HFO-1234yf is subject to a typical haloolefin biotransformation with a cytochrome P-450 2E1 mediated initial oxidation of the C-C double bond at low rates, followed by conjugation of glutathione or hydrolysis (not observed in the rabbit). Species differences in metabolite pattern did not indicate differences in potential toxicity. Thus, no explanation was found regarding the mortality of pregnant rabbits after multiple exposures.

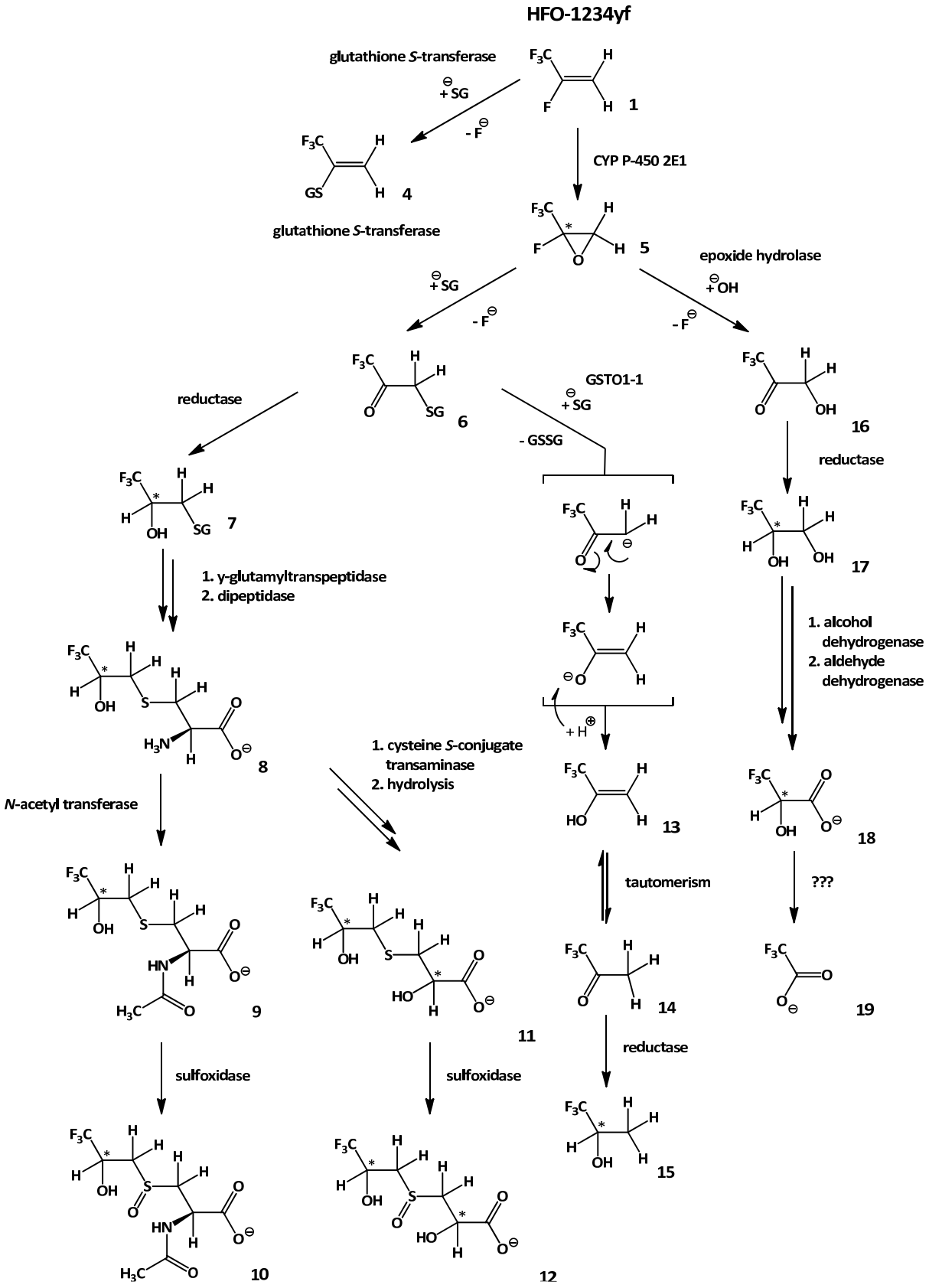

Fig. 8. Biotransformation of HFO-1234yf *in vitro* and *in vivo* modified from Schuster, 2009; (**1**) 2,3,3,3-tetrafluoropropene (HFO-1234yf), (**4**) 2-*S*-(3,3,3-trifluoropropenyl)-glutathione, (**5**) 2,3,3,3-tetrafluoroepoxyprpane, (**6**) *S*-(3,3,3-trifluoro-2-oxopropanyl)-glutathione, (**7**) *S*-(3,3,3-trifluoro-2-hydroxypropanyl)-glutathione, (**8**) *S*-(3,3,3-trifluoro-2-hydroxypropanyl)-*L*-cysteine, (**9**) *N*-acetyl-*S*-(3,3,3-trifluoro-2-hydroxypropanyl)-*L*-cysteine, (**10**) *N*-acetyl-*S*-(3,3,3-trifluoro-2-hydroxypropanyl)-*L*-cysteine sulfoxide, (**11**) *S*-(3,3,3-trifluoro-2-hydroxypropanyl)-mercaptolactic acid, (**12**) *S*-(3,3,3-trifluoro-2-hydroxypropanyl)-mercaptolactic acid sulfoxide, (**13**) 3,3,3-trifluoro-1-propen-2-ol, (**14**) 1,1,1-trifluoroacetone, (**15**) 3,3,3-trifluoro-2-propanol, (**16**) 3,3,3-trifluoro-1-hydroxyacetone, (**17**) 3,3,3-trifluoro-1,2-propanediol, (**18**) 3,3,3-trifluorolactic acid, (**19**) trifluoroacetic acid; GSSG, glutathione disulfide; -SG, thiolate anion of glutathione; GSTO1-1, glutathione S-transferase omega-class 1.

1.3 *trans*-1-Chloro-3,3,3-trifluoropropene (*trans*-HCFO-1233zd)

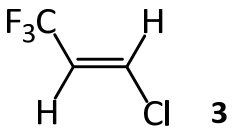

3

1.3.1 Chemical properties and applications

trans-1-Chloro-3,3,3-trifluoropropene is a new solvent intended for use as a foam blowing agent and preceding cleaning agent for special applications. Additionally, it may be used as a propellant in pharmaceutical applications such as metered dose-inhalators.

It is a colorless gas with light odor, incombustible and has a log *P* value of approximately 2.2. Its vapor pressure of 152 kPa (at 30 °C) and its low boiling point of 19 °C are characteristic for a volatile substance (Honeywell, 2008). Its blood/air partition coefficients were determined as 0.6 in humans, 0.9 in rabbits and as 1.5 in the rat. With an ODP of 0.003 (relative to $CFCl_3$), a GWP of 7 (relative to CO_2) and an atmospheric life time of 26 days (Andersen et al., 2008) *trans*-HCFO-1233zd is more environmentally sustainable compared to older compounds used for similar applications (e.g. CFC-113, Table 1).

1.3.2 Toxicity testing results

The available toxicity data on *trans*-HCFO-1233zd generally demonstrate a low potential for toxicity. An acute inhalation toxicity study in SD rats (OECD 403) revealed LC_{50} (median lethal concentration) values of 118,200 ppm for male and 121,700 ppm for female animals. Repeated dose inhalation studies in SD rats (14/28 days, OECD 410) with exposure levels up to 20,000 ppm (14 days) and 10,000 ppm (28 days) showed no treatment related abnormalities during clinical examinations as well as no effects on body weight, body weight gain or food consumption. An increase in blood potassium levels observed in male rats, not correlating with any clinical effect, was the basis for the definition of a NOEL of 4,500 ppm. Subchronic toxicity testing (90 days, OECD 413) in SD rats revealed a NOAEL of 4,000 ppm on account of multifocal mononuclear cell infiltrates in the heart seen at the higher levels of exposure. NOELs observed in prenatal developmental toxicity studies in SD rat and NZW rabbit (OECD 414) with exposure concentrations up to 15,000 ppm, were 10,000 ppm for rats and 15,000 ppm in rabbits. Whereas no substance related findings occurred in the rabbit, the rat showed an increased number of pups with a dilated bladder at 15,000 ppm. Cardiac sensitization testing in beagle dogs (10 min inhalation exposure) revealed a NOEL of 25,000 ppm (Honeywell, 2011).

In vitro testings for genotoxicity and mutagenicity in several bacteria strains (Salmonella typhimurium, TA 1535, TA 1537, TA 98, TA 100; E. coli, WP2 uvrA) as well as in human lymphocytes, were negative regarding mutation induction or structural chromosome aberrations, both in presence or absence of S9 mix (Honeywell, 2011).

1.4 Task and scope

Being aware of global warming and the ozone layer depletion based on human activities has led to efforts to reduce and replace compounds with high ODP and GWP values. The large chemical class of chlorofluorocarbons with their high ODP and GWP potential and various application forms is subject to search for replacement compounds since their negative environmental impact was discovered in the 1970s (Molina and Rowland, 1974). Thus, several CFC replacements with enhanced environmental characteristics were introduced in recent decades (HCFCs, HFCs). To achieve stricter governmental regulatory directives (e.g. Clean Air Act 1990, US; Regulation (EC) No 1005/2009) the haloolefines *trans*-1-chloro-3,3,3-trifluoropropene (*trans*-HCFO-1233zd) and 2,3,3,3-tetrafluoropropene (HFO-1234yf) were recently developed by Honeywell International (Morristown, New Jersey).

Part of the risk assessment and registration of new chemical compounds is the evaluation of mammalian biotransformation and identification of possible human health risks (in the European Union according to Regulation (EC) No 1907/2006, “REACH”). Principle aims of this thesis were to investigate the unknown metabolism of the new solvent *trans*-HCFO-1233zd and to further investigate a possible biotransformation based toxicity of HFO-1234yf observed in rabbits (WIL, 2011, 2008).

Metabolism of *trans*-HCFO-1233zd was studied *in vitro* in rat, rabbit and human liver subcellular fractions and *in vivo* in rats and rabbits to confirm predictions based on the results of the *in vitro* assays. In the *in vitro* work, the extent of biotransformation by different enzymatic pathways was compared in subcellular fractions from rat, rabbit and human liver for a comparative assessment of potential toxicity possibly mediated by the different pathways of biotransformation (cytochrome P-450 or glutathione *S*-transferase). *In vivo* metabolism was determined in urine of rats and rabbits exposed to different concentrations of *trans*-HCFO-1233zd by whole-body inhalation. To identify fluorine-containing metabolites urine was analyzed by ^{19}F-NMR spectroscopy and mass spectrometry coupled with liquid or gas chromatography (LC-MS/MS and GC/MS). To evaluate excretion kinetics of relevant *trans*-HCFO-1233zd metabolites, time courses were also determined in urine and blood.

Observed cardiotoxicity in a NZW rabbit prenatal developmental toxicity study (OECD 414) was the basis for the second objective of this study. Therefore two *in vivo* studies with NZW rabbits were conducted at Huntingdon Life Sciences (East Millstone, New Jersey). An acute inhalation toxicity study was designed to investigate whether there is a gender-based or

pregnancy-based difference in acute toxic response and biotransformation of HFO-1234yf in rabbits. A second study evaluated the effects of a multiple HFO-1234yf inhalation exposure (28 days) on possible biotransformation and cytochrome P-450 activity (2E1 and 3A4) alterations in female and male rabbits. In particular, the formation and accumulation of monofluoroacetate, a known cardiotoxic compound (Gooneratne et al., 1995; Sherley, 2004), was determined in heart tissue. Study specimens were analyzed by ^{19}F-NMR spectroscopy, mass spectrometry (LC-MS/MS and GC/MS) and potentiometry (fluoride sensitive electrode).

2 Materials and methods

2.1 Chemicals

2,3,3,3-Tetrafluoroprop-1-ene (HFO-1234yf, purity of 99,99%) and *trans*-1-chloro-3,3,3-trifluoropropene (*trans*-HCFO-1233zd, purity of 99,99%) were supplied by Honeywell (Morristown, New Jersey, USA). 3,3,3-trifluoro-1,2-epoxypropane was purchased from Matrix Scientific (Columbia, South Carolina, USA), 3,3,3-trifluorolactic acid (96%) was purchased from Alfa Aesar (Karlsruhe, Germany) and ammonia (purity ≥ 99.98%) was purchased from Linde (Pullach, Germany). All other chemicals were purchased from Sigma-Aldrich (Taufkirchen, Germany) in the highest available purity. Synthesis and characterization of *S*-(1,2-dichlorovinyl)-glutathione and *S*-(3,3,3-trifluoro-*trans*-propenyl)-mercaptolactic acid were reported previously (Schuster et al., 2009; Vamvakas et al., 1988).

2.2 Chemical synthesis

2.2.1 ^{1}H-NMR, ^{13}C-NMR and ^{19}F-NMR spectroscopy

^{1}H-NMR and ^{13}C-NMR spectra were recorded with a Bruker 600 DMX NMR spectrometer equipped with a 5 mm DCH cryoprobe operating at 600.133 MHz (Bruker Biospin. GmbH, Rheinstetten). Chemical shifts were referenced to external tetramethylsilane (TMS). ^{1}H-NMR spectra were recorded with a 30° pulse, a pulse length of 10.1 µsec and a cycle delay of 6 µsec. The acquisition time was 5 sec and 32 scans were recorded with a spectral width of 22 ppm. ^{13}C-NMR spectra were recorded with a 30° pulse, a pulse length of 9.5 µsec, a cycle delay of 6 µsec and a spectral width of 269 ppm. The acquisition time was set to 5 sec. All spectra were manually baseline corrected and analyzed with TopSpin 3.0 (Bruker Biospin GmbH, Rheinstetten).

^{19}F-NMR spectra were recorded with a Bruker DRX 300 NMR spectrometer with a 5 mm fluoride probe operating at 282.404 MHz (Bruker Biospin GmbH, Rheinstetten). ^{19}F-chemical shifts were referenced to external $CFCl_3$. Spectra were recorded with a 30° pulse, a pulse length of 13.6 µsec and a cycle delay of 6 µsec. The acquisition time was 3 sec and 200 scans were recorded. The ^{19}F-spectra were acquired with proton coupling and a spectral width of 200 ppm (+10 to -190 ppm). Before integration of peak areas, an accurate baseline correction and spectra phasing was performed between chemical shifts of -60 and -85 ppm.

Following abbreviations are used for the description of the NMR spectra: s = singlet, d = doublet, t = triplet, q = quartet, dd = doublet of doublet, dq = doublet of quartet, m = multiplet. Diastereomeric ratios were determined by comparison of integrals assigned to single-proton signals of each diastereomer. Compound impurities were calculated by division of integrals assigned to single-proton signals of each impurity (solvent and reactant residues) by the integral of a single-proton signal of the product.

2.2.2 HFO-1234yf metabolites

2.2.2.1 *N*-Acetyl-*S*-(3,3,3-trifluoro-2-hydroxypropanyl)-*L*-cysteine (8)

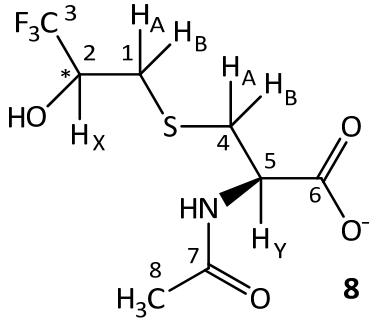

8

M_w (molecular weight) = 275 g/mol

M_w (as dicyclohexylammonium salt) = 456 g/mol

N-Acetyl-*S*-(3,3,3-trifluoro-2-hydroxypropanyl)-*L*-cysteine was synthesized according to the published procedure by Schuster et al., 2008. Two diastereomers of *N*-acetyl-*S*-(3,3,3-trifluoro-2-hydroxypropanyl)-*L*-cysteine were obtained in a ratio of 5:1 according to HPLC-separation (HP 1090, Agilent, Waldbronn, Germany) on a Partisil ODS 3 column (250 x 8 mm; Bischoff Chromatography, Leonberg, Germany) with 0.1% formic acid in water and acetonitrile as eluents (R_t = 13.3/13.8 minutes). For gradient elution the concentration of acetonitrile was elevated from 2% to 40% within 30 minutes. The detection wavelength was set to 225 nm.

For further purification, the reaction products were precipitated as dicyclohexylammonium (DCHA) salts (Mennicke et al., 1983).

Purity was determined > 96% based on ^{1}H-NMR (DMSO-d_6, δ [ppm], *J* [Hz]): 1.82 (3 H, s, **H8**), 2.60 (1 H, dd, $^{2}J_{AB}$ = 13.6, $^{3}J_{AX}$ = 10.0, **H1$_A$**), 2.73 (1 H, dd, $^{2}J_{BA}$ = 13.6, $^{3}J_{BX}$ = 3.3, **H1$_B$**), 2.82 (1 H, dd, $^{2}J_{AB}$ = 13.5, $^{3}J_{AY}$ = 6.1, **H4$_A$**), 2.97 (1 H, dd, $^{2}J_{BA}$ = 13.5, $^{3}J_{BY}$ = 5.1, **H4$_B$**), 4.01 (1 H, m, **H2$_X$**), 4.1 (1 H, m, **H5$_Y$**), 7.58 (1 H, d, ^{3}J = 7.3, N**H**); ^{13}C-NMR (DMSO-d_6, δ [ppm], *J* [Hz]): 22.73 (s, **C8**), 31.97 (s, **C1**), 34.90 (s, **C4**) 51.76 (s, **C5**), 69.12 (q, **C2**), 125.25 (q, **C3**), 168.52 (s, **C7**), 172.40 (s, **C6**); ^{19}F-NMR (D_2O): -78.7 (3 F, d, $^{3}J_{HF}$ = 6.6, **F3**).

2.2.3 *trans*-HCFO-1233zd metabolites

2.2.3.1 *N*-Acetyl-*S*-(3,3,3-trifluoro-*trans*-propenyl)-*L*-cysteine (20)

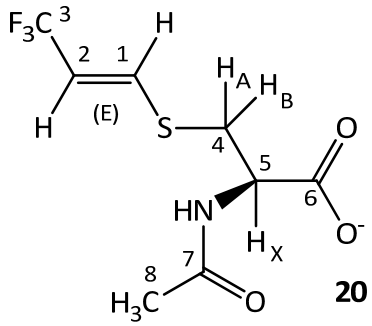

20

M_w = 257 g/mol

N-Acetyl-*S*-(3,3,3-trifluoro-*trans*-propenyl)-*L*-cysteine was synthesized according to published procedures for the synthesis of *S*-1,2-dichlorovinyl-*L*-cysteine (Mckinney et al., 1959a; Mckinney et al., 1959b). Sodium (6.6 mmol) was dissolved in 50 mL of dry liquid ammonia and *N*-acetyl-*L*-cysteine (app. 6.7 mmol) was added until the blue color of the reaction mixture disappeared. An excess of *trans*-HCFO-1233zd was then condensed and the obtained reaction mixture was stirred for 1 hour under cooling by a CO_2/isopropanol mixture. The mixture was allowed to reach ambient temperature to evaporate the excess of HFCO-1233zd and the ammonia. The crystalline residue obtained was dissolved in water. After acidification to pH 2 with 2 N hydrochloric acid, *N*-acetyl-*S*-(3,3,3-trifluoro-*trans*-propenyl)-*L*-cysteine was extracted with ethylacetate and further purified by HPLC separation (same conditions as describes for the HPLC analysis of *N*-acetyl-S-(3,3,3-trifluoro-2-hydroxypropanyl)-*L*-cysteine [2.2.2.1]). Fractions eluting after approximately 19 minutes were collected to obtain purified *N*-acetyl-*S*-(3,3,3-trifluoro-*trans*-propenyl)-*L*-cysteine.

Purity was determined > 95% based on ^{1}H-NMR (DMSO-d_6, δ [ppm], *J* [Hz]): 1.85 (3 H, s, **H8**), 3.09 (1 H, dd, $^{2}J_{AB}$ = 13.7, $^{3}J_{AX}$ = 8.3, **H4$_A$**), 3.26 (1 H, dd, $^{2}J_{BA}$ = 13.7, $^{3}J_{BX}$ = 5.0, **H4$_B$**), 4.44 (1 H, m, **H5$_X$**), 5.96 (1 H, dq, ^{3}J = 15.4, ^{3}J = 6.8, **H2**), 7.39 (1 H, dq, ^{3}J = 15.4, ^{4}J = 2.0, **H1**), 8.38 (1 H, d, ^{3}J = 8.0, N**H**);^{13}C-NMR (DMSO-d_6, δ [ppm], *J* [Hz]): 22.27 (s, **C8**), 32.80 (s, **C4**), 51.44 (s, **C5**), 110.60 (q, **C1**), 123.32 (q, **C3**), 139.35 (q, **C2**), 169.44 (s, **C7**), 171.47 (s, **C6**); ^{19}F-NMR (D_2O, δ [ppm], *J* [Hz]): -61.8 (3 F, dd, $^{3}J_{HF}$ = 6.6, $^{4}J_{HF}$ = 2.1, **F3**).

2.2.3.2 *S*-(3,3,3-Trifluoro-*trans*-propenyl)-*L*-cysteine (21)

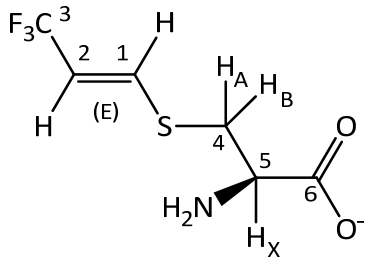

21

M_w = 215 g/mol

S-(3,3,3-Trifluoro-*trans*-propenyl)-*L*-cysteine was synthesized as described for *N*-acetyl-*S*-(3,3,3-trifluoro-*trans*-propenyl)-*L*-cysteine but adding 10 mmol *L*-cysteine to approximately 20 mmol sodium dissolved in liquefied ammonia. The crystalline residue obtained was dissolved in water. After acidification to pH 2 with 2 N hydrochloric acid, *S*-(3,3,3-Trifluoro-*trans*-propenyl)-*L*-cysteine was extracted with ethylacetate.

Two diastereomers (E/Z) were obtained in a ratio of 10:3 based on ^{1}H-NMR analysis. Purity of the E/Z mixture was determined > 95% based on ^{1}H-NMR (D_2O, δ [ppm], *J* [Hz]): 3.27 (1 H, dd, $^{2}J_{AB}$ = 15.0, $^{3}J_{AX}$ = 7.5, **H4$_A$**),3.42 (1 H, dd, $^{2}J_{BA}$ = 15.0, $^{3}J_{BX}$ = 4.2, **H4$_B$**), 4.03 (1 H, dd, $^{3}J_{AX}$ = 7.5, $^{3}J_{BX}$ = 4.2, **H5$_X$**), 5.86 (1 H, dq, ^{3}J = 15.5, ^{3}J = 6.5, **H2**), 7.15 (1 H, dq, ^{3}J = 15.5, ^{4}J = 2.1, **H1**); ^{13}C-NMR (D_2O, δ [ppm], *J* [Hz]): 32.26 (s, **C4**), 53.24 (s, **C5**), 113.55 (q, **C1**), 122.78 (q, **C3**), 136.44 (q, **C2**), 171.70 (s, **C6**); ^{19}F-NMR (D_2O, δ [ppm], *J* [Hz]): -62.1 (3 F, dd, $^{3}J_{HF}$ = 6.5; $^{4}J_{HF}$ = 2.1, **F3**).

2.2.3.3 *N*-Acetyl-d_3-*S*-(3,3,3-trifluoro-*trans*-propenyl)-*L*-cysteine (22)

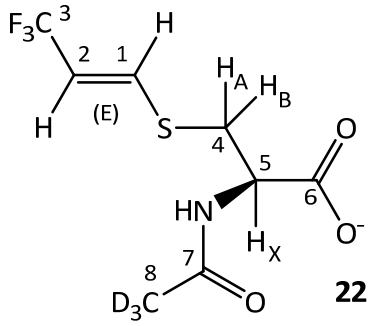

22

M_w = 260 g/mol

N-Acetyl-d_3-*S*-(3,3,3-trifluoro-*trans*-propenyl)-*L*-cysteine was synthesized by acetylation of approximately 1 mmol *S*-(3,3,3-trifluoro-*trans*-propenyl)-*L*-cysteine (20) with acetic anhydride-d_6 (Stoll and Seebeck, 1948).

Two diastereomers (E/Z) were obtained in a ratio of 10:3 based on ^{1}H-NMR analysis. The purity of the E/Z mixture was determined > 92% based on ^{1}H-NMR (DMSO-d_6, δ [ppm], *J* [Hz]): 3.09 (1 H, dd, $^{2}J_{AB}$ = 13.7, $^{3}J_{AX}$ = 8.3, **H4$_A$**), 3.26 (1 H, dd, $^{2}J_{BA}$ = 13.7, $^{3}J_{BX}$ = 5.0, **H4$_B$**), 4.44 (1 H, m, **H5$_X$**), 5.96 (1 H, dq, ^{3}J = 15.5, ^{3}J = 6.8, **H2**), 7.39 (1 H, dq, ^{3}J = 15.5, ^{4}J = 2.0, **H1**), 8.18 (1 H, d, ^{3}J = 8.0, N**H**). ^{13}C-NMR (DMSO-d_6, δ [ppm], *J* [Hz]): 21.69 (sept, **C8**), 33.50 (s, **C4**), 52.12 (s, **C5**), 110.28 (q, **C1**), 123.42 (q, **C3**), 139.71 (q, **C2**), 169.40 (s, **C7**), 171.76 (s, **C6**).

2.2.3.4 *S*-(3,3,3-Trifluoro-*trans*-propenyl)-glutathione (23)

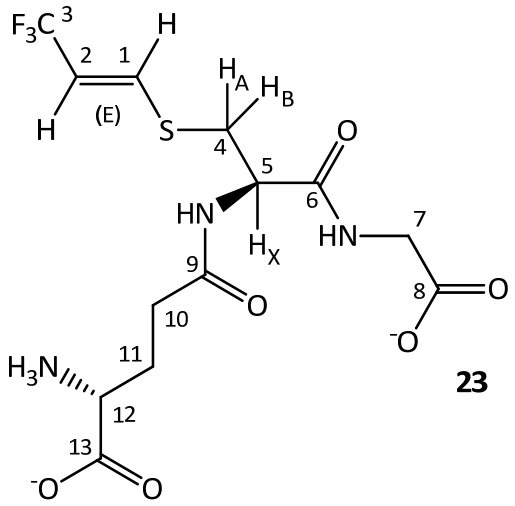

23

M_w = 401 g/mol

S-(3,3,3-Trifluoro-*trans*-propenyl)-glutathione was synthesized as described for *N*-acetyl-*S*-(3,3,3-trifluoro-*trans*-propenyl)-*L*-cysteine but adding 3 mmol *L*-glutathione to approximately 9 mmol sodium dissolved in liquefied ammonia. After the evaporation of remaining *trans*-HCFO-1233zd and ammonia, the crystalline residue was dissolved in water and acidified to pH 3 with 2 N hydrochloric acid. The formed precipitate was twice recrystallized from water with ethanol.

Two diastereomers were obtained (E/Z) in a ratio of approximately 1:1 based ^{1}H-NMR analysis. Purity of the E/Z mixture was determined > 95% based on ^{1}H-NMR (D_2O, δ [ppm], *J* [Hz]): 2.09 (2 H, m, **H11**), 2.47 (2 H, m, **H10**), 3.12 (1 H, dd, $^{2}J_{AB}$ = 14.4, $^{3}J_{AX}$ = 7.8, **H4$_A$**), 3.30 (1 H, dd, $^{2}J_{BA}$ = 14.4, $^{3}J_{BX}$ = 5.2, **H4$_B$**), 3.71 (1 H, t, ^{3}J = 6.6, **H12**), 3.87 (2 H, s, **H7**), 4.60 (1 H, dd, $^{3}J_{AX}$ = 7.9, $^{3}J_{BX}$ = 5.2, **H5$_X$**), 5.72 (1 H, dq, ^{3}J = 15.5, ^{3}J = 6.5, **H2**), 6.88 (1 H, dq, ^{3}J = 15.5, ^{4}J = 2.0, **H1**); ^{13}C-NMR (D_2O, δ [ppm], *J* [Hz]): 25.92 (s, **C11**), 31.18 (s, **C10**), 32.83 (s, **C4**), 41.72 (s, **C7**), 52.71 (s, **C5**), 53.80 (s, **C12**), 112.54 (q, **C1**), 123.20 (q, **C3**), 139.11 (q, **C2**), 171.78 (s, **C6**), 173.60 (s, **C9**), 173.79 (s, **C8**), 174.72 (s, **C13**); ^{19}F-NMR (D_2O, δ [ppm], *J* [Hz]): -62.0 (3 F, dd, $^{3}J_{HF}$ = 6.5, $^{4}J_{HF}$ = 2.1, **F3**).

2.3 Animals and treatment

2.3.1 Inhalation studies conducted with *trans*-HCFO-1233zd

Male Sprague Dawley (SD) rats (Harlan, Venray, Netherlands) and female New Zealand White (NZW) rabbits (Charles River, Sulzfeld, Germany) were used for all exposures. Animal weights ranged from 212 g to 244 g for male rats and from 2.4 kg to 2.8 kg for female rabbits. All animals were stabilized for at least 7 days and examined daily (general conditions, skin and fur, eyes, respiration, nose, oral cavity and external genitalia) during stabilization period to confirm suitability for the studies. Rats were housed in groups of five in Makrolon-IV cages (Bayer Makrolon, Leverkusen, Germany) and rabbits in single cages (Scanbur A/S, Karlslunde, Denmark). All animals had free access to water and standard diet (rat: Ssniff, Soest, Germany; rabbit: Altromin, Lage, Germany). Environmental conditions were set to standard conditions (12 hour light/dark cycle, room temperature 21-23 °C). Body weights and signs of toxic effects were recorded during treatment and post treatment period.

Study details will be described in the particular sections. SD rats were acclimatized to the metabolic cages 2 days before inhalation exposure. Urine was collected at approximately 12 hours before initiation of the inhalation exposure and for approximately 48 hours after exposure, at 6 and 12 hour intervals. Urine was collected at 4 °C and volume was measured for each collection interval. Blood samples were taken from rats approximately 12 hours before initiation of the inhalation exposure and 0, 24 and 48 hours after end of inhalation exposure (Fig. 9). All samples were stored at -20 °C until analysis.

Rats were sacrificed by CO_2 asphyxiation and cardiocentesis. Rabbits were sacrificed by injection of the α-2-receptor agonist xylazine hydrochloride followed by an injection of ketamine, a glutamate receptor (NMDAR) antagonist. All animal studies were performed under permit of the appropriate authorities in approved animal care facilities of the department.

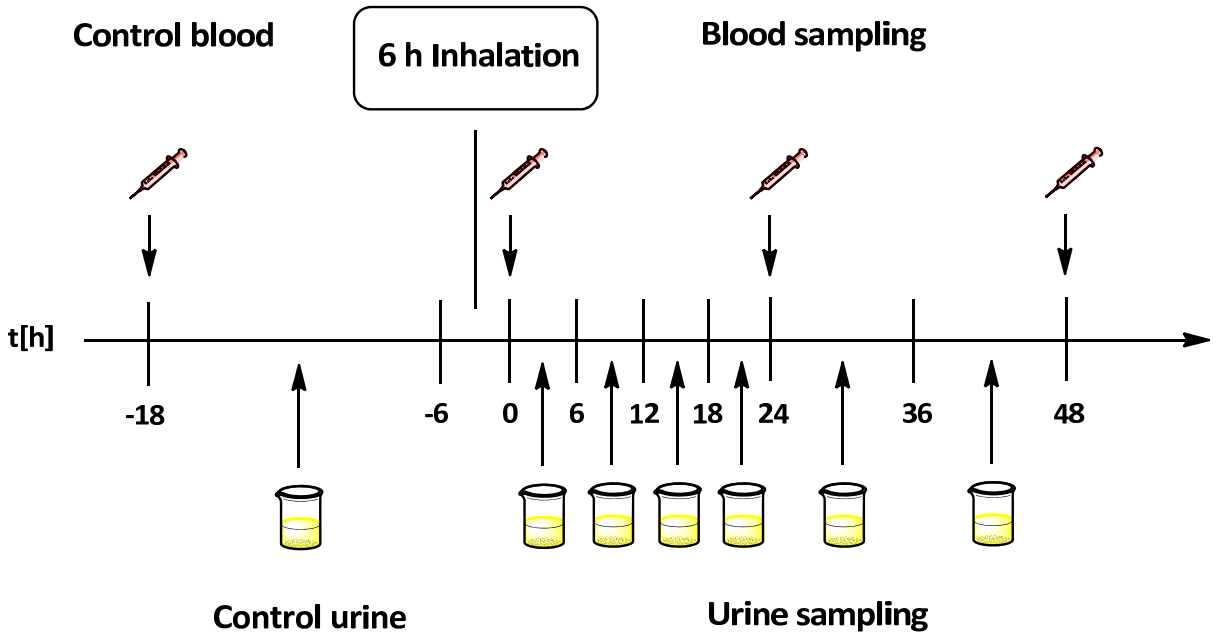

Fig. 9. Urine and blood sampling for *trans*-HCFO-1233zd inhalation exposures.

2.3.2 Inhalation studies conducted with HFO-1234yf by Huntingdon Life Sciences

Studies were conducted by Huntingdon Life Sciences (East Millstone, New Jersey, USA) under GLP conditions and the currently acceptable practice of animal husbandry was followed. All animals were stabilized for at least 5 days and examined during stabilization period to confirm suitability for the studies. Body weights and signs of toxic effects were recorded during treatment and post treatment period. Rabbits were sacrificed by phenobarbital injection. Study details will be described in the corresponding section.

2.3.2.1 Single high dose inhalation exposure of male, pregnant and non-pregnant female New Zealand White rabbits to HFO-1234yf

Male and female (pregnant and non-pregnant) NZW rabbits (Robinson Services, Inc., Mocksville, North Carolina, USA) were used for all exposures. Animal weights were determined as 3.0 kg on average (range 2.6 kg to 3.7 kg) for the male rabbits, 3.3 kg on average (range 3.0 kg to 3.5 kg) for non-pregnant female rabbits and 3.4 kg on average (range 3.1 kg to 3.7 kg) for presumed pregnant female rabbits at the initiation of dosing. Age at the receipt was approximately 5 to 6 months and the pregnant animals were on gestation day (GD) 2 where GD 0 was the day of mating.

Urine was collected at approximately 12 hours before initiation of the inhalation exposure and for approximately 48 hours after exposure, at approximately 12 hour intervals from 5 males/group, up to 6 pregnant females/group and 5 non-pregnant females/group (Fig. 10). Urine was collected in ice chilled containers and volume was measured for each interval. All samples were shipped on dry ice and stored at -20 °C until analysis.

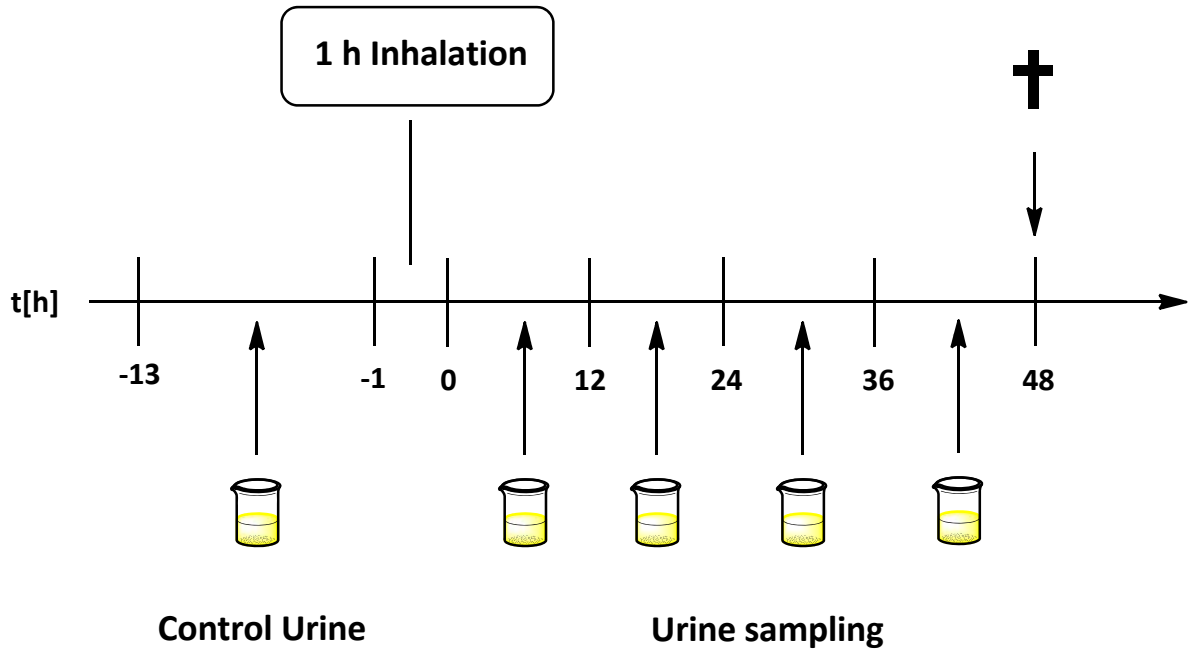

Fig. 10. Urine sampling for single high dose HFO-1234yf inhalation exposures.

2.3.2.2 Multiple inhalation exposure (28 days) of female and male New Zealand White rabbits to HFO-1234yf

Male and female NZW rabbits (Robinson Services, Inc., Mocksville, North Carolina) were used for all exposures. Animal weights ranged from 2.5 kg to 3.6 kg for male rabbits and from 2.8 kg to 3.8 kg for female rabbits.

Urine was collected in ice chilled containers for 18 hours after the final exposure (Fig. 11). Urine volumes were measured and samples obtained were then split into aliquots (approximately 10 mL), frozen in methanol/dry ice and stored at -20 °C until shipping. Blood for fluoride determination was collected into tubes with no anticoagulant at each necropsy (Fig. 11) via an auricular artery, was allowed to clot and was centrifuged to obtain serum. Samples were frozen in methanol and dry ice and stored at -20 °C until shipping. Liver (left lobe) and heart (section of the left ventricle) were obtained at each necropsy (Fig. 11), frozen in liquid nitrogen and stored at -80 °C until shipping. All samples were shipped on dry ice and stored at -20 °C or -80 °C until analysis.

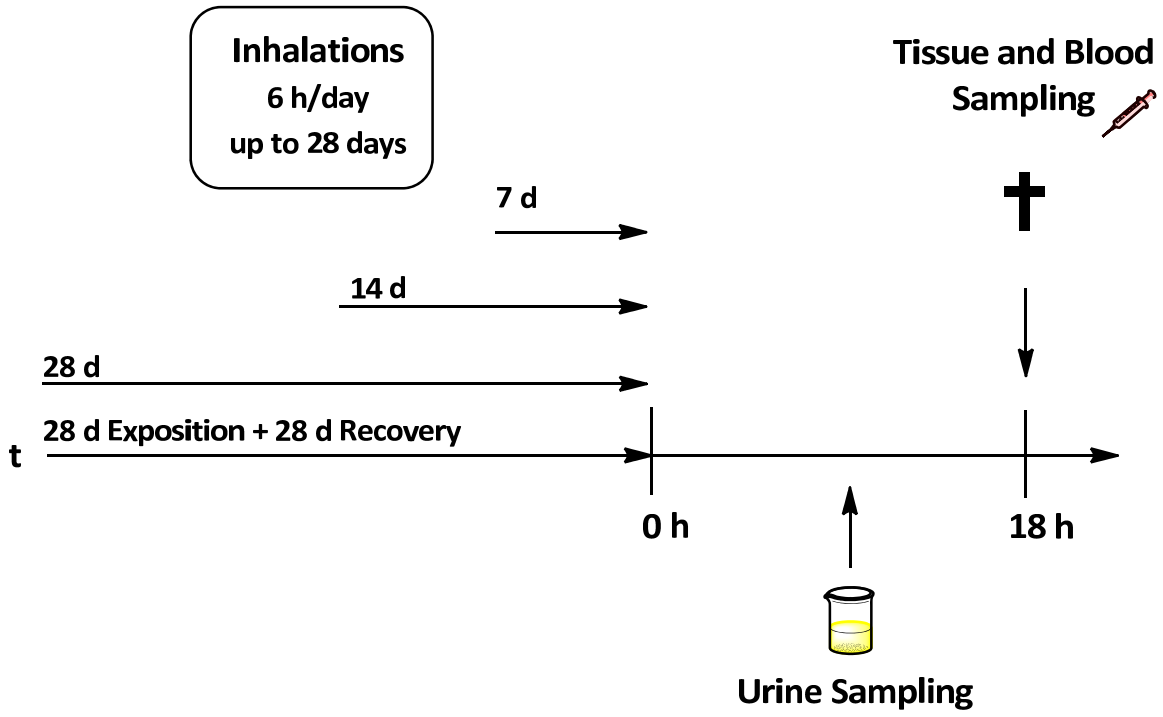

Fig. 11. Urine, blood and tissue sampling for multiple HFO-1234yf inhalation exposures.

2.4 *In vivo* studies

2.4.1 Inhalation exposures conducted with *trans*-HCFO-1233zd

Male rats (n = 5/concentration) and female rabbits (n = 3/concentration) were exposed to target concentrations of 0, 2,000, 5,000 and 10,000 ppm of *trans*-HCFO-1233zd for 6 hours in open dynamic exposure chambers (Fig. 12). Rats were exposed in a 20.6 L desiccator equipped with a magnetic fan to achieve exposure atmosphere homogeneity. Rabbits were exposed in a 360 L chamber with a base of 0.6 m^2, equipped with an electric fan and divided in equal compartments for animal separation. Exposure chambers were connected to compressed air, a cylinder of *trans*-HCFO-1233zd and gas flows were controlled by flow meters. Metered amounts of *trans*-HCFO-1233zd were mixed with air and fed into the exposure chamber. The generated test atmosphere was controlled by taking 100 µL samples with a gas-tight syringe every 15 minutes. Total gas flow provided at least 20 air changes per hour for rats and 1 air change per hour for rabbits.

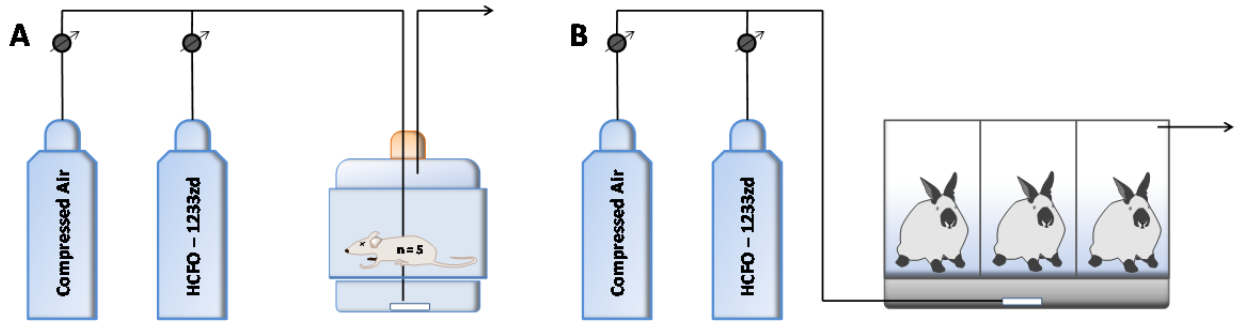

Fig. 12. Inhalation exposure of rats in 20.6 L desiccator (**A**) and rabbit in a 360 L chamber (**B**).

2.4.2 Studies conducted by Huntingdon Life Sciences with HFO-1234yf

2.4.2.1 Single high dose inhalation exposure of male, pregnant and non-pregnant female New Zealand White rabbits to HFO-1234yf

Non-pregnant female (n = 5/concentration), presumed pregnant female (n = 6/concentration; GD 12) and male (n = 5/concentration) NZW were exposed to target concentrations of 0, 50,000 and 100,000 of HFO-1234yf for 1 hour in open dynamic exposure chambers. Non-pregnant females were not exposed to 50,000 ppm because of available data from previous studies (Schuster, 2009; Schuster et al., 2010).

The whole-body exposure chambers (volume approximately 1 m^3) were operated at a minimum flow rate of 200 L/min. HFO-1234yf was metered into this air flow and thus diluted to the target exposure concentrations. These settings provided at least 12 air changes per hour. Chamber oxygen levels were measured every 30 minutes with an oxygen analyzer and maintained at a concentration of at least 19% (v/v) throughout each inhalation experiment. Determination of the exposure levels was made using a MIRAN® Ambient Air analyzer equipped with a strip chart recorder. The test atmosphere was monitored continuously and exposure levels were determined by comparison of the measured absorbance to a calibrated response curve.

2.4.2.2 Multiple inhalation exposure (28 days) of female and male New Zealand White rabbits to HFO-1234yf

Female and male NZW rabbits were exposed 6 hours a day for 7 days per week for 7, 14 or 28 consecutive days. Exposure levels were 0 (control), 500 (low dose), 1,000/1,500 (mid dose) and 4,500/5,500 (high dose) ppm. A recovery group was observed for at least 28 days after the last exposure of the 28 days exposure period (Table 2).

Due to unexpected deaths of two rabbits in the 7-day high dose exposure groups, exposure concentrations were changed. For rabbits of the 14-day exposures, the high dose exposure level was lowered to 4,500 ppm on day 8, with no exposure of high dose rabbits on day 7 in both 7- and 14-day exposure groups. Mid dose exposure levels were changed to 1,000 ppm

on day 8. No changes were made for low dose groups. Rabbits of the 28-day exposure groups were exposed to 0 (control), 500 (low dose), 1,000 (mid dose) and 4,500 (high dose) ppm for the whole 28 days. Whole-body exposures were performed as described under 2.4.2.1.

Table 2. Study design for multiple HFO-1234yf inhaltion exposures; exposure levels and number of animals; male (M), female (F).

Group	Exposure level [ppm]	Number of test animals									
		Total on study		Interim necropsy day 8		Interim necropsy day 15		Terminal necropsy day 29		Recovery necropsy day 59	
		M	F	M	F	M	F	M	F	M	F
1	0 (control)	25	25	5	5	5	5	10	10	5	5
2	500 (low dose)	25	25	5	5	5	5	10	10	5	5
3	1,000/1,500 (mid dose)	25	25	5	5	5	5	10	10	5	5
4	4,500/5,500 (high dose)	25	25	5	5	5	5	10	10	5	5

2.5 *In vitro* subcellular liver fraction incubations

2.5.1 Cytochrome P-450 2E1 induction in male Sprague Dawley rats

To induce cytochrome P-450 2E1, Sprague Dawley rats were treated with pyridine (100 mg/kg ip, dissolved in isotonic chloride solution) once daily for 5 days (Urban et al., 1994). Animals were fasted for 18 hours before sacrifice. Liver microsomes were prepared as described under 2.5.2 and cytochrome P-450 2E1 activity was determined as described under 2.5.4 (measured activity: 3.33 ± 0.05 nmol/min x mg (protein)).

2.5.2 Preparation of liver microsomes and protein determination

Microsomes were prepared according to standard protocols of the institute (SOP 21-A/2) (Herbst et al., 1994; Koster et al., 1994; Urban et al., 1994). 800 mg of liver tissue was homogenized with 2.5 mL of 0.154 M KCl solution pH 7.4 and then centrifuged at 10,000 x *g* and 4 °C for 10 minutes. The supernatant was centrifuged a second time at 40,000 x *g* and

4 °C for 1 hour. The resulting pellet was suspended in 10 mM phosphate buffer pH 7.4 and centrifuged once more at 40,000 x *g* and 4 °C for 1 hour. The cleaned pellet was suspended in 500 µL of 10 mM phosphate buffer pH 7.4 and aliquots were immediately frozen in liquid nitrogen. Microsomes were stored at -80 °C.

Microsomal protein concentration was determined with the DC™ assay kit from Biorad® and bovine serum albumin (BSA) as standard. The assay is an improved colorimetric method based on the method of Lowry (Lowry et al., 1951). The first step of the assay is the reaction of peptide bonds with Cu^{2+} ions resulting in a blue-violet complex (biuret reaction). In a second step Cu^{2+} is reduced to Cu^{1+} by peptide bond oxidation. The peptide-bound Cu^{1+} ions finally reduce added Folin-Ciocalteu (mixture of phosphomolybdate and phosphotungstate) reagent leading to blue color development that can be measured at 750 nm.

Before protein quantification, microsomal protein samples were diluted 1:50 with ice-cold 10 mM phosphate buffer pH 7.4. Calibration standards (range 0 to 1 mg/mL) were prepared by diluting the stock solution of BSA (1mg/mL) in the same buffer as for the samples. 20 µL of standards or samples were added to 100 µl of reagent A and vortexed. After adding 800 µL of reagent B, samples and standards were vortexed and incubated for 15 minutes at room temperature. The developed blue color is stable for at least one hour and the absorbance was determined at 750 nm using a UV-Vis spectrometer. Protein concentrations were determined by the linear equation obtained for the measured standards.

2.5.3 *In vitro* incubations for biotransformation analysis

To study biotransformation of *trans*-HCFO-1233zd *in vitro*, pooled human liver microsomes (Becton Dickinson, Heidelberg, Germany), rabbit liver S9 (Becton Dickinson, Heidelberg, Germany), or rat liver microsomes from pyridine-induced male rats (3 mg protein/mL) were incubated in sealed GC vials with either 10 mM glutathione or a NADPH regenerating system (10 mM nicotinamide adenine dinucleotide phosphate (NADP), 10 mM glucose-6-phosphate and 0.25 units/ml glucose-6-phosphate dehydrogenase) or 10 mM glutathione and a regenerating system in potassium phosphate buffer pH 7.4 containing 1 mM EDTA (final volume of 1 mL). Liquid *trans*-HCFO-1233zd (20 µL) was added through a septum with a microsyringe and the incubations were performed for up to 12 hours at 37 °C. Reactions were stopped by placing the opened GC vials on ice.

For *in vitro* kinetic experiments either pooled human, male rat, or female rabbit S9 liver fractions (4 mg protein/mL) were pre-incubated with 10 mM glutathione in 100 mM potassium phosphate buffer pH 7.4 containing 1 mM EDTA (end volume 0.5 mL) in sealed GC vials for 5 minutes at 37 °C. Reaction mixtures were incubated for another 30 minutes, after adding gaseous *trans*-HCFO-1233zd (100, 250, 500, 750, 1,000 or 2,000 µL) through the septum with a gastight microliter syringe. Reactions were stopped by placing the opened GC vials on ice and adding 50 µL of acetonitrile.

2.5.4 Cytochrome P-450 2E1 activity

This assay is based on the specific hydroxylation of p-nitrophenol to p-nitrocatechol by cytochrome P-450 2E1 (conducted according to internal SOP 89-S/3). The latter can be quantified by UV/Vis spectroscopy (Fig. 13).

Liver microsomes (end-concentration 2 mg protein/mL) were pre-incubated with 45 µL of a NADPH regenerating system, containing 20 µL of a 200 mM glucose-6-phosphate solution, 20 µL of a 50 mM NADP solution and 5 µl of a 0.1 Units/µl glucose-6-phosphate-deydrogynase stock solution for 3 minutes at 37 °C. Following 250 µL of a 450 µM p-nitrophenol solution was added and the incubation mixture was filled up to 1 mL with 100 mM phosphate buffer pH 6.8. The mixture was incubated for another 20 minutes and stopped by adding 40 µL of 43% perchloric acid.

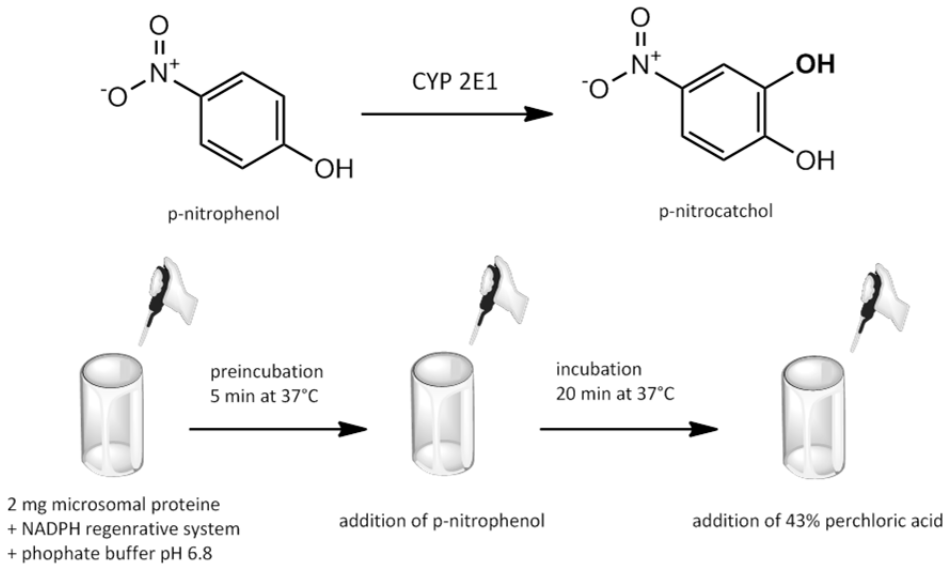

Fig. 13. Cytochrome P-450 2E1 activity assay.

After centrifugation at 20,000 x *g*, 700 µL of the supernatant obtained was mixed with 70 µl of 10 M NaOH and measured three times at a wavelength of 510 nm. Calibration standards were worked up and measured as described before but adding known concentrations of p-nitrocatechol instead of p-nitrophenol (Table 3). p-Nitrocatechol concentrations were determined by the linear equation obtained for the measured standards. The R^2-values of the calibration curves were > 0.99.

Table 3. Concentrations of calibration standards used for the quantification of p-nitrocatechol.

Calibration standard	p-Nitrocatechol concentration	
	[µg/mL]	[nmol/mL]
1	0.00	0.00
2	12.21	78.75
3	8.72	56.25
4	5.23	33.75
5	1.74	11.25
6	1.05	6.75
7	0.87	5.63

2.5.5 Cytochrome P-450 3A4 activity

Testosterone is hydroxylated by cytochrome P-450 3A4 specifically in 6-ß position. In this assay (conducted according to internal SOP 85-S/2) testosterone is incubated with liver microsomes in phosphate buffer pH 7.4 together with a NADPH regenerating system. The amount of 6-ß-hydroxy-testosterone formed is determined by HPLC/UV-Vis analysis (Fig. 14).

Liver microsomes (end-concentration 1 mg protein/mL) were pre-incubated with 22.5 µL of NADPH regenerating system, containing 10 µL of a 200 mM glucose-6-phosphate solution, 10 µL of a 50 mM NADP solution and 2.5 µL of a of a 0.1 Units/µl glucose-6-phosphate-deydrogynase stock solution in 100 mM phosphate buffer pH 7.4 (final incubation volume 500 µL) at 37 °C for 5 minutes. Testosterone (end-concentration 0.2 mM) was added and the mixture was incubated for another 10 minutes at 4 °C. To stop the reaction, 500 µl methanol was added and the mixture was centrifuged at 20,000 x *g*. The supernatant was evaporated and the residue was dissolved in 200 µL of 100 mM phosphate buffer pH 7.4 Calibration curves were prepared by spiking 6-ß-hydroxy-testosterone standards in incubation matrix (Table 4), prepared as described before, but adding methanol already before starting the incubation.

Table 4. Concentrations of calibration standards used for the quantifiction of 6-ß-hydroxy-testosterone.

Calibration standard	6-ß-Hydroxy-testosterone concentration	
	[µg/mL]	[nmol/mL]
1	0.00	0.00
2	30.44	100.00
3	15.22	50.00
4	7.61	25.00
5	4.56	15.00
6	3.04	10.00
7	1.52	5.00

For HPLC analysis (HP 1090, Agilent, Waldbronn, Germany), 50 µL of the sample or standard solutions were injected. Quantification was performed with a Hypersil ODS 3 column (250 x 4.6 mm, 5 µm, Bischoff Chromatography, Leonberg, Germany), a solvent flow rate of 1 mL/min with gradient elution and a detection wavelength of 242 nm. Mobile phases were 0.1% formic acid in H_2O (A) and 0.1% formic acid in MeOH (B). The gradient was set up as follows: increase of 40% to 95% solvent B within 20 minutes and further to 100% in 2 minutes; 100% solvent B is held for 5 minutes before decreasing back to 40%. 6-ß-Hydroxy-testosterone concentrations were determined by the linear equation obtained for the measured standards. R^2-values of all calibration curves were > 0.99.

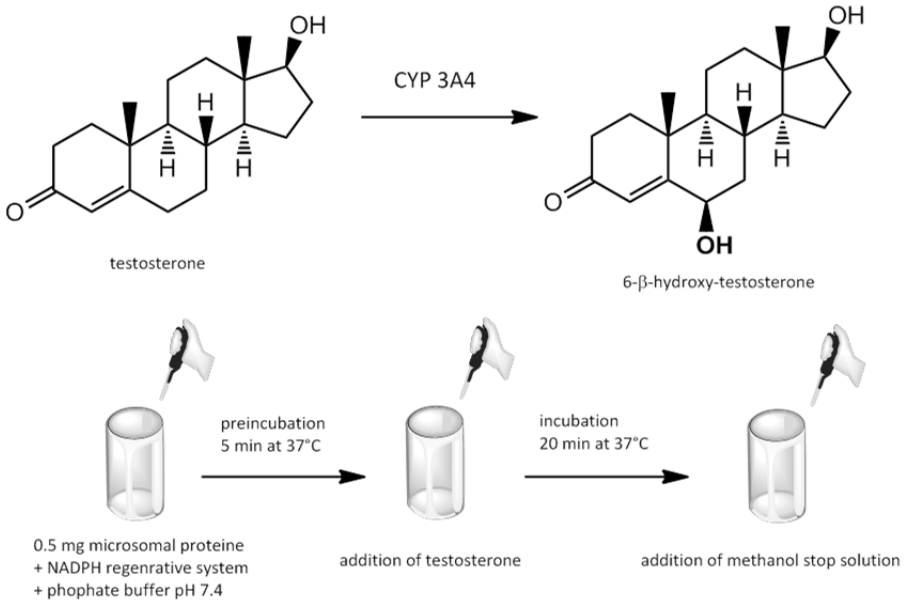

Fig. 14. Cytochrome P-450 3A4 activity assay.

2.6 Instrumental analysis

2.6.1 Development of LC-MS/MS and GC/MS methods according to IUPAC

Method development followed international standards of the *International Union Of Pure And Applied Chemistry* (IUPAC) (Leiterer, 2008; Thompson et al., 2002; Wellmitz and Gluschke, 2005). Due to single laboratory use, all methods were not evaluated regarding their reproducibility, robustness and uncertainty of measurement. Despite, the linearity, accuracy, precision (repeatability) and the limit of detection (LOD) and limit of quantification (LOQ) were evaluated for all metabolite quantifications.

Therefore calibration curve standards in blank matrix were separately diluted at least twice for each quantification and LOD/LOQ were determined according to DIN 32645 (calibration curve method with equidistant standards). Calculations were performed with DINTEST (Institut für Rechtmedizin und Verkehrsmedizin, Universität Heidelberg, Version 2004 DE). All calibration curves standards achieved an accuracy of ± 15%. For repeatability, all samples were worked up and analyzed twice (except chamber atmosphere samples). For quality control (accuracy, specificity), samples with known concentrations as well as blank matrix samples were included in all metabolite quantifications. If calibration curves standards were not prepared in blank matrix (fluoride quantification) the recovery of the method was determined by quantification of samples of known concentrations within the linear range of the calibration curve (three with low, three with mid and three with high fluoride concentrations; twice separate analysis).

For metabolite identification, specificity was ensured by the measurement of blank and standard samples in matrix. Moreover, the LOD was either determined by the calibration curve method (DIN 32645) or the evaluation of signal to noise (> 3).

Achieved values of the validation parameters are stated in the specific sections.

2.6.2 ^{19}F-NMR spectroscopy - trace analysis

^{19}F-NMR spectra were recorded with a Bruker DRX 300 NMR spectrometer with a 5 mm fluoride probe operating at 282.404 MHz (Bruker Biospin GmbH, Rheinstetten). ^{19}F-chemical shifts were referenced to external $CFCl_3$. Spectra were recorded with a 30° pulse, a pulse length of 13.6 µsec and a cycle delay of 6 µsec. The acquisition time was 3 sec and 10,240 scans were recorded. The ^{19}F-spectra were acquired with proton coupling and a spectral width of 200 ppm (+10 to -190 ppm). Before integration of peak areas, an accurate baseline correction and spectra phasing was performed between chemical shifts of -60 and -85 ppm.

One heart extract sample was measured with a Bruker AV-III 500 NMR spectrometer operating at 470.799 MHz, equipped with a 5 mm fluoride probe (Bruker, BBFO) and coupled with a cryo platform working at 15 K (Bruker, CPBBO swi) at the NMR lab of Bruker GmbH, Rheinstetten. Spectra were recorded with a 90° pulse, a pulse length of 16.1 µsec and a cycle delay 6.5 µsec. Acquisition time was 0.35 sec and 10,240 scans were recorded. ^{19}F-spectra were acquired with proton coupling and a spectral width of 200 ppm (+10 to -190 ppm).

Sample preparation for ^{19}F-NMR analysis: After thawing at 4 °C, urine samples (1mL) were vortexed and then centrifuged for 15 minutes at 20,000 x *g* and at 4 °C. Aliquots (720 µL) of the obtained supernatants were added to 80 µL of deuterium oxide. Heart tissue (200 mg of the left ventricle) was homogenized in a glass potter with 800 µL of 100 mM phosphate buffer pH 6.8. The mixture was vortexed for 10 minutes and centrifuged at 20,000 x *g* at 4 °C for 15 minutes. For further purification the supernatant was filtered through a 0.2 µm filter (Whatman®, Dassel, Germany) and 720 µL of the filtrate were added to 80 µL of deuterium oxide.

NMR spectra were analyzed with TopSpin 3.0 (Bruker Biospin. GmbH, Rheinstetten) and *trans*-HCFO-1233zd/HFO-1234yf metabolites were identified by comparison of their chemical shifts, multiplicities and coupling constants with standard spectra of HFO-1234yf metabolites already available of previous studies (Schuster, 2009; Schuster et al., 2008; Schuster et al., 2010) and standard spectra of *trans*-HCFO1233zd metabolites purchased or synthesized (Table 5). LOD (S/N > 3) for monofluoroacetate and monofluorocitrate was 10 ppm (Bruker DRX 300 NMR spectrometer).

Table 5. ^{19}F-NMR data of relevant compounds (dissolved in D_2O).

Compound	Chemical shift [ppm]	Multiplicity	^{1}H -^{19}F Coupling constants [Hz]
S-(3,3,3-Trifluoro-*trans*-propenyl)-mercaptolactic acid	-61.7	dd	$^{3}J_{HF}$ = 6.6; $^{4}J_{HF}$ = 2.1
N-Acetyl-*S*-(3,3,3-trifluoro-*trans*-propenyl)-*L*-cysteine	-61.8	dd	$^{3}J_{HF}$ = 6.5; $^{4}J_{HF}$ = 2.1
S-(3,3,3-Trifluoro-*trans*-propenyl)-*L*-glutathione	-62.0	dd	$^{3}J_{HF}$ = 6.5; $^{4}J_{HF}$ = 2.1
trans-1-Chloro-3,3,3-trifluoropropene (*trans*-HCFO-1233zd)	-63.2	dd	$^{3}J_{HF}$ = 6.6, $^{4}J_{HF}$ = 2.2
S-(3,3,3-Trifluoro-*trans*-propenyl)-*L*-cysteine	-62.1	dd	$^{3}J_{HF}$ = 6.5; $^{4}J_{HF}$ = 2.1
3,3,3-Trifluoropropionic acid*	-63.5	t	$^{3}J_{HF}$ = 11.4
3,3,3-Trifluoro-1-propanol*	-64.3	t	$^{3}J_{HF}$ = 11.2
3,3,3-Trifluorolactic acid	-75.3	d	$^{3}J_{HF}$ = 8.2
Trifluoroacetic acid*	-75.4	s	-
3,3,3-Trifluoro-1,2-propanediol	-77.2	d	$^{3}J_{HF}$ = 7.4
N-Acetyl-*S*-(3,3,3-trifluoro-2-hydroxypropanyl)-*L*-cysteine	-78.7	d	$^{3}J_{HF}$ = 6.6
N-Acetyl-*S*-(3,3,3-trifluoro-2-hydroxypropanyl)-mercaptolactic acid*	-78.9	d	$^{3}J_{HF}$ = 6.9
3,3,3-Trifluoro-1-hydroxyacetone*	-83.4	s	-
1,1,1-Trifluoroacetone*	-86.4	s	-
Monofluorocitrate	-200.6	d	$^{3}J_{HF}$ = 48.0
Monofluoroacetate	-216.9	t	$^{3}J_{HF}$ = 48.3

*standard compounds measured by Schuster (Schuster, 2009; Schuster et al., 2008; Schuster et al., 2010)

2.6.3 Mass spectrometry

2.6.3.1 Mass spectrometry coupled with liquid chromatography (LC)

LC-MS/MS analyses were performed with an API 3000 mass spectrometer (Applied Biosystems, Darmstadt, Germany) or an API/Q-Trap 2000 mass spectrometer (Applied Biosystems-MDS Sciex, Darmstadt, Germany) both coupled to an Agilent 1100 HPLC-pump equipped with an Agilent 1100 autosampler (Agilent, Waldbronn, Germany). Both mass spectrometers were set to a vaporizer temperature of 400 °C and a TurboIon® Spray voltage of -4.0 kV. Spectral data were recorded with nitrogen as collision gas (CAD [collisionally activated dissociation] = 4 or 9). Further instrument settings will be described in the corresponding sections.

Sample preparation for LC-MS/MS analysis: Before analysis, frozen urine samples were thawed at 4 °C. Urine aliquots (1 mL) or incubation solutions were vortexed and then centrifuged for 15 minutes at 20,000 x *g* and 4 °C.

Plasma (20 µL) was added to 40 µL of methanol. After keeping samples on ice for 30 minutes followed by centrifugation (20,000 x *g*, 4 °C, 10 min), obtained supernatants were mixed with 40 µL of acetonitrile and subjected to a second centrifugation at 20,000 x *g* (4 °C, 10 min).

Urine and plasma supernatants obtained were diluted with water (1:10). If sample values were outside the linear range of the calibration curve, an additional 10- or 100-fold dilution was performed.

2.6.3.2 Mass spectrometry coupled with gas chromatography (GC)

GC/MS analyses were performed with an Agilent 5973 mass spectrometer, equipped with an electron impacted ionizer, coupled to an Agilent 6890 GC (Agilent, Santa Clara, United States). Analytical columns were either a HP-Plot Q column (30 m x 0.32 mm i.d., 20 µm film thickness; Agilent, Santa Clara, United States) or an Agilent DB-WAX capillary column (30m x 0.25 mm i.d., 25 µm film thickness; Agilent, Santa Clara, United States). Helium served as carrier gas and mass spectrometer temperatures were set as follows: interface 270 °C, ion source 250 °C and quadrupole 150 °C. The dwell time was 100 ms for all experiments. Further instrument settings will be described in the particular sections. For sample injection, gas-tight syringes (volumes 10, 100 and 1,000 µL) were used (Hamilton Bonaduz AG, Bonaduz, Switzerland) and gas was diluted with gas-tight 1 L Tedlar® sampling bags (Supelco, Bellefonte, Pennsylvania, USA).

2.6.4 Potentiometric quantification of inorganic fluoride

Urine and serum were analyzed using a fluoride selective electrode (Einstabmesskette F800 of WTW, Weilheim, Germany) coupled with a potentiometer (WTW, Weilheim, Germany).

Urine and serum samples (1 mL) were thawed, vortexed and centrifuged. The supernatants were diluted with 1 mL of total ionic strength adjustment buffer (TISAB) (containing 29 g NaCl, 2.2 g 1,2-diaminocyclohexanetetraacetic acid monohydrate, 28.5 mL of acetic acid per liter H_2O; pH adjustment by NaOH to pH 5.0-5.5) and directly measured without any further work up. All samples were measured with the fluoride selective electrode till a constant mV value was obtained. Every sample was measured twice and mean values were used for further calculation. Calibration standards were freshly prepared every day by dissolving known amounts of NaF in Millipore® water (Table 6). Work-up and measurement of calibration standards was carried out as described for the samples.

The applied method was linear within the range of the calibration curves (R^2-value range, 0.995 - 0.999). Deviations between repeatedly measured samples were calculated as 1.2 ± 1.5% for serum and 1.2 ± 1.9% for urine analysis. The overall fluoride recovery was determined as 101.8 ± 2.4% for serum samples and 99.5 ± 2.0% for urine samples.

Table 6. Concentrations of the calibration standards used for the quantification of inorganic fluoride in rabbit serum and urine.

Calibration standard	Inorganic fluoride concentration [ppm]	
	Urine	Serum
1	0.10	0.10
2	0.25	0.25
3	0.50	0.50
4	0.75	0.75
5	1.00	1.00
6	5.00	-
7	10.00	-

2.7 Qualitative analysis by mass spectrometry

2.7.1 Qualitative analysis by GC-MS

2.7.1.1 Determination of 1,1,1-trifluoroacetone

1,1,1-Trifluoroacetone was identified following a previous publication (Schuster et al., 2008) by GC/MS using a HP Q-Plot column. Head-space samples (1,000 µL) taken with a warmed syringe from 200 µL urine samples heated to 30 °C for 30 minutes were injected splitless. The linear temperature gradient was run from 100 °C to 170 °C with heating rate of 10 °C/min and helium flow of 2 mL/min. The inlet temperature was set to 100 °C. The characteristic mass fragments of 1,1,1-trifluoroacetone (m/z 69 and 43) eluted after 4.2 minutes. The LOD was determined as 2 nmol/mL (S/N > 3).

2.7.1.2 Determination of trifluoroacetic acid and 3,3,3-trifluoropropionic acid

Trifluoroacetic acid was determined after esterification with methanol. For this purpose, 200 µL of urine was added to 80 µL of 0.1 N NaOH and samples were taken to dryness in an evacuated desiccator containing anhydrous P_2O_5. 100 µL of methanol and sulfuric acid (97%) was added to the dried residue and heated in a gas tight GC vial at 80 °C for 1 hour. For analysis, head-space samples (500 µL) were removed with a warmed syringe.

Samples were separated on a HP Q-Plot column using a linear temperature program, after initially holding 100 °C for 1 minute, from 100 °C to 220 °C with a heating rate of 15 °C/min and an inlet temperature of 250 °C. The helium flow rate was set to 2 mL/min and injection was performed with split ratio of 5:1. Trifluoroacetic acid was eluted after 4.6 minutes (m/z 69 and 59) and 3,3,3-trifluoropropionic acid (m/z 142, 111, 83 and 69) after 7.5 minutes.

2.7.1.3 Determination of 3,3,3-trifluoro-1,2-propanediol

3,3,3-Trifluoro-1,2-propanediol was determined as published previously (Schuster et al., 2008). Urine samples (500 µL) were extracted with 100 µL dichloromethane three times, the organic phases were combined and dried under a gentle stream of nitrogen. The residue was dissolved in 40 µL dichloromethane and 1 µl samples were analyzed by GC/MS using a DB-WAX column. The linear temperature gradient was run from 40 °C to 220 °C with heating rate of 10 °C/min, a helium flow of 2 mL/min and an inlet temperature of 100 °C. The characteristic mass fragments of 3,3,3-trifluoro-1,2-propanediol (m/z 80 and 69) eluted after 9.6 minutes.

2.7.1.4 Determination of 3,3,3-trifluoro-1-propanol

3,3,3-Trifluoro-1-propanol was detected by heating 200 µl of urine at 85 °C for 30 minutes. A 1 mL headspace sample was injected splitless on a HP-Plot Q column with a carrier gas flow rate of 2 mL/min. Oven temperature was kept at 40 °C for 1 minute, followed by an increase

to 160 °C within 8 minutes and holding the final temperature for 1 minute. Inlet temperature was set to 100 °C. The intensities of m/z 95, 69 were recorded during analysis. 3,3,3-Trifluoro-1-propanol eluted at 9.1 minutes. The LOD was determined as 10 nmol/mL (S/N >3).

2.7.1.5 Determination of 3,3,3-trifluoro-2-propanol

3,3,3-Trifluoro-2-propanol was determined on a HP Q-Plot column. 500 µL urine samples were heated to 85 °C for 1 hour and 500 µL head-space samples were withdrawn with a warmed syringe. The linear temperature program was set from 40 °C (held for 1 minute) to 160 °C with a heating rate of 15 °C/min, a helium flow of 2mL/min and an inlet temperature set to 100 °C. The characteristic mass fragments of 3,3,3-trifluoro-2-propanol (m/z 99, 69, 45) eluted after 8.2 minutes. The LOD was determined as 9 nmol/mL (S/N >3).

2.7.2 Qualitative analysis by LC-MS/MS

2.7.2.1 Determination of monofluoroacetate in heart tissue

For sample preparation, 200 mg of the left heart ventricle was homogenized with 1 mL of 25 mM ammonium acetate buffer pH 4.2 in a glass potter. The homogenate was centrifuged at 15,000 rpm and 4 °C for 15 minutes and the resulting supernatant was further processed by SPE extraction (Strata X-AW 30mg, Phenomenex, Aschaffenburg, Germany). Before samples were loaded on the SPE column, it was conditioned with 1 mL of methanol and 1 mL of water pH 4.2. Further, 1 mL of a 25 mM ammonium acetate pH 4.2 buffer was applied as washing solution and monofluoroacetate was eluted by adding 1 mL of 2% ammonium hydroxide. The eluate was evaporated under a gentle stream of nitrogen and the residue was dissolved in 50 µl of 0.1% formic acid. For further purification, the solution was centrifuged twice at 20,000 x *g* and 4 °C for 15 minutes.

Heart extracts were separated on a Synergi Polar RP column (2 x 150 mm; 4 µm; Phenomenex, Aschaffenburg, Germany). Separation was performed by isocratic elution with water containing 0.1% formic acid (solvent A) and acetonitrile (solvent B) using the following conditions: 98% A, 2% B for 8 minutes at a flow rate of 200 µL/min. Characteristic mass transitions for monofluoroacetate monitored during the separation are listed in Table 7. Achieved limit of detection in heart tissue was 0.01 ppm monofluoroacetate (S/N >3).

2.7.2.2 Determination of *S*-(3,3,3-trifluoro-*trans*-propenyl)-mercaptolactic acid

S-(3,3,3-Trifluoro-*trans*-propenyl)-mercaptolactic acid was identified by LC-MS/MS. Urine samples were separated on a Reprosil Pur C18 AQ column (2 x 150 mm, 5µm; Maisch, Ammerbuch, Germany) using gradient elution with 0.1% formic acid in methanol and 0.1% formic acid in water at a flow rate of 200 µL/min. Methanol content of the mobile phase was increased from 10% to 90% within 30 minutes and hold for further 2 minutes. Characteristic mass transitions monitored during the separation are listed in Table 7.

2.7.2.3 Determination of *S*-(3,3,3-trifluoro-*trans*-propenyl)-*L*-cysteine

S-(3,3,3-trifluoro-*trans*-propenyl)-*L*-cysteine was identified as described for *S*-(3,3,3-trifluoro-*trans*-propenly)-mercaptolactic acid. Characteristic mass transitions monitored during the separation are listed in Table 7.

Table 7. Mass spectrometric parameters settings (MS-MS-transitions, declustering potential and collision energy) used for metabolite identification.

Compound	Transition [m/z]	Declustering potential [V]	Collision energy [V]	Retention time [min]	Mass spectrometer device
Monofluoroacetate	77 → 77 77 → 57	-35 -30	-16 -17	2.4	API 3000
S-(3,3,3-Trifluoro-*trans*-propenly)-mercaptolactic acid	215 → 127 215 → 107	-50	-30	20.3-20.5	API/Q-Trap 2000
S-(3,3,3-Trifluoro-*trans*-propenly)-*L*-cysteine	214 → 127 214 → 107	-26	-20	8.8	API/Q-Trap 2000

2.7.2.4 Screening for unknown metabolites

Screening for unknown urinary metabolites was done by LC-MS/MS analysis on a Reprosil Pur C18 AQ column (2 x 150 mm, 5µm; Maisch, Ammerbuch, Germany) using gradient elution with 0.1% formic acid in ACN or methanol and 0.1% formic acid in water at a flow rate of 200 µL/min. Organic mobile phase content was increased from 10% to 90% within 30 minutes and held for further 2 minutes. Mass spectrometer (API/Q-Trap 2000 - Applied Biosystems-MDS Sciex, Darmstadt, Germany) parameters were set to -50 V for declustering potential, -10 V for entrance potential and either -20 V, -30 V or -40 V for collision energy. Scans were performed with negative ionization either in the EMS (enhanced mass spectrometry)/EPI (enhanced product ion), the CNL (constant neutral loss)/EPI (Table 8) or the sensitive MRM (multiple reaction monitoring)/EPI mode respectively, monitoring transitions of conceivable metabolites.

Table 8. Constant neutral loss(CNL) of metabolic conjugation compounds and hydrogen fluoride.

Compound	CNL [Da]	Reference
Hydrogen fluoride	20	(Schuster, 2009)
Glycine	73	(Schmidt et al., 1995)
Sulfate	80	(Lenz et al., 2005; Xia et al., 2003)
Mercaptopyruvic acid	86	-
Cysteine	87	(Schmidt et al., 1995)
Mercaptolactic acid	88	-
Mercapturic acid/glutathione	129	(Mutlib et al., 2005; Wagner et al., 2006)
Glucuronide	176	(Xia et al., 2003)

The used API/Q-Trap 2000 is a hybrid quadrupole linear ion trap mass spectrometer (QqLIT) offering various operation modes. Specific scan functions used in this study are illustrated in Fig. 15. Generally, tandem mass spectrometers consist of three quadrupoles (Q1, Q2, Q3) with Q1 and Q3 serving as mass filters and Q2 serving as collision cell for fragment ion formation by collision with gas molecules (i.e. nitrogen). For multiple reaction monitoring (MRM) Q1 filters selected masses that subsequently fragment into product ions in Q2. The resulting daughter ions get specifically filtered by Q3. A constant neutral loss, induced by gas collision in Q2, can be analyzed if Q1 and Q3 both scan but with a constant difference between the two scan ranges.

In novel hybrid mass spectrometers, Q3 can also operate as a linear ion trap (LIT). This technique is used in the enhanced mass spectrometry scan mode (EMS) with Q1 and Q2 not operating and ions of a specific m/z rage are trapped and scanned in Q3. Furthermore, hybrid mass spectrometers can switch between the operation modes. By this, scan combinations of triple quadrupole mode and trap mode can be combined in the same run (Hopfgartner et al., 2004). If Q3 operates as a LIT, specific ions can be collected in Q3, additionally fragmented and scanned (enhanced product ion scan, EPI). A combination of specific survey scans, such as EMS, MRM or CNL, with an EPI scan as dependent scan enables an improved characterization of unknown structures or the possibility to confirm known analytes. To increase sensitivity of combined scan modes, the signal intensity of the first experiment (EMS, CNL, MRM) can be set to a specific abundance value, and, only in case of accordance with this criterion, an enhanced product ion scan is performed (information dependent acquisition - IDA).

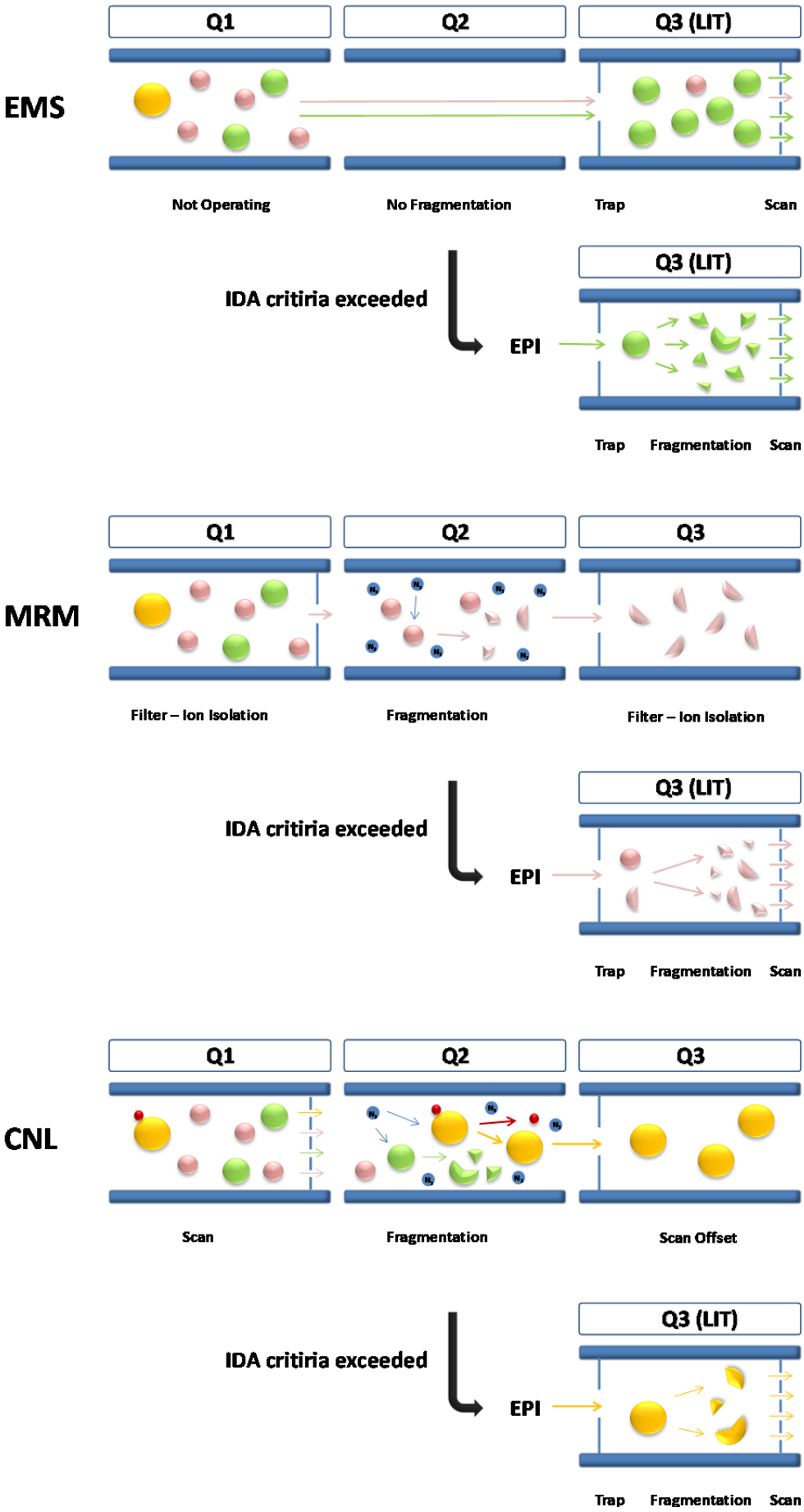

Fig. 15. Mass spectrometer scanning modes; EMS, enhanced mass spectrometry; MRM, multiple reaction monitoring; CNL, constant neutral loss; EPI, enhanced product ion.

2.8 Quantification by mass spectrometry

2.8.1 Quantification by GC-MS

2.8.1.1 Quantification of *trans*-HCFO-1233zd

trans-HCFO-1233zd chamber concentrations were determined by GC/MS (HP-Plot Q column). Chamber air samples (100 µL) were injected (split 5:1). The oven temperature was increased from 60 to 180 °C within 7 minutes, the inlet temperature was set to 100 °C and characteristic mass fragment were recorded (*trans*-HCFO-1233zd, 95 [m/z], R_t = 7.7 min; internal standard – oxygen, 32 [m/z], R_t = 1.8 min). Quantification of *trans*-HCFO-1233zd was based on calibration curves of air samples containing known amounts of *trans*-HCFO-1233zd (Table 9).

The method was linear within the concentration ranges of the different calibration curves (R^2-value range, 0.995 - 0.999). The deviation of quality controls from their nominal concentration was determined as 5.7 ± 3.0%.

Table 9. Concentrations of the calibration standards used for the determination of *trans*-HCFO-1233zd chamber concentrations.

Calibration standard	*trans*-HCFO-1233zd concentration [ppm]		
	2,000 ppm exposure	5,000 ppm exposure	10,000 ppm exposure
1	500	1,248	2,494
2	999	2,494	4,975
3	1,996	4,975	9,901
4	2,991	7,444	14,778
5	3,984	9,901	19,608

2.8.2 Quantification by LC-MS/MS

2.8.2.1 Quantification of *N*-acetyl-*S*-(3,3,3-trifluoro-2-hydroxypropanyl)-*L*-cysteine

Diluted urine samples (10 µL) were added to 90 µL of a 500 pg/µL internal standard solution (*N*-acetyl-*S*-(2-chloro-1,1,2-trifluoroethyl)-*L*-cysteine), vortexed, transferred into glass autosampler vials, sealed and aliquots (10 µL) were analyzed. Samples were separated on a Reprosil Pur C18 AQ column (2 mm x 150 mm; 5 µm; Maisch, Ammerbuch, Germany). Separation was performed by gradient elution with water containing 0.1% formic acid

(solvent A) and acetonitrile (solvent B) using the following conditions: 98% A, 2% B, isocratic for 1 minute, linear increase to 90% B within 5 minutes, followed by 90% B for 5 minutes, at a flow rate of 300 µL/min. Mass spectrometer parameters are listed in Table 14. Quantification was based on calibration curves of urine samples spiked with known amounts of *N*-acetyl-*S*-(3,3,3-trifluoro-2-hydroxypropanyl)-*L*-cysteine (Table 10).

The method was linear within the concentration range of the calibration curve (R^2-value range, 0.998 - 0.999). The LOQ (calculated according to DIN 32645) for *N*-acetyl-*S*-(3,3,3-trifluoro-2-hydroxypropanyl)-*L*-cysteine ranged from 0.20 to 0.45 µg/L (0.72 - 1.63 nmol/L) and the LOD (calculated according to DIN 32645) was between 0.06 and 0.14 µg/L (0.22 - 0.51 nmol/L) in rabbit urine for the different studies. Deviations between repeatedly measured samples were 2.1 ± 6.2%. The deviation of quality controls from their nominal concentration was 5.0 ± 3.1%.

Table 10. Concentrations of the calibration standards used for the quantification of *N*-acetyl-S-(3,3,3-trifluoro-2-hydroxypropanyl)-*L*-cysteine.

Calibration standard	***N*-Acetyl-*S*-(3,3,3-trifluoro-2-hydroxypropanyl)-*L*-cysteine concentration**	
	[µg/L]	**[nmol/L]**
1	0.0	0.0
2	0.3	1.1
3	0.6	2.2
4	0.9	3.3
5	1.2	4.4
6	1.5	5.5
7	5.0	18.2
8	10.0	36.4
9	50.0	181.8
10	100.0	363.6

2.8.2.2 Quantification of 3,3,3-trifluorolactic acid

An ion pair chromatography method was developed based on a published procedure (Loos and Barcelo, 2001). Samples (7.5 µL) were added to 92.5 µL of a 150 pg/µL internal standard

solution (dichloroacetic acid), vortexed and transferred into glass autosampler vials. Aliquots (10 µL) were analyzed. Quantification was performed using a Reprosil Pur C18 column (2 x 150 mm, 5 µm; Maisch, Ammerbuch, Germany) with an isocratic elution by water containing 5 mM triethylamine and 5% acetonitrile adjusted to pH 6.2 with acetic acid at a flow rate of 200 µL/min for 10 minutes. Mass spectrometer parameters are listed in Table 14. Quantification was based on calibration curves of urine samples spiked with known amounts of 3,3,3-trifluorolactic acid (Table 11).

Linearity was observed within the concentration range of the calibration curve (R^2-value range, 0.993 - 0.997). The LOQ (calculated according to DIN 32645) for 3,3,3-trifluorolactic acid was between 0.43 and 0.54 µg/L (2.99 - 3.75 nmol/L) with a LOD (calculated according to DIN 32645) between 0.14 and 0.21 µg/L (0.97 - 1.46 nmol/L) in rat urine. Deviations between repeatedly measured samples were 0.5 ± 11.4%. The deviation of quality controls from their nominal concentration was 7.0 ± 5.5%.

Table 11. Concentrations of the calibration standards used for the quantification of 3,3,3-trifluorolactic acid.

Calibration standard	3,3,3-Trifluorolactic acid concentration	
	[µg/L]	[nmol/L]
1	0.00	0.00
2	0.60	4.17
3	0.90	6.25
4	1.20	8.33
5	1.50	10.42
6	1.80	12.50
7	5.00	34.72
8	7.50	52.08
9	10.00	69.44
10	13.75	95.49
11	17.50	121.53

2.8.3 Quantification of *N*-acetyl-*S*-(3,3,3-trifluoro-*trans*-propenyl)-*L*-cysteine

Diluted samples (10 µL) were added to 90 µL of a 90 pg/µL internal standard solution (*N*-acetyl-d_3-*S*-(3,3,3-trifluoro-*trans*-propenyl)-*L*-cysteine), vortexed, transferred into glass autosampler vials and sealed aliquots (10 µL) were injected into the LC. Quantification was performed using a Reprosil Pur C18 AQ column (2 x 150 mm, 5µm; Maisch, Ammerbuch, Germany) with a gradient elution using water containing 0.1% formic acid (solvent A) and methanol containing 0.1% formic acid (solvent B). The elution conditions were: flow rate of 300 µL/min; 2% solvent B for 1 minute followed by a linear increase to 90% solvent B within 5 minutes, then 90% solvent B for another 3 minutes. Mass spectrometer parameters are listed in Table 14. Quantification was based on calibration curves of urine or plasma samples spiked with known amounts of *N*-acetyl-*S*-(3,3,3-trifluoro-*trans*-propenyl)-*L*-cysteine (Table 12).

The method in rat and rabbit urine and plasma was linear within the concentration range of the calibration curves (R^2-value ranges, 0.995 - 0.996 [urine] respectively 0.998 - 0.999 [plasma]). The LOQ (calculated according to DIN 32645) for *N*-acetyl-*S*-(3,3,3-trifluoro-*trans*-propanyl)-*L*-cysteine was between 0.21 and 0.26 µg/L (0.81 - 1.00 nmol/L) in rat and rabbit urine, with LODs (calculated according to DIN 32645) between 0.05 and 0.07 µg/L (0.19 - 0.26 nmol/L). *N*-acetyl-*S*-(3,3,3-trifluoro-*trans*-propanyl)-*L*-cysteine quantification in plasma achieved a LOQ (calculated according to DIN 32645) of 0.62 µg/L (2.38 nmol/L) and a LOD (calculated according to DIN 32645) of 0.17 µg/L (0.65 nmol/L). Deviations between repeatedly measured samples were 5.4 ± 5.0% (urine) respectively 6.6 ± 4.5% (plasma). The deviation of quality controls from their nominal concentration was 1,9 ± 1,8% (urine) respectively 5,6 ± 3,8% (plasma).

Table 12. Concentrations of the calibration standards used for the quantification of *N*-acetyl-*S*-(3,3,3-trifluoro-*trans*-propenyl)-*L*-cysteine.

Calibration standard	***N*-Acetyl-*S*-(3,3,3-trifluoro-*trans*-propenyl)-*L*-cysteine concentration in**			
	Urine		**Plasma**	
	[µg/L]	**[nmol/L]**	**[µg/L]**	**[nmol/L]**
1	0.00	0.00	0.00	0.00
2	0.34	1.32	0.41	1.60
3	0.68	2.64	0.82	3.20
4	1.35	5.25	1.65	6.42
5	2.03	7.90	2.47	9.61
6	2.70	10.51	3.30	12.84
7	3.38	13.15	4.12	16.03
8	4.83	18.79	5.88	22.88
9	9.65	37.55	11.80	45.91
10	19.30	75.10	23.50	91.44

2.8.4 Quantification of *S*-(3,3,3-trifluoro-*trans*-propenyl)-glutathione

Incubation supernatants (50 µL) were added to 50 µL of a 500 pg/µL solution of the internal standard *S*-(1,2-dichlorovinyl)-glutathione, vortexed and transferred into glass autosampler vials. Aliquots (10 µL) were injected. Analytes were separated on a Reprosil Pur C18 column (2 x 150 mm, 5µm; Maisch, Ammerbuch, Germany) by gradient elution with water containing 0.1% FA (solvent A) and acetonitrile containing 0.1% FA (solvent B) at a flow rate of 200 µL/min. Conditions were set to 10% solvent B for 1 minute, increasing to 90% solvent B within 9 minutes and solvent B at 90% for 3 minutes. Mass spectrometer parameters are listed in Table 14. Quantification was based on calibration curves of incubation matrix samples spiked with known amounts of *S*-(3,3,3-trifluoro-*trans*-propenyl)-glutathione (Table 13).

The method was linear within the concentration range of the calibration curve (R^2-value range, 0.998-0.999). The LOQ (calculated according to DIN 32645) for *S*-(3,3,3-trifluoro-*trans*-propenyl)-glutathione in the incubation matrix was 5.5 µg/L (13.7 nmol/L) and the LOD (calculated according to DIN 32645) was 1.7 µg/L (4.2 nmol/L). Deviations between

repeatedly measured samples were 7.7 ± 3.7%. The deviation of quality controls from their nominal concentration was 6.0 ± 4.8%.

Table 13. Concentrations of the calibration standards used for the quantification of *S*-(3,3,3-trifluoro-*trans*-propenyl)-glutathione.

Calibration standard	***S*-(3,3,3-Trifluoro-*trans*-propenyl)-glutathione concentration**	
	[µg/L]	**[nmol/L]**
1	0.00	0.00
2	1.92	4.78
3	3.84	9.58
4	5.76	14.36
5	7.68	19.15
6	9.60	23.94
7	16.00	39.90
8	32.00	79.80
9	64.00	159.60
10	320.00	798.00

Table 14. Mass spectrometric parameters settings (MS-MS-transitions, declustering potential and collision energy) used for metabolite quantifications in negative ionization.

Compound	Transition [m/z]	Declustering potential [V]	Collision energy [V]	Retention time [min]	Mass spectrometer device
N-Acetyl-*S*-(3,3,3-trifluoro-*trans*-propenyl)-*L*-cysteine	256 → 127 256 → 107	-26	-30	8.9	API 3000
N-Acetyl-d_3-*S*-(3,3,3-trifluoro-*trans*-propenyl)-*L*-cysteine (internal standard)	259 → 127 259 → 107	-26	-30	8.9	
3,3,3-Trifluorolactic acid	143 → 143 143 → 79	-30	-10	2.7	API/Q-Trap 2000
Dichloroacetic acid (internal standard)	127 → 127	-30	-10	3.1	
S-(3,3,3-Trifluoro-*trans*-propenyl)-glutathione	400 → 272 400 → 254	-41 -41	-18 -40	10.1	API/Q-Trap 2000
S-(1,2-Dichlorovinyl)-glutathione (internal standard)	400 → 272 400 → 143	-41 -41	18 -40	9.5	
N-Acetyl-*S*-(3,3,3-trifluoro-2-hydroxypropanyl)-*L*-cysteine	274 → 145 274 → 75	-26	-30	8.1	API 3000
N-Acetyl-*S*-(2-chloro-1,1,2-trifluoroethyl)-*L*-cysteine (internal standard)	278 → 149 278 → 129	-26	-30	8.1	

3 Results

3.1 Biotransformation of HFO-1234yf in pregnant, non-pregnant female and male New Zealand White rabbits after single high dose inhalation exposure

3.1.1 Inhalation exposures

To obtain information on differences in the biotransformation of HFO-1234yf in male (n = 5/concentration), non-pregnant (n = 5/concentration) and pregnant female (n = 6/concentration) NZW rabbits, animals were exposed to 0 ppm, 50,000 ppm and 100,000 ppm of 2,3,3,3-tetrafluoroprop-1-ene by whole-body inhalation. Measured exposure chamber concentrations were 47,000 ± 1,530 ppm, 102,000 ± 7,640 ppm for non-pregnant and pregnant female and 45,000 ± 4,000 ppm, 100,000 ± 0 ppm for male rabbits.

3.1.2 Identification of HFO-1234yf metabolites by ^{19}F-NMR spectroscopy

Biotransformation products of HFO-1234yf were identified by ^{19}F-NMR spectroscopy (Table 15, Fig. 16), comparing the chemical shifts and fluorine-proton coupling constants with spectra of standards (Table 5). No ^{19}F-NMR signals were found in urine samples of control animals. Signals found in the spectra of urine fractions collected within 48 hours after the inhalation were assigned to trifluoroacetic acid (**19**, Fig. 16), 3,3,3-trifluoro-1,2-propanediol (**17**, Fig. 16), *N*-acetyl-*S*-(3,3,3-trifluoro-2-hydroxypropanyl)-*L*-cysteine (**9**, Fig. 16) and *S*-(3,3,3-trifluoro-2-hydroxypropanyl)-mercaptolactic acid (**11**, Fig. 16). Beside known metabolites, there were two unidentified metabolites present (**24** and **25**, Fig. 16).

Metabolite 24 (Fig. 16) is probably a conjugation product of 3,3,3-trifluoro-1,2-propanediol considering its similar ^{19}F-chemical shift, multiplicity and $^{3}J_{HF}$-coupling constant. The slightly more positive ^{19}F-chemical shift as well as the lower $^{3}J_{HF}$-coupling constant may indicate sulfation or glucuronidation of the hydroxide group leading to a higher polar chemical bond. Metabolite 25 (Fig. 16) is likely an alternative derivative of the 2,3,3,3-tetrafluoroprop-1-ene glutathione-*S* conjugation pathway also because of its similar ^{19}F-chemical shift, multiplicity and $^{3}J_{HF}$-coupling constant compared to *S*-(3,3,3-trifluoro-2-hydroxypropanyl) mercaptolactic acid and *N*-acetyl-*S*-(3,3,3-trifluoro-2-hydroxypropanyl)-*L*-cysteine. The more positive ^{19}F-chemical may again indicate the introduction of a higher electronegative substituent, likely by sulfation or glucuronidation of the hydroxide group. To assess possible differences in the biotransformation of 2,3,3,3-tetrafluoroprop-1-ene between the groups of rabbits, ^{19}F-NMR data were compared. Figure 16 illustrates that there are no significant differences between the ^{19}F-spectra of urine from male (A), non-pregnant female (B) and pregnant female rabbits (C) after a single one-hour exposure to 100,000 ppm. All spectra show the same major signals with very similar relative intensities. The determined metabolic pattern of fluorine-containing metabolites was similar to that previously reported by Schuster et al. (2010). The only difference observed was that *S*-(3,3,3-trifluoro-2-hydroxypropanyl)-mercaptolactic acid

was the major biotransformation product instead of *N*-acetyl-*S*-(3,3,3-trifluoro-2-hydroxypropanyl)-*L*-cysteine (Schuster et al., 2010).

Table 15. Biotransformation products of HFO-1234yf identified in rabbit urines after singel high dose exposures.

Compound	Chemical shift [ppm]	Multiplicity	^{1}H - ^{19}F Coupling constants [Hz]
Trifluoroacetic acid (19)	-75.4	s	-
Unidentified metabolite (24)	-77.1	d	$^{3}J_{HF}$ = 7.2
3,3,3-Trifluoro-1,2-propanediol (17)	-77.2	d	$^{3}J_{HF}$ = 7.4
Unidentified metabolite (25)	-78.4	d	$^{3}J_{HF}$ = 6.8
N-Acetyl-*S*-(3,3,3-trifluoro-2-hydroxypropanyl)-*L*-cysteine (9)	-78.7	d	$^{3}J_{HF}$ = 6.6
N-Acetyl-*S*-(3,3,3-trifluoro-2-hydroxypropanyl)-mercaptolactic acid (11)	-78.9	d	$^{3}J_{HF}$ = 6.9

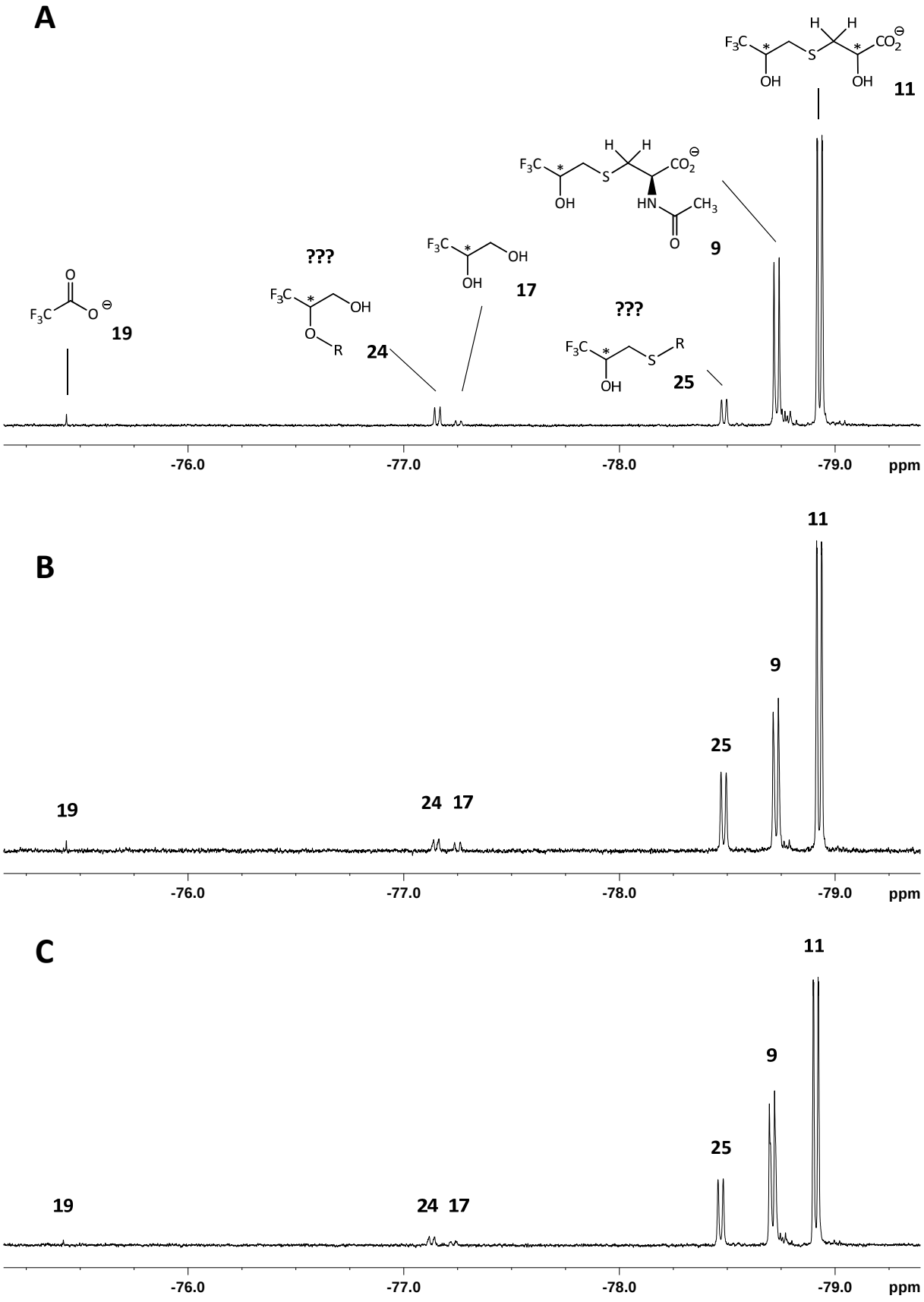

Fig. 16. ^{19}F-NMR spectra of urine samples from (**A**) male, (**B**) non-pregnant female, (**C**) pregnant female rabbits exposed to HFO-1234yf by whole-body inhalation (100,000 ppm, 12-24 h).

3.1.3 Quantification of 3,3,3-trifluoro-2-propanol and 1,1,1-trifluoroacetone by GC-MS

The nucleophile metabolite 1,1,1-trifluoroacetone was previously observed as a minor urinary metabolite in rats and mice and in incubation experiments with rabbit liver S9 fractions (Schuster, 2009; Schuster et al., 2008). More sensitive GC/MS determination of 1,1,1-trifluoroacetone and its precursor metabolite 3,3,3-trifluoro-2-propanol was performed to confirm negative ^{19}F-NMR analysis (Fig. 16). GC/MS analysis revealed no positive signal for 1,1,1-trifluoroacetone in any analyzed sample, despite 3,3,3-trifluoro-2-propanol was detected in traces (Fig. 17).

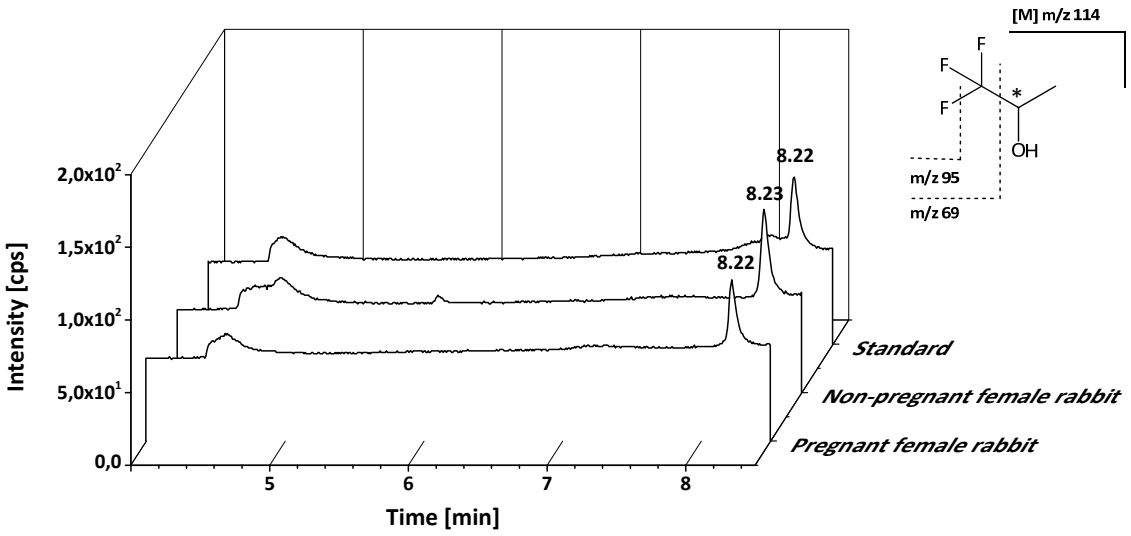

Fig. 17. GC/MS chromatogram of 3,3,3-trifluoro-2-propanol (m/z 69 monitored) in urine samples of pregnant and non-pregnant female rabbits exposed to HFO-1234yf by inhalation (0-12 h post-inhalation fraction, 100,000 ppm); standard: 1ng/µL 3,3,3-trifluoro-2-propanol in water.

3.1.4 Determination of minor metabolites by LC-MS/MS

The screening of urine samples for still uncharacterized metabolites seen in ^{19}F-NMR spectra revealed *N*-acetyl-2-*S*-(3,3,3-trifluoropropenyl)-*L*-cysteine as a possible further metabolite of HFO-1234yf (Fig. 18). The gained EPI spectra showed a typical constant neutral loss for mercapturic acid conjugates of 129 m/z and a precursor ion mass of 256 m/z. Further, a double loss of hydrogen fluoride (20 m/z), that was seen before in EPI spectra of other HFO-1234yf metabolites (see also Fig. 33, B/D, p. 82), indicated the presence of the CF_3 group. *N*-acetyl-2-*S*-(3,3,3-trifluoropropenyl)-*L*-cysteine was not confirmed by comparison with a synthesized standard. No further HFO-1234yf metabolites could be identified by LC-MS/MS analysis.

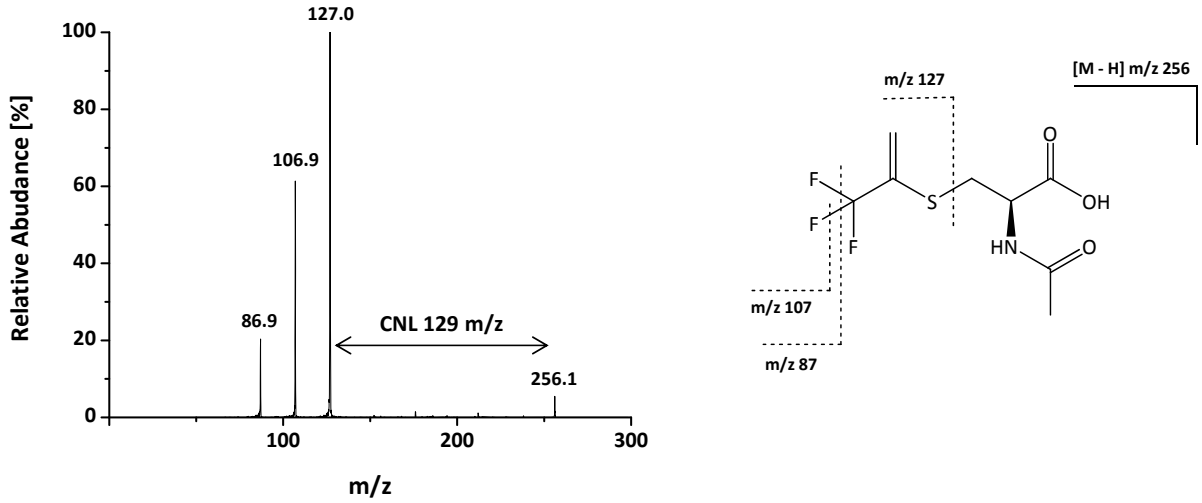

Fig. 18. EPI spectra of *N*-acetyl-2-*S*-(3,3,3-trifluoropropenyl)-*L*-cysteine in rabbit urine (pregnant female, 100,000 ppm exposure); CNL, constant neutral loss.

3.1.5 Quantification of urinary *N*-acetyl-*S*-(3,3,3-trifluoro-2-hydroxypropanyl)-*L*-cysteine excretion kinetics

In all urine samples, concentrations of *N*-acetyl-*S*-(3,3,3-trifluoro-2-hydroxypropanyl)-*L*-cysteine were determined by LC-MS/MS in order to evaluate any difference in the excretion kinetics of the glutathione *S*-conjugation pathway (Fig. 19, A/B). Peak urine excretions were reached within 12 hours after termination of the exposures (mean values: male 100,000 ppm – 63.55 µmol, male 50,000 ppm – 53.76 µmol, non-pregnant female 100,000 ppm – 32.51 µmol, pregnant female 50,000 ppm – 45.07 µmol) except for the study group pregnant females 100,000 ppm. For this group, the peak excretion was reached between 12 and 24 hours after the end of exposure (mean value: 27.17 µmol). The metabolite elimination followed 1st order kinetics with a half-life time of 6.0 ± 3.5 hours in all groups and > 83% of *N*-acetyl-*S*-(3,3,3-trifluoro-2-hydroxypropanyl)-*L*-cysteine was recovered within 24 hours. Elimination within the first 12 hours in the 100,000 ppm pregnant female group (35.9 ± 24.4% of total metabolite excretion) was slower compared to all other groups (mean value: 71.8 ± 14.5% of total metabolite excretion within 48 hours). However, this result is probably due to significant lower urine output in pregnant female rabbits within the first 12 hours after inhalation exposure compared to the non-pregnant female group (Table 16). The total urinary recovery of *N*-acetyl-*S*-(3,3,3-trifluoro-2-hydroxypropanyl)-*L*-cysteine within 48 hours after exposure was higher in males (mean values: male 100,000 ppm – 86.40 ± 38.87 µmol; male 50,000 ppm – 67.86 ± 22.95 µmol) than in females (mean values: pregnant 100,000 ppm – 50.47 ± 19.72 µmol; pregnant 50,000 ppm – 60.97 ± 13.05 µmol; non-pregnant 100,000 ppm – 43.10 ± 22.35 µmol). No significant difference (Student's t-test, p = 0.58) was observed between non-pregnant females and pregnant females as well as

between pregnant and male (Student's t-test, p = 0.08) and non-pregnant and male (Student's t-test, p = 0.06) rabbits in the 100,000 ppm group. Since the quantity of metabolite recovered at 100,000 ppm is close to the quantity recovered at 50,000 ppm, uptake and/or metabolism of HFO-1234yf are presumably saturated above concentrations of 50,000 ppm, as observed for similar substances in previous studies (Gargas et al., 1986).

Table 16. Urinary excretion of inorganic fluoride, *N*-acetyl-*S*-(3,3,3-trifluoro-2-hydroxypropanyl)-*L*-cysteine and urine output by non-pregnant (100,000 ppm) and pregnant female (100,000 ppm) rabbits within 24 hours after inhalation exposure to HFO-1234yf; *p < 0.05, **p < 0.01.

Fraction	Compound and Specimen	Non-pregnant	Pregnant	Student's t-test, p-value
0-12 h	**Inorganic fluoride – F^- [µmol]**	2.7 ± 1.3	1.5 ± 1.3	0.17
12-24 h		0.6 ± 0.3	0.8 ± 0.4	0.37
24-36 h		0.6 ± 0.3	0.5 ± 0.2	0.20
36-48 h		0.5 ± 0.4	0.3 ± 0.1	0.10
0-48 h		4.4 ± 1.7	3.0 ± 1.8	0.12
0-12 h	***N*-Acetyl-*S*-(3,3,3-trifluoro-2-hydroxypropanyl)-*L*-cysteine [µmol]**	32.5 ± 20.5	19.9 ± 14.9	0.29
12-24 h		8.1 ± 4.0	27.2 ± 11.8	0.01 **
24-36 h		2.0 ± 1.5	5.3 ± 3.2	0.11
36-48 h		0.9 ± 1.0	2.8 ± 1.6	0.05
0-48 h		43.1 ± 22.4	50.5 ± 19.7	0.58
0-12 h	**Urine volume [mL]**	193.2 ± 98.2	44.7 ± 41.6	0.01 **
12-24 h		66.4 ± 44.3	64.5 ± 36.6	0.94
24-36 h		87.2 ± 79.8	63.8 ± 43.1	0.24
36-48 h		93.6 ± 68.0	45.8 ± 34.7	0.20
0-48 h		446.4 ± 209.3	200.5 ± 136.0	0.04 *

3.1.6 Quantification of urinary inorganic fluoride excretion

As inorganic free fluoride is known as a cardiotoxic compound by decreasing extracellular calcium levels and causing a hyperkalemia (Cummings and McIvor, 1988; McIvor et al., 1987), urine levels were determined by potentiometry (fluoride selective electrode). Total urinary excretion of inorganic fluoride within 48 hours showed no significant difference (Student's t-test, p = 0.1) between pregnant (2.60 ± 1.89 µmol) and non-pregnant (4.44 ± 1.65 µmol) rabbits (100,000 ppm exposure) (Fig. 19, C).

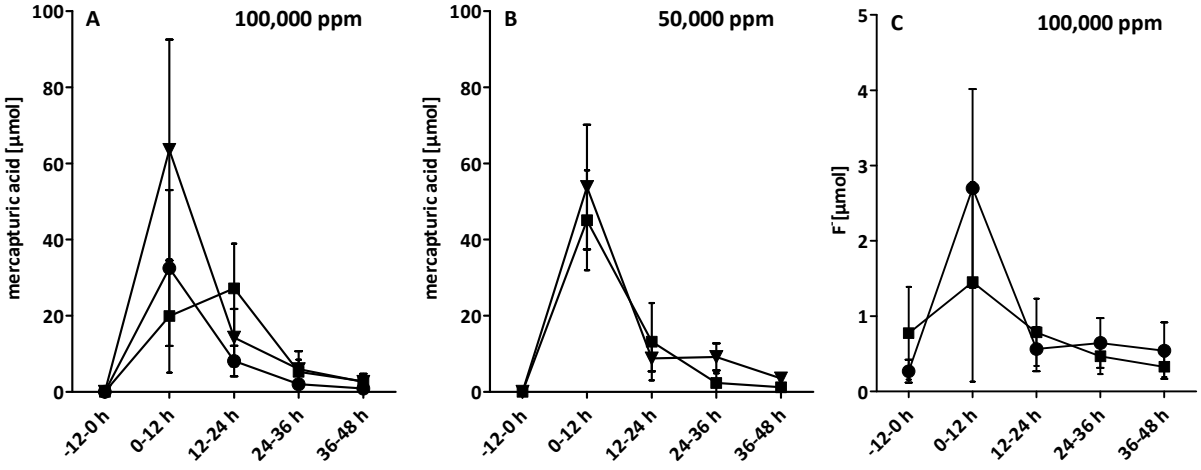

Fig. 19. Kinetics of urinary elimination of *N*-acetyl-*S*-(3,3,3-trifluoro-2-hydroxypropanyl)-*L*-cysteine (**A**, **B**) and inorganic fluoride (**C**) within 48 hours after whole-body inhalation of male (▼), non-pregnant female (●) and pregnant female (■) rabbits to 100,000 or 50,000 ppm of HFO-1234yf.

3.1.7 Quantification of minor metabolites by LC-MS/MS and ^{19}F-NMR spectroscopy

For further characterization of metabolism, relative peak areas in ^{19}F-NMR spectra of the six major metabolic products were determined and compared between the different study groups by including absolute *N*-acetyl-*S*-(3,3,3-trifluoro-2-hydroxypropanyl)-*L*-cysteine excretion amounts determined by LC-MS/MS (see 3.1.5). Due to time consuming ^{19}F-NMR trace analysis and only shared access to^{19}F-NMR facilities only one animal per group was analyzed. As shown in Fig. 20, there were no major differences in metabolite excretion between male and female as well as between non-pregnant female and pregnant female rabbits at any time intervals collected. Dose-dependency was not seen between all 50,000 ppm and 100,000 ppm dose groups. All fluoro metabolites were excreted nearly completely within 36 hours after termination of the single high dose exposure, except trifluoroacetic acid.

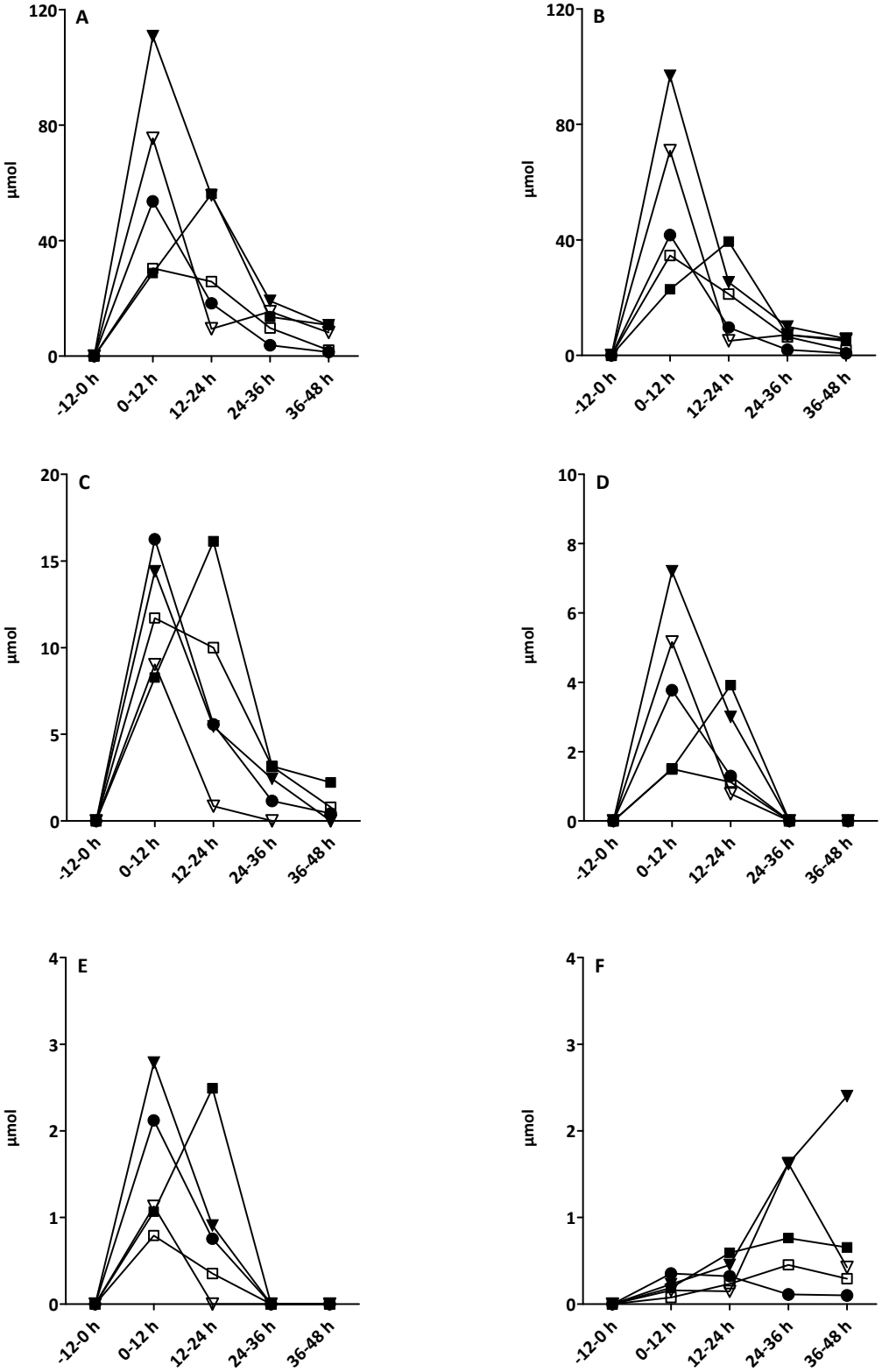

Fig. 20. Urinary excretion kinetics of major metabolites within 48 hours based on their relative quantification by ^{19}F-NMR and LC-MS/MS in one rabbit per exposure group: male (100,000 ppm [▼]/50,000 ppm [▽]), pregnant female (100,000 ppm [■]/50,000 ppm [□]) and non-pregnant female (100,000 ppm [●]); (**A**) *S*-(3,3,3-trifluoro-2-hydroxypropanyl)-mercaptolactic acid, (**B**) *N*-acetyl-*S*-(3,3,3-trifluoro-2-hydroxypropanyl)-*L*-cysteine, (**C**) unidentified metabolite (25), (**D**) unidentified metabolite (24), (**E**) 3,3,3-trifluoro-1,2-propanediol, (**F**) trifluoroacetic acid.

3.2 Biotransformation of HFO-1234yf in female and male New Zealand White rabbits after multiple inhalation exposure (28 days)

3.2.1 Inhalation exposures

Female and male NZW rabbits (n = 5/concentration for 7-day exposures, 14-day exposures and recovery group; n = 10/concentration for 28-day exposures) were exposed to HFO-1234yf by inhalation for 6 hours a day, 7 days a week for up to 7, 14 or 28 consecutive days. Exposure levels were 0 (control), 500 (low dose), 1,000/1,500 (mid dose) and 4,500/5,500 (high dose) ppm. A recovery group was observed for at least 28 days after the last exposure of the 28 days exposure period (see also Table 2, page 29 and Fig. 11, page 27).

Due to unexpected deaths of two rabbits in the 7-day high dose exposure groups, high dose exposures were halted on day 7 (7-day and 14-day high dose exposure groups). In addition to that, concentrations were changed. For rabbits of the 14-day exposures the high dose exposure level was lowered to 4,500 ppm on day 8. No changes were made for low (500 ppm) and mid dose (1,500 ppm) groups. Rabbits of the 28-day exposure groups were exposed to 0 (control), 500 (low dose), 1,000 (mid dose) and 4,500 (high dose) ppm for the whole 28 days.

Measured exposure chamber concentrations were 497 ± 38 ppm, 1,508 ± 81 ppm, 5,533 ± 137 ppm (day 1 to 6) and 4,338 ± 177 ppm (day 8 to 15) for rabbits of the 7- and 14-day exposure groups and 478 ± 64 ppm, 1,010 ± 57 ppm and 4,378 ± 209 ppm for rabbits of the 28-day exposure groups.

3.2.2 Identification of HFO-1234yf metabolites

3.2.2.1 Urine analysis by ^{19}F-NMR spectroscopy

Figure 21 and Table 17 give an overview of all fluoro containing metabolites found in rabbit urine collected after multiple inhalation exposure to HFO-1234yf for up to 28 consecutive days. Signals found in urine collected within 48 hours were assigned to trifluoroacetic acid (**19**, Fig. 21), 3,3,3-trifluoro-1,2-propanediol (**17**, Fig. 21), *N*-acetyl-*S*-(3,3,3-trifluoro-2-hydroxypropanyl)-*L*-cysteine (**9**, Fig. 21), *S*-(3,3,3-trifluoro-2-hydroxypropanyl)-mercaptolactic acid (**11**, Fig. 21), 3,3,3-trifluoro-2-propanol (**15**, Fig. 21) and *S*-(3,3,3-trifluoro-2-hydroxypropanyl)-*L*-cysteine (**8**, Fig. 21). Beside these known metabolites, there were two unidentified metabolites present (**24** and **25**, Fig. 21). As previously elucidated in section 3.1.2 (single-exposure inhalation), metabolite 24 is probably a conjugation product of 3,3,3-trifluoro-1,2-propanediol whereas metabolite 25 is likely an alternative derivative of the 2,3,3,3-tetrafluoroprop-1-ene glutathione-*S* conjugation pathway.

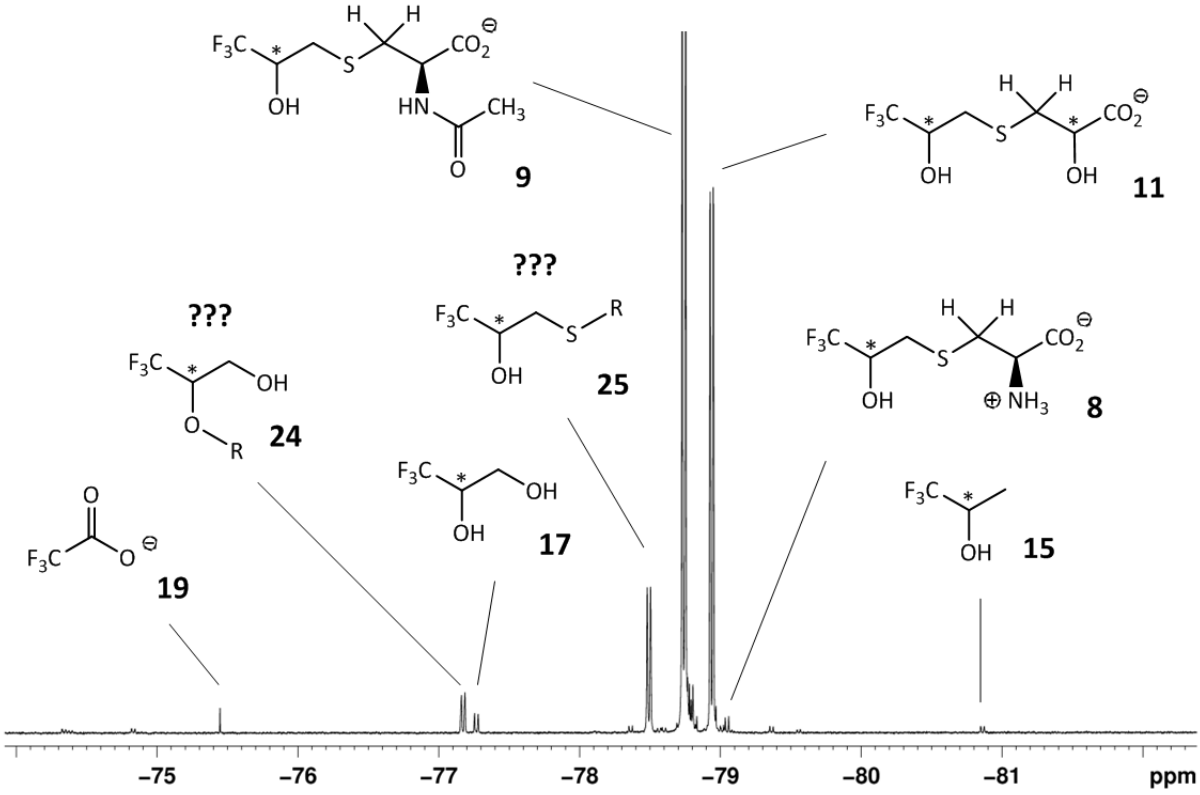

Fig. 21. ^{19}F-NMR spectrum of a post-inhalation urine sample of a male rabbit exposed to 4,500 ppm of HFO-1234yf (high dose) for 28 days (0-18 h collection interval).

Table 17. Metabolites of HFO-1234yf in rabbit urines after multiple exposures.

Compound	Chemical shift [ppm]	Multiplicity	$^{1}H - ^{19}F$ Coupling constants [Hz]
Trifluoroacetic acid (19)	-75.4	s	-
Unidentified metabolite (24)	-77.1	d	$^{3}J_{HF}$ = 7.2
3,3,3-Trifluoro-1,2-propanediol (17)	-77.2	d	$^{3}J_{HF}$ = 7.4
Unidentified metabolite (25)	-78.4	d	$^{3}J_{HF}$ = 6.8
N-Acetyl-*S*-(3,3,3-trifluoro-2-hydroxypropanyl)-*L*-cysteine (9)	-78.7	d	$^{3}J_{HF}$ = 6.6
N-Acetyl-*S*-(3,3,3-trifluoro-2-hydroxypropanyl)-mercaptolactic acid (11)	-78.9	d	$^{3}J_{HF}$ = 6.9
S-(3,3,3-Trifluoro-2-hydroxypropanyl)-*L*-cysteine (8)	-79.0	d	$^{3}J_{HF}$ = 6.6
3,3,3-Trifluoro-2-propanol (15)	-80.8	d	$^{3}J_{HF}$ = 7.0

3.2.2.2 Heart tissue analysis by ^{19}F-NMR spectroscopy

For evaluation whether potentially toxic metabolites (monofluoroacetate or monofluorocitrate) were formed or accumulated in heart tissue, several heart extract samples of rabbits with significantly increased cardiac toxicity biomarkers were analyzed by ^{19}F-NMR spectroscopy. Five samples of animals with extremely increased creatine kinase values (total creatine kinase, CK; creatine kinase heart muscle isoform, CK-MB), and two samples with slightly increased CK and CK-MB values, compared to control, were analyzed (Table 18). No ^{19}F-NMR signals were observed in any sample analyzed. Spectra of references showed clear signals for monofluoroacetate (δ = -216.9; t, $^{3}J_{HF}$ = 48.3 Hz) and monofluorocitrate (δ = -200.6; d, $^{3}J_{HF}$ = 48.0 Hz).

Table 18. Heart extract samples analyzed by ^{19}F-NMR spectroscopy.

Animal	Exposure duration [days]	Exposure concentration [ppm]	CK* [U/L]	CK-MB* [U/L]	NMR device
M 4037	14	4,500/5,500	2,790	8.4	Bruker DRX 300
F 4564	14	4,500/5,500	8,343	133.5	Bruker DRX 300
M 4049	28	4,500	3,915	19.6	Bruker DRX 300
F 4571	28	4,500	6,034	54.3	Bruker DRX 300
M 4047	28	4,500	611	2.4	Bruker DRX 300
F 4575	28	4,500	431	4.7	Bruker DRX 300
F 3552	14	1,500	11,632	46.5	Bruker AV-III 500

*Clinical parameters were determined by Huntington Life Sciences, East Millstone, New Jersey, USA.

3.2.2.3 Determination of monofluoroacetate in heart tissue by LC-MS/MS

In addition to ^{19}F-NMR analysis, heart samples of rabbits showing either clinical effects (3 or more significantly increased clinical parameters: CK, CK-MB, creatine kinase skeletal muscle isoform (CK-MM), fatty-acid-binding proteins (FABPs), myoglobin (MYG) - determined by Huntington Life Sciences, East Millstone, New Jersey, USA) or pathological changes in the heart muscle or in the heart and in the skeletal muscle (determined by Huntington Life Sciences, East Millstone, New Jersey, USA) were also analyzed for monofluoroacetate by LC-MS/MS (Table 19). No monofluoroacetate specific signal could be observed in any of the heart extract samples analyzed. The chromatogram of a standard sample containing 0.02 ppm monofluoroacetate is shown in Fig. 22.

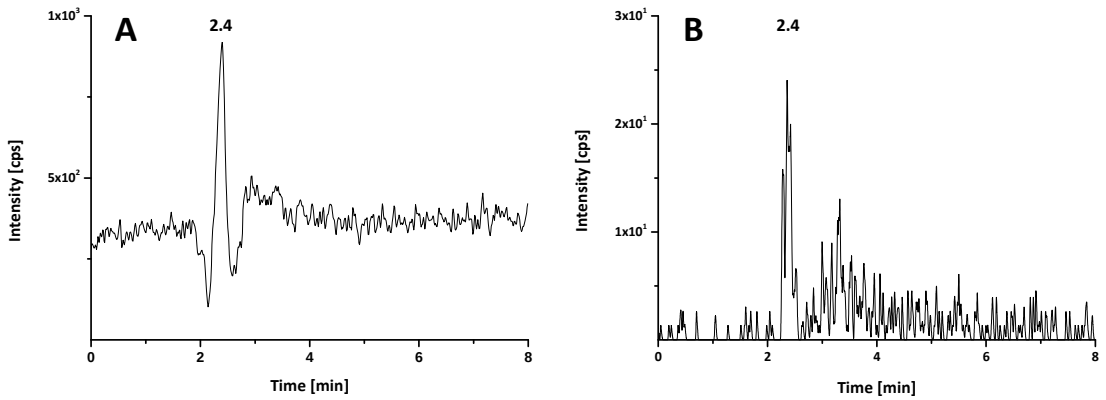

Fig. 22. LC-MS/MS chromatogram of a monofluoroacetate standard sample (0.02 ppm - in heart tissue). Recorded mass transitions: 77-77 m/z (**A**), 77-57 m/z (**B**).

Table 19. Animals analyzed for monofluoroacetate by LC-MS/MS, showing either effects in clinical chemistry, heart pathology or heart and muscle pathology.

Animal	Exposure duration [days]	Exposure concentration [ppm]	Effects in clinical chemistry	Effects in heart pathology	Effects in heart and muscle pathology
M 3066	7	1,500		X	
M 4035	7	5,500		X	
F 3552	14	1,500	X		X
F 3553	14	1,500		X	
F 4564	14	5,500/4,500	X*		
M 4037	14	5,500/4,500	X		X
F 4568	28	4,500	X		X
F 4574	28	4,500	X*		
F 4576	28	4,500	X		X
F 4569	28	4,500			X
M 3084	28	1,000		X	
M 4041	28	4,500	X		X
M 4042	28	4,500	X		X
M 4046	28	4,500	X		X
M 4048	28	4,500		X	
M 4049	28	4,500	X		X

* rabbits showing only extremely high CK and CK-MB values

3.2.3 Determination of 3,3,3-trifluoro-2-propanol and 1,1,1-trifluoroacetone by GC-MS

The nucleophile metabolite 1,1,1-trifluoroacetone was previously observed as a minor urinary metabolite in rats and mice and in incubation experiments with rabbit liver S9 fractions (Schuster, 2009; Schuster et al., 2008). 3,3,3-trifluoro-2-propanol was identified as a minor HFO-1234yf metabolite in rabbit urine after single exposures (Schuster et al., 2010). More sensitive GC/MS determination of 1,1,1-trifluoroacetone and its precursor metabolite

3,3,3-trifluoro-2-propanol was performed to confirm negative ^{19}F-NMR analysis (Fig. 21). GC/MS spectra revealed no positive signal for 1,1,1-trifluoroacetone in any analyzed sample, 3,3,3-trifluoro-2-propanl was only detected in traces in female and male rabbit urine (Fig. 23).

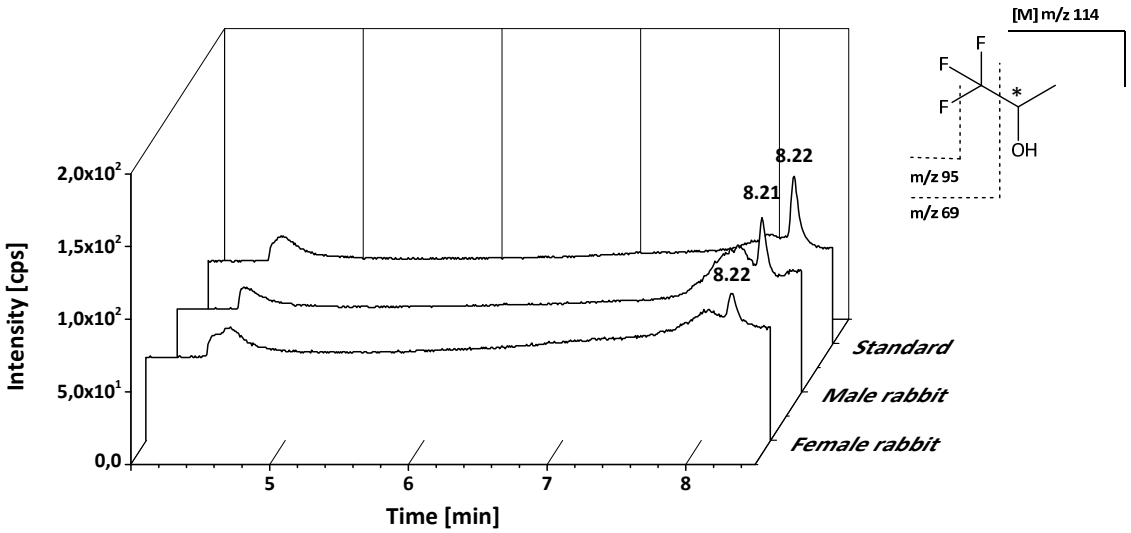

Fig. 23. GC/MS chromatogram of 3,3,3-trifluoro-2-propanol in urine samples (m/z 69 monitored) of female and male rabbits exposed to HFO-1234yf by inhalation (0-18 h post-inhalation fraction, 4,500 ppm, 28 day exposure); standard: 1ng/µL 3,3,3-trifluoro-2-propanol in water.

3.2.4 Quantitative analysis

3.2.4.1 Inorganic fluoride determination

Inorganic fluoride was quantified in urine and serum (Fig. 24 and Fig. 25). Urinary excretion of inorganic fluoride within 18 hours after termination of the last inhalation exposure was not dose-dependent in all female and male exposure groups. Significant differences could only be determined between the mid and high dose groups of female and male rabbits exposed for 28 days and between the low and mid dose groups of male rabbits exposed for 7 days (Fig. 24, C and D). Expected low fluoride excretion amounts were observed for high dose animals exposed for 7 days, due to exposition interruption on day 7 (male: 0.65 ± 0.37 µmol; female: 1.87 ± 0.80 µmol).

Further, no significant changes between controls and 28-day recovery groups were determined at any exposure level. An exposure time-dependent increase in fluoride excretion was not observed in any of the exposure groups (Fig. 24, A and B). A low significant increase in urinary fluoride excretion was only observed for female rabbits (14 days: 5.27 ± 1.47 µmol; 28 days: 10.11 ± 2.85 µmol) of the high dose exposure groups.

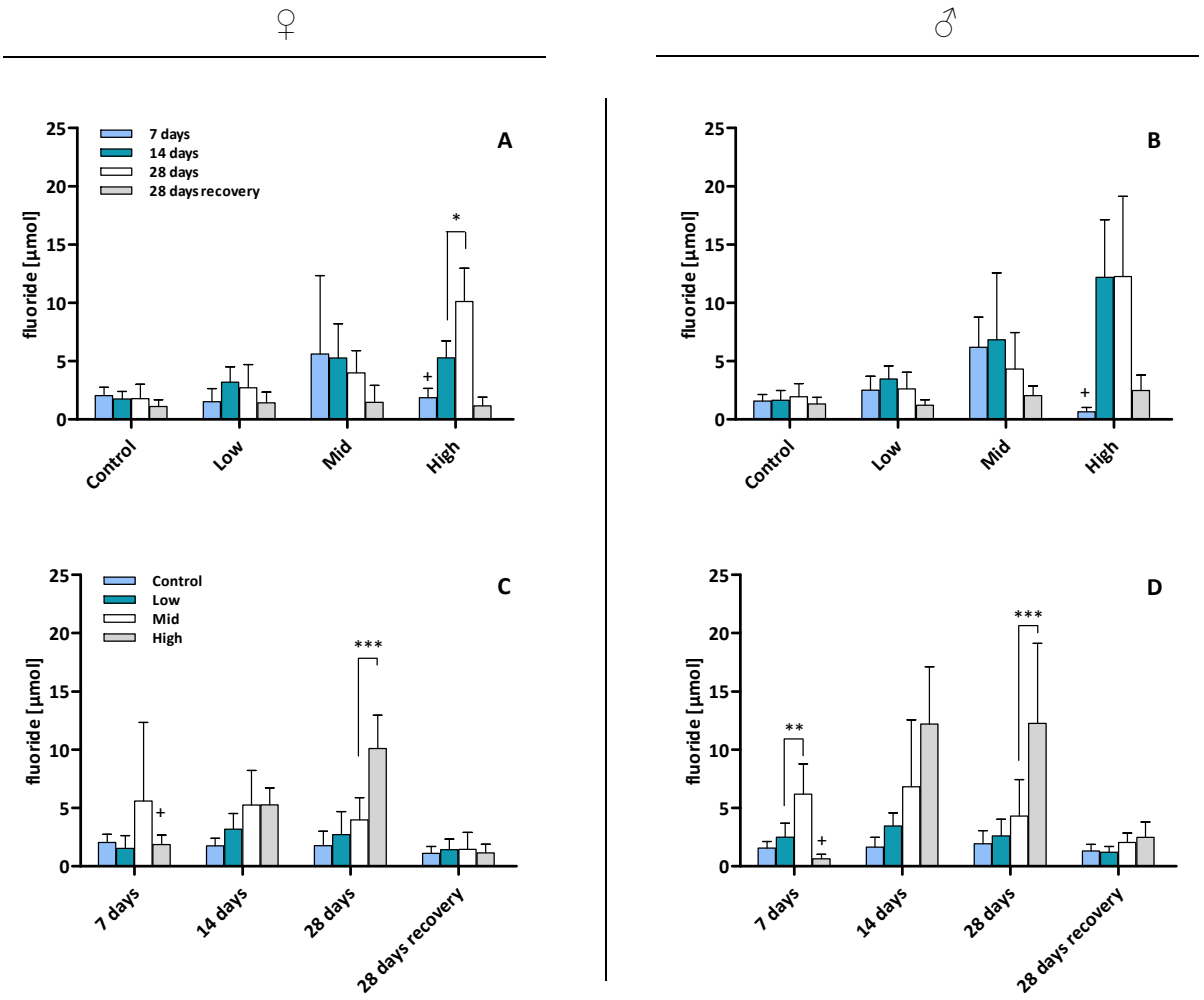

Fig. 24. Total inorganic fluoride excreted in urine within 18 hours after inhalation exposure in female (**A**, **C**) and male (**B**, **D**) rabbits; + no inhalation exposure on day 7; one-way ANOVA, Tukey post test, * $p < 0.05$, ** $p < 0.01$, *** $p < 0.001$.

Inorganic fluoride levels in serum in general increased dose-dependently in male rabbits of the 7- and 28-day exposure groups and in female rabbits exposed for 28 days (Fig. 25, C and D). Nevertheless these trends were not consistently significant. In the 7 day exposure groups of female rabbits, serum fluoride levels increased only in the low and mid dose exposures with only the latter difference being significant. The increase observed for male rabbits exposed to the high dose for 14 days, was not significant (Fig. 25, D). As already determined for urinary inorganic fluoride excretion, also no significant differences in inorganic fluoride levels were observed for all control serum samples compared with the 28-day recovery groups (Fig. 25, C and D). An exposure time-dependent increase in serum fluoride was seen for high dose exposures of female rabbits, with a significant difference only between 14 and 28 days of exposure (Fig. 25, A; female 14-day exposure, high dose: 3.95 ± 0.20 nmol/mL; female 28-day exposure, high dose: 6.20 ± 1.35 nmol/mL).

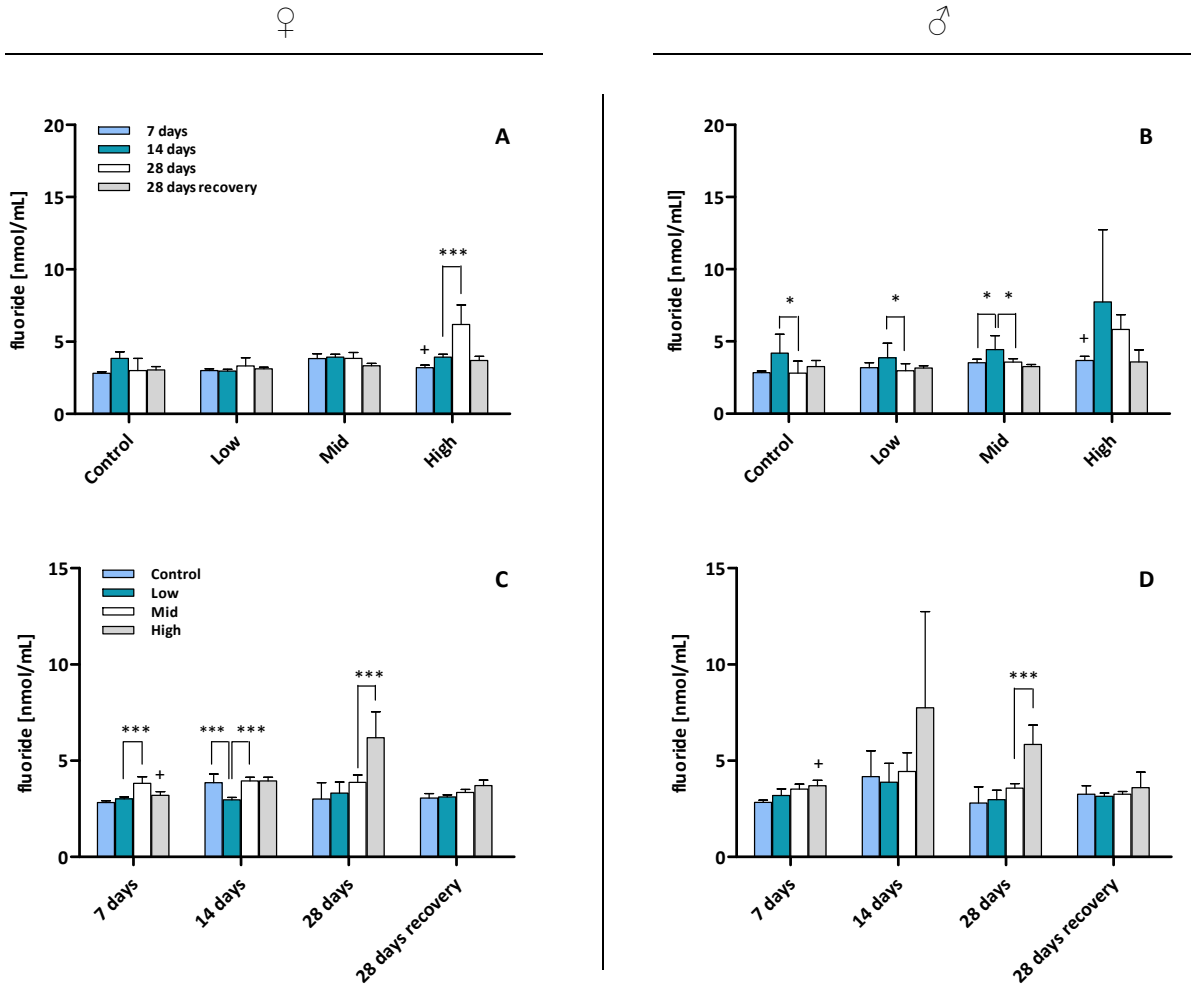

Fig. 25. Inorganic fluoride levels in serum after sacrifice in female (**A**, **C**) and male (**B**, **D**) rabbits; + no inhalation exposure on day 7; one-way ANOVA, Tukey post test, * $p < 0.05$, ** $p < 0.01$, *** $p < 0.001$.

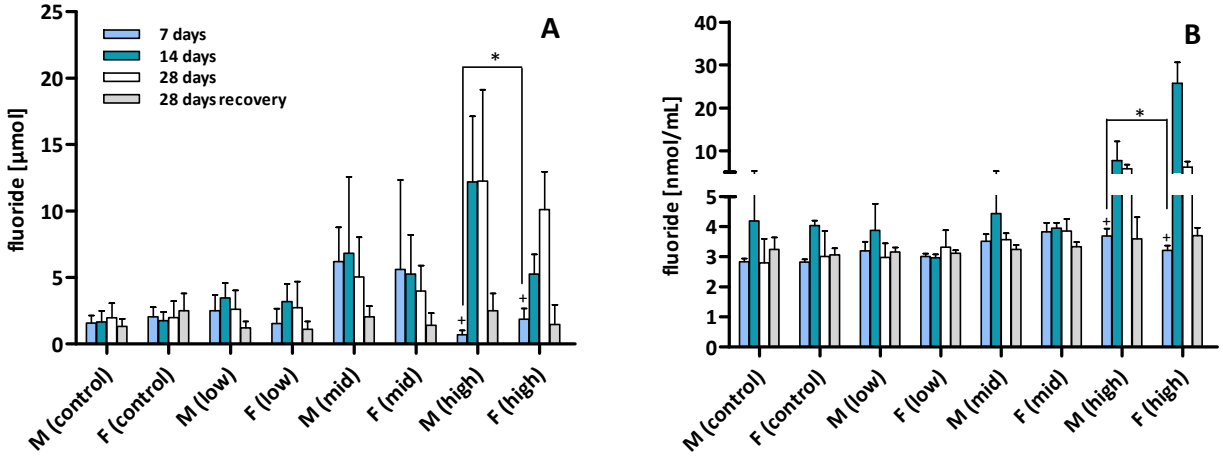

Fig. 26. Total urinary inorganic fluoride excretion within 18 hours after inhalation exposure(**A**); inorganic serum fluoride levels (**B**) after termination of each exposure interval; + no inhalation exposure on day 7; Student's t-test, * $p < 0.05$.

Differences in urinary fluoride excretion and serum levels between male and female rabbits were only significant in the 7-day high dose exposures (Student's t-test – urine: $p = 0.03$; serum: $p = 0.02$). The exposure interruption of the high dose groups on day 7 has to be taken into account (Fig. 26).

3.2.4.2 Quantification of urinary *N*-acetyl-*S*-(3,3,3-trifluoro-2-hydroxypropanyl)-*L*-cysteine excretion by LC-MS/MS

Concentrations of *N*-acetyl-*S*-(3,3,3-trifluoro-2-hydroxypropanyl)-*L*-cysteine in urine were well above the LOQ in all samples of the low, mid and high dose groups exposed to HFO-1234yf for 7, 14 and 28 days. In all samples of the control groups and of the 28-day recovery groups concentrations of *N*-acetyl-*S*-(3,3,3-trifluoro-2-hydroxypropanyl)-*L*-cysteine were below the LOD. Total urinary amounts of *N*-acetyl-*S*-(3,3,3-trifluoro-2-hydroxypropanyl)-*L*-cysteine excreted within 18 hours after the last exposure were generally determined to be dose-dependent (Fig. 27, D and E) but no significant excretion increases were observed between low and mid dose groups of the 14- and 28-day exposures. A time-dependent increase in *N*-acetyl-*S*-(3,3,3-trifluoro-2-hydroxypropanyl)-*L*-cysteine was not observed (Fig. 27, A and B). A significant difference between male and female rabbits (Fig. 27, C) was only observed in low dose 7-day exposure groups (male: 15.58 ± 7.15 µmol; female: 6.76 ± 2.35 µmol; Student's t-test, $p = 0.03$). Expected low absolute excretion values were determined for male (0.09 ± 0.09 µmol) and female (0.20 ± 0.13 µmol) rabbits of the 7-day high dose exposure groups due to the interruption of the inhalations on day 7.

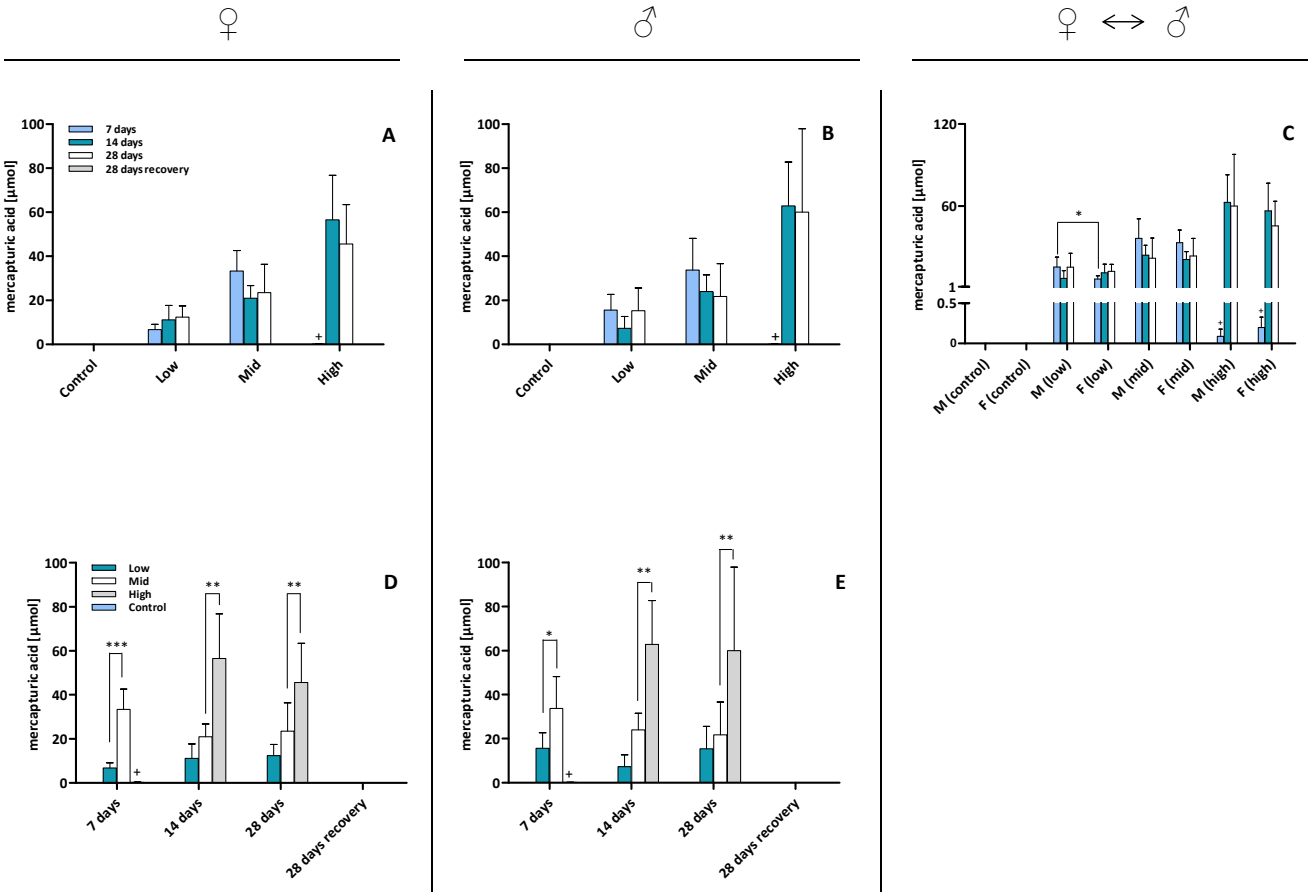

Fig. 27. Total *N*-acetyl-*S*-(3,3,3-trifluoro-2-hydroxypropanyl)-*L*-cysteine excreted in urine within 18 hours after inhalation exposure in female - F (**A**, **C**, **D**) and male - M (**B**, **C**, **E**) rabbits; + no inhalation exposure on day 7; one-way ANOVA, Tukey post test, * $p < 0.05$, ** $p < 0.01$, *** $p < 0.001$ (A, B, C, D); * Student's t-test $p < 0.05$ (C).

3.2.4.3 Quantification of metabolites by LC-MS/MS and ^{19}F-NMR spectroscopy

For relative metabolite quantification, all obtained ^{19}F-NMR signal intensities (normalized to the signal of *N*-acetyl-*S*-(3,3,3-trifluoro-2-hydroxypropanyl)-*L*-cysteine, male rabbit, 28-day high dose exposure) were compared by taking absolute excretion amounts of *N*-acetyl-*S*-(3,3,3-trifluoro-2-hydroxypropanyl)-*L*-cysteine (determined by LC-MS/MS) into account (Fig. 28, Table 20).

An exposure duration-dependent increase in signal intensity could be seen between rabbits exposed for 14 and 28 days. Due to the exposure interruption on day 7, very low signal intensities were obtained for female and male samples of the high dose 7-day exposure groups. This demonstrated the very rapid clearance of both the parent compound and its metabolites. In all analyzed samples, the two main metabolites were identified as *S*-(3,3,3-trifluoro-2-hydroxypropanyl)-mercaptolactic acid and *N*-acetyl-*S*-(3,3,3-trifluoro-2-hydroxypropanyl)-*L*-cysteine representing 43.1 ± 7.4% and 43.3 ± 7.2% of total ^{19}F-NMR signal intensity respectively.

Table 20. Relative HFO-1234yf metabolite excretion: (**A**) *S*-(3,3,3-trifluoro-2-hydroxypropanyl)-mercaptolactic acid, (**B**) *N*-acetyl-*S*-(3,3,3-trifluoro-2-hydroxypropanyl)-*L*-cysteine, (**C**) unidentified metabolite (25), (**D**) unidentified metabolite (24), (**E**) trifluoroacetic acid, (**F**) 3,3,3-trifluoro-1,2-propanediol, (**G**) 3,3,3-trifluoro-2-propanol, (**H**) *S*-(3,3,3-trifluoro-2-hydroxypropanyl)-*L*-cysteine.

Sex	Exposure duration [days]	Exposure conc. [ppm]	Metabolite excretion [µmol]							
			A	B	C	D	E	F	G	H
M	7	500	23.94	21.36	2.47	1.35	0.00	0.00	0.00	0.00
F	7	500	7.40	7.35	3.68	0.70	0.11	0.00	0.00	0.00
M	7	5,500	0.21	0.08	0.02	0.00	0.06	0.00	0.00	0.00
F	7	5,500	0.20	0.03	0.03	0.00	0.01	0.00	0.00	0.00
M	14	5,500/4,500	42.35	31.36	6.72	0.00	0.00	2.26	0.00	0.00
F	14	5,500/4,500	38.27	37.11	13.16	2.11	0.36	1.20	0.00	1.40
M	28	4,500	155.77	269.87	47.03	12.74	1.57	5.37	2.34	2.52
F	28	4,500	70.89	63.95	5.68	6.60	0.55	1.35	0.00	1.02

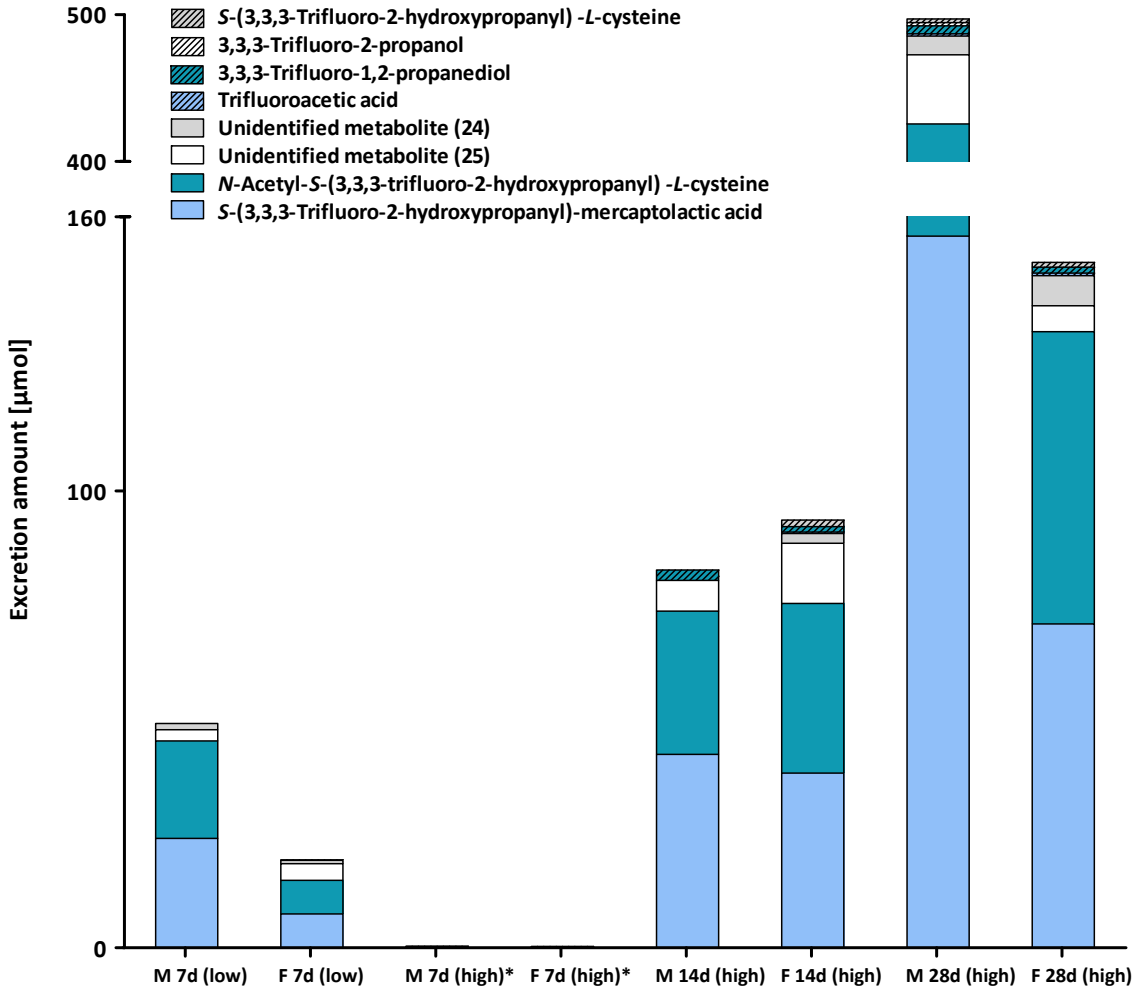

Fig. 28. Totalized excretion of major metabolites in female (F) and male (M) rabbit urines within 18 hours after inhalation exposure (relative quantification by LC-MS/MS and ^{19}F-NMR, one animal per group); normalized to the total excretion amount of *N*-acetyl-*S*-(3,3,3-trifluoro-2-hydroxypropanyl)-*L*-cystein – male rabbits 28 days, high dose exposure; * no inhalation exposure on day 7; low, low dose (500 ppm); high, high dose (5,500/4,500 ppm).

3.2.4.4 Cytochrome P-450 2E1 and 3A4 activity determination

The cytochrome P-450 2E1 and 3A4 activities were evaluated for 3 rabbits per group of the control and the high dose exposures of all four different exposure periods (Fig. 29) to evaluate a possible inductive effect of an HFO-1234yf exposure.

The evaluation for cytochrome P-450 2E1 showed quite stable turnover rates in a range between approximately 0.4 to 0.7 nmol p-nitrocatechol formation per minute and mg protein. Significant increases were only determined between animals of control and high dose subgroups for male rabbits of the 28-day exposure (Student's t-test, $p = 0.03$) and female rabbits of the 7-day exposure (Student's t-test, $p = 0.03$). No changes in enzyme activity, after multiple exposures to HFO-1234yf, were observed for cytochrome P-450 3A4. Turnover rates lay between 2 and 4 nmol 6-ß-hydroxy-testosterone per minute and mg protein.

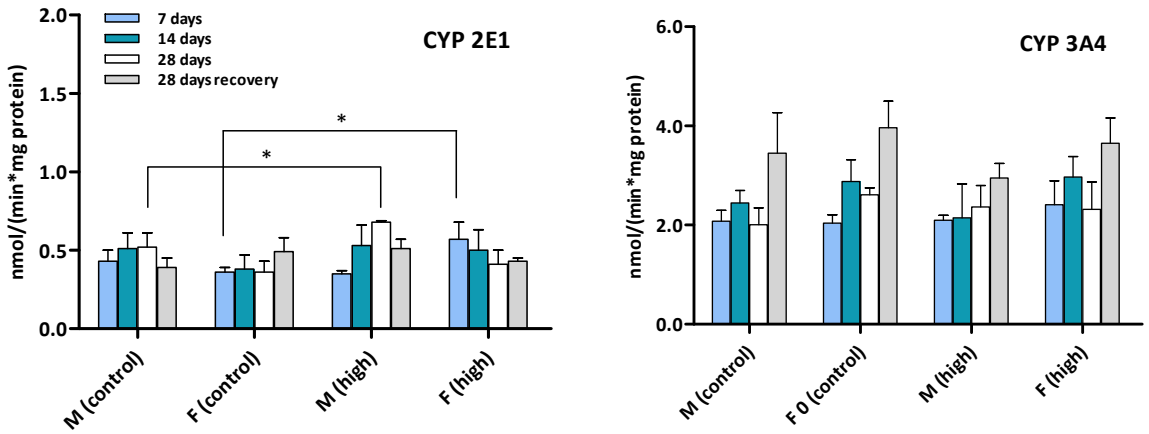

Fig. 29. Cytochrome P-450 2E1 and 3A4 activity in liver microsomes; female (F), male (M); Student's t-test, * $p < 0.05$.

3.3 Biotransformation of *trans*-HCFO-1233zd in male Sprague Dawley rats and female New Zealand White rabbits after single exposure

3.3.1 Inhalation exposures

For *in vivo* biotransformation analysis of HFCO-1233zd, female NZW rabbits (n = 3/concentration) and male SD rats (n = 5/concentration) were exposed to 2,000, 5,000 and 10,000 ppm for 6 hours in an open dynamic exposure system. Measured chamber concentrations of HFCO-1233zd were 1,961 ± 261 ppm, 5,084 ± 549 ppm and 10,089 ± 818 ppm for rabbit and 1,977 ± 256 ppm, 5,220 ± 1,147 ppm and 10,128 ± 714 ppm for rat exposures.

3.3.2 Identification of *trans*-HCFO-1233zd metabolites

3.3.2.1 Urine analysis by ^{19}F-NMR spectroscopy

Predominant metabolites in ^{19}F-NMR spectra of SD rat urine (Fig. 30 and Table 21) were 3,3,3-trifluorolactic acid (**18**, Fig. 30) and *N*-acetyl-*S*-(3,3,3-trifluoro-*trans*-propenyl)-*L*-cysteine (**20**, Fig. 30), representing 32% and 40% of total fluoro related signal intensity (0-6 hour post inhalation urine fraction). Further identified metabolites were *S*-(3,3,3-trifluoro-*trans*-propenyl)-mercaptolactic acid (**26**, Fig. 30), trifluoroacetic acid (**19**, Fig. 30) and 3,3,3-trifluoro-1,2-dihydroxypropane (**17**, Fig. 30). A very weak signal was observed for 3,3,3-trifluoropropionic acid (**27**, Fig. 30). The structures of the chemical entities giving the doublets at -71.3, -72.4 and -77.1 ppm (**24**, Fig. 30) as well as the doublet of doublets at -61.5 ppm could not be identified. Nevertheless, metabolite 24 (Fig. 30) is probably a conjugation product of 3,3,3-trifluoro-1,2-propanediol as previously mentioned for the metabolism of HFO-1234yf. Spectra from rabbit urine (Fig. 31 and Table 22) did not show a signal for 3,3,3-trifluorolactic acid. The major metabolite was assigned to *N*-acetyl-*S*-(3,3,3-trifluoro-*trans*-propenyl)-*L*-cysteine (**20**, Fig. 31) representing 46% of total ^{19}F-NMR signal intensity (0-6 hour post inhalation urine fraction). *S*-(3,3,3-trifluoro-*trans*-propenyl)-mercaptolactic acid (**26**, Fig. 31), trifluoroacetic acid (**19**, Fig. 31) and 3,3,3-trifuoro-1,2-dihydroxypropane (**17**, Fig. 31) were also present in rabbit urine. Besides, additional signals were observed at -72.3, -72.4, -77.1 and -62.1 ppm, the latter assigned to *S*-(3,3,3-trifluoro-*trans*-propenyl)-*L*-cysteine (**21**, Fig. 31). A weak signal for 3,3,3-trifluoro-1-propanol was seen at -64.3 ppm (**28**, Fig. 31) chemical shift. Again, the chemical entity giving the doublets appearing at – 72.3, -72.4 and -77.1 ppm (**24**, Fig. 31) could not be elucidated.

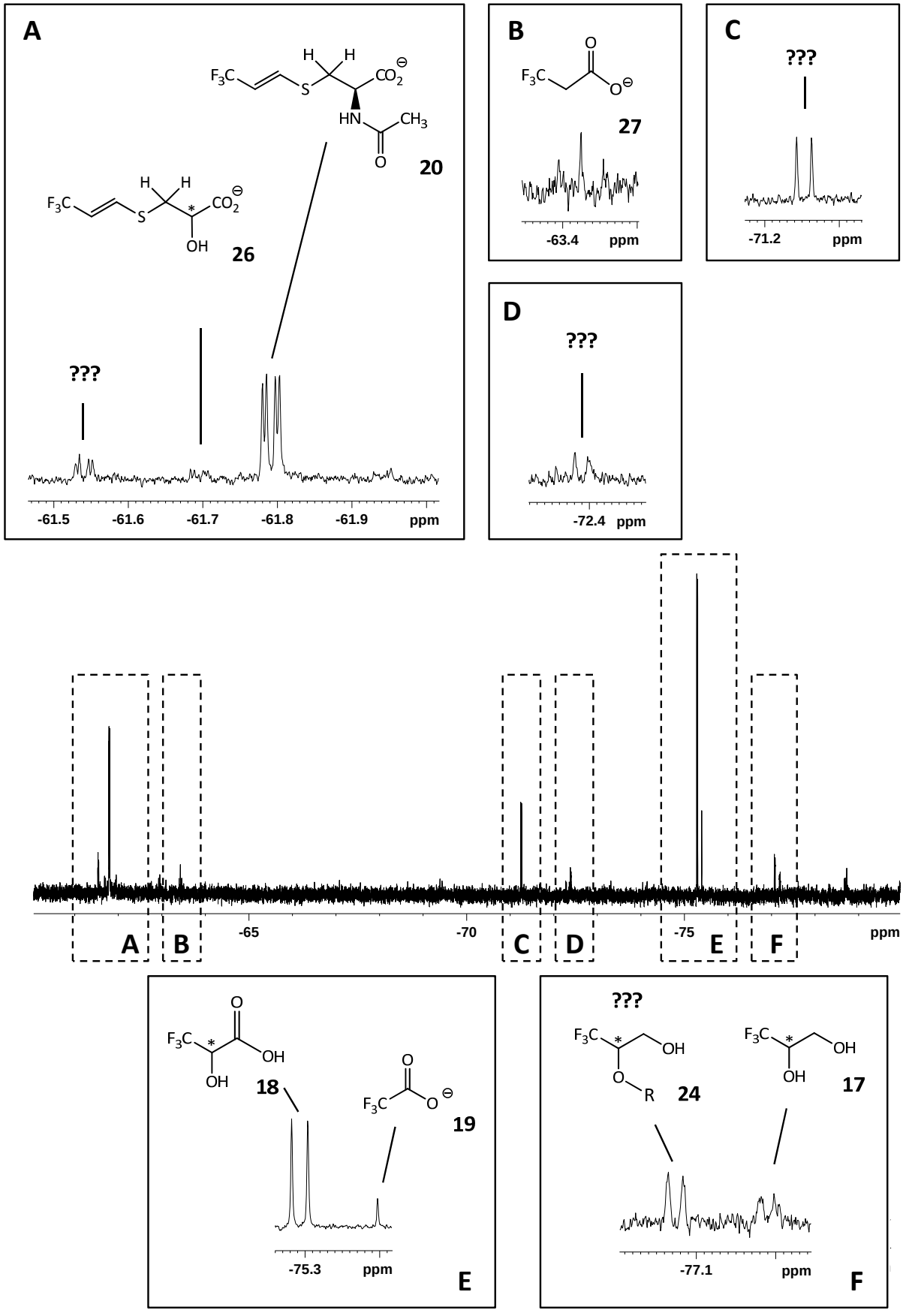

Fig. 30. ^{19}F-NMR spectra of urine sample from SD rat (0-6 hour post inhalation urine fraction) exposed to 10,000 ppm of *trans*-HCFO-1233zd for 6 hours.

Table 21. Metabolites of *trans*-HCFO-1233zd observed in ^{19}F-NMR spectra of SD rat urine after a 6-hour inhalation exposure.

Compound	Chemical shift [ppm]	Multiplicity	^{1}H - ^{19}F Coupling constants [Hz]
Unidentified metabolite	- 61.5	dd	$^{3}J_{HF}$ = 6.7 Hz, $^{4}J_{HF}$ = 2.1 Hz
S-(3,3,3-Trifluoro-*trans*-propenyl)-mercaptolactic acid (26)	- 61.7	dd	$^{3}J_{HF}$ = 6.6 Hz, $^{4}J_{HF}$ = 2.1 Hz
N-Acetyl-*S*-(3,3,3-trifluoro-*trans*-propenyl)-*L*-cysteine (20)	-61.8	dd	$^{3}J_{HF}$ = 6.6 Hz, $^{4}J_{HF}$ = 2.1 Hz
3,3,3-Trifluoropropionic acid (27)	-63.4	t	$^{3}J_{HF}$ = 11.4 Hz
Unidentified metabolite	- 71.3	d	$^{3}J_{HF}$ = 7.5 Hz
Unidentified metabolite	- 72.4	d	$^{3}J_{HF}$ = 6.3 Hz
3,3,3-Trifluorolactic acid (18)	-75.3	d	$^{3}J_{HF}$ = 8.2 Hz
Trifluoroacetic acid (19)	-75.4	s	-
Unidentified metabolite (24)	- 77.1	d	$^{3}J_{HF}$ = 7.0 Hz
3,3,3-Trifluoro-1,2-propanediol (17)	-77.2	d	$^{3}J_{HF}$ = 7.3 Hz

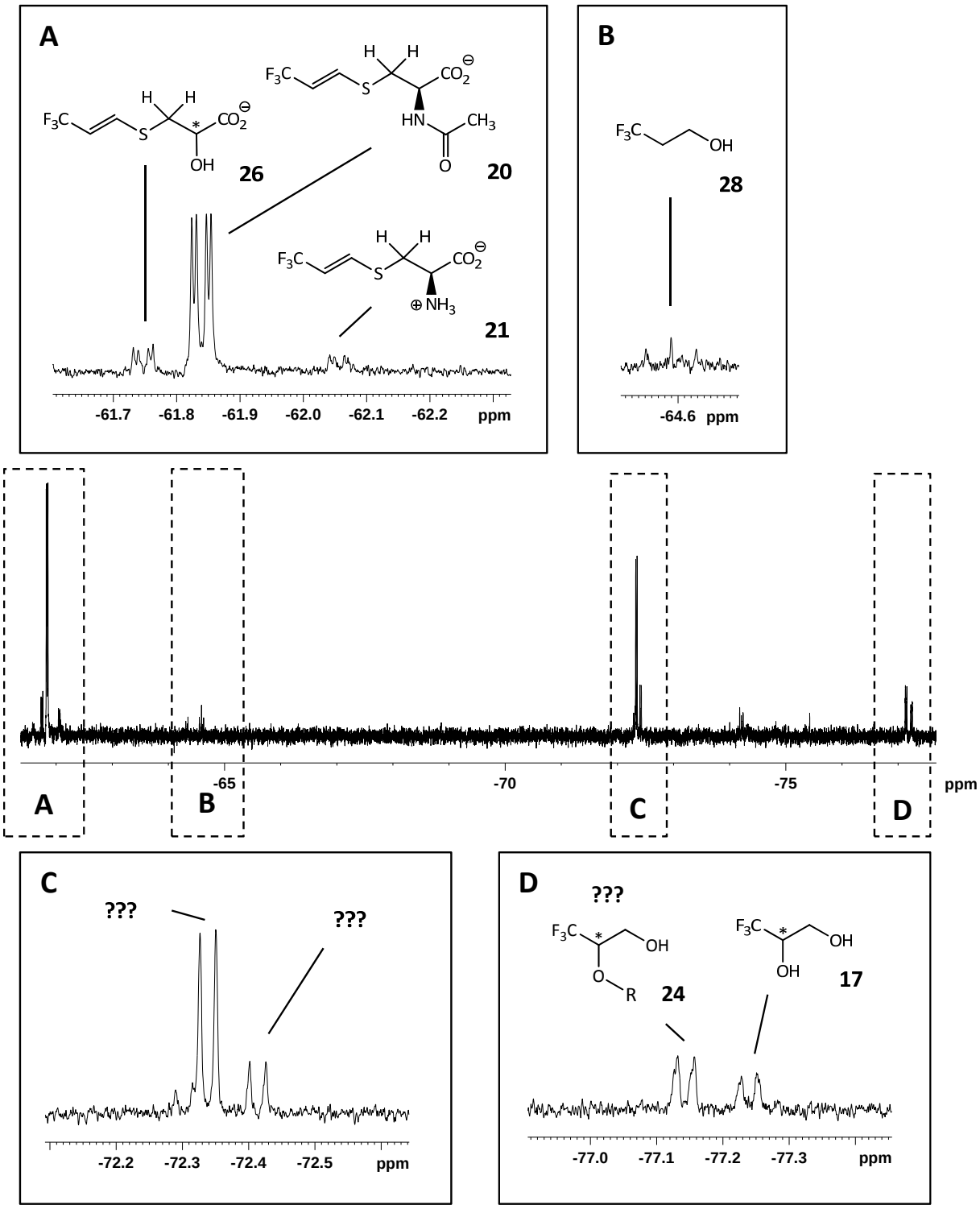

Fig. 31. ^{19}F-NMR spectra of urine sample from NZW rabbit (0-6 hour post inhalation urine fraction) exposed to 10,000 ppm of *trans*-HCFO-1233zd for 6 hours.

Table 22. Metabolites of trans-HCFO-1233zd observed in ^{19}F-NMR spectra of NZW rabbit urine after a 6-hour inhalation exposure.

Compound	Chemical shift [ppm]	Multiplicity	^{1}H - ^{19}F Coupling constants [Hz]
S-(3,3,3-Trifluoro-*trans*-propenyl)-mercaptolactic acid (26)	- 61.7	dd	$^{3}J_{HF}$ = 6.6 Hz, $^{4}J_{HF}$ = 2.1 Hz
N-Acetyl-*S*-(3,3,3-trifluoro-*trans*-propenyl)-*L*-cysteine (20)	-61.8	dd	$^{3}J_{HF}$ = 6.6 Hz, $^{4}J_{HF}$ = 2.1 Hz
S-(3,3,3-Trifluoro-*trans*-propenyl)-*L*-cysteine (21)	-62.1	dd	$^{3}J_{HF}$ = 6.5 Hz, $^{4}J_{HF}$ = 2.1 Hz
3,3,3-Trifluoro-1-propanol (28)	- 64.6	t	$^{3}J_{HF}$ = 11.2 Hz
Unidentified metabolite	- 72.3	d	$^{3}J_{HF}$ = 6.7 Hz
Unidentified metabolite	- 72.4	d	$^{3}J_{HF}$ = 7.0 Hz
Unidentified metabolite (24)	- 77.1	d	$^{3}J_{HF}$ = 7.0 Hz
3,3,3-Trifluoro-1,2-propanediol (17)	-77.2	d	$^{3}J_{HF}$ = 7.3 Hz

3.3.2.2 Urine analysis by GC/MS

Minor volatile metabolites in urine were detected by GC/MS analysis (Fig. 32). Trifluoroactetic acid, 3,3,3-trifluoropropionic acid and 3,3,3-trifluoro-1,2-propanediol could be confirmed in rat and rabbit urine with similar retention times and fragmentation as standard substances. As observed in ^{19}F-NMR spectra, 3,3,3-trifluoro-1-propanol could only be determined in rabbit urine.

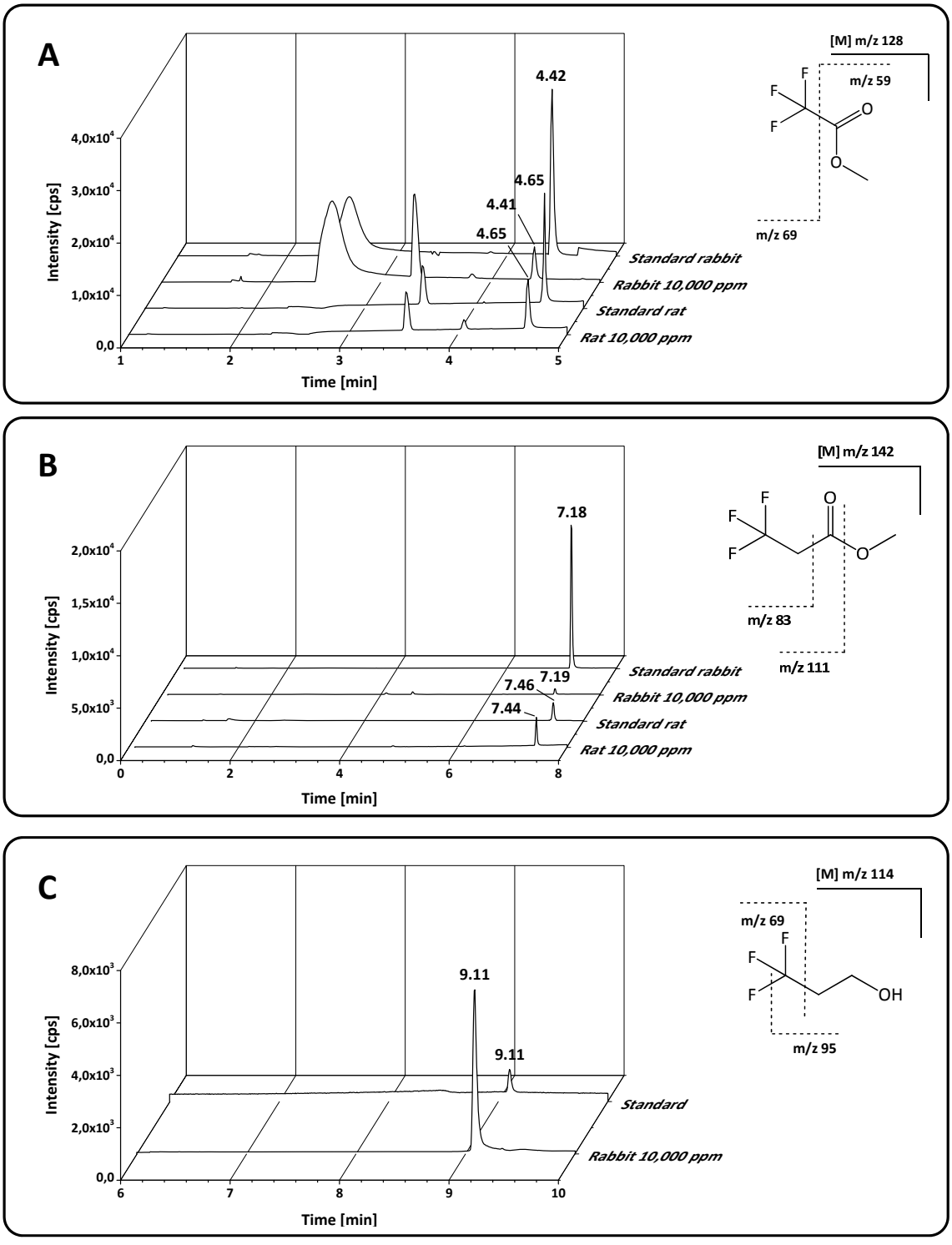

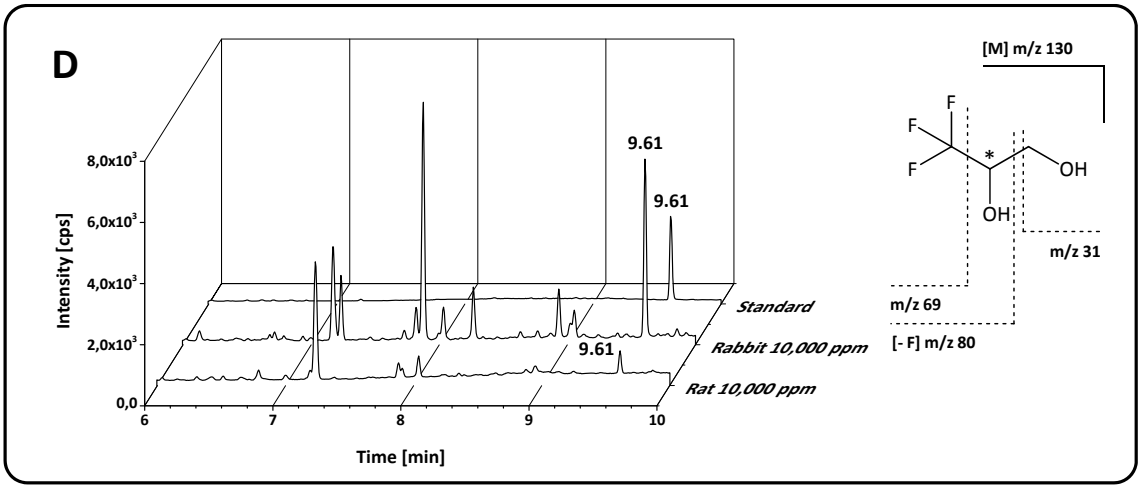

Fig. 32. GC/MS chromatogram of (**A**) trifluoroacetic acid, methyl ester (m/z 59 monitored), (**B**) 3,3,3-trifluoropropionic acid, methyl ester (m/z 111 monitored), (**C**) 3,3,3-trifluoro-1-propanol (m/z 95 monitored), (**D**) 3,3,3-trifluoro-1,2-propanediol (m/z 80 monitored) in urine samples from rats (6-12 hour post-inhalation fraction; 10,000 ppm) and rabbits (0-6 hour post-inhalation fraction; 10,000 ppm). Standard substances were solved in rat or rabbit urine.

3.3.2.3 Urine and plasma analysis by LC-MS/MS

The main *in vitro* and *in vivo* metabolites, already determined by ^{19}F-NMR, were confirmed by LC-MS/MS in the sensitive MRM-EPI scan mode (Fig. 33): *S*-(3,3,3-trifluoro-*trans*-propenyl)-glutathione (A)*, N*-acetyl-*S*-(3,3,3-trifluoro-*trans*-propenyl)-*L*-cysteine (B)*,* 3,3,3-trifluorolactic acid (C)*, S*-(3,3,3-trifluoro-*trans*-propenyl)-mercaptolactic acid (D), *S*-(3,3,3-trifluoro-*trans*-propenyl)-*L*-cysteine (E). Metabolite retention times and their fragmentation patterns in the negative scan mode were compared to synthesized or purchased standards. In all samples, metabolites showed the same retention times and fragmentation patterns as their standard substances. Only *S*-(3,3,3-trifluoro-*trans*-propenyl)-mercaptolactic acid in rabbit urine (R_t = 20.3 min) showed a slight retention time drift compared to the standard spectrum in water (R_t = 20.5 min).

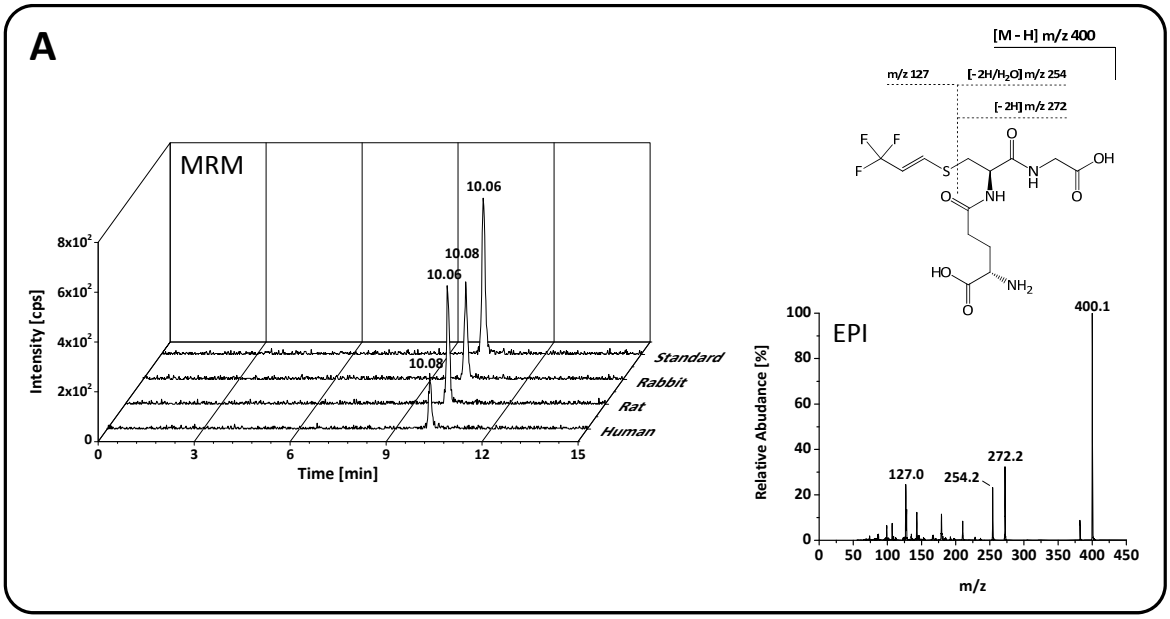
A
MRM
Intensity [cps]
Time [min]
10.06
10.08
10.06
10.08
Standard
Rabbit
Rat
Human
[M - H] m/z 400
m/z 127
[- 2H/H2O] m/z 254
[- 2H] m/z 272
EPI
Relative Abudance [%]
m/z
400.1
272.2
254.2
127.0

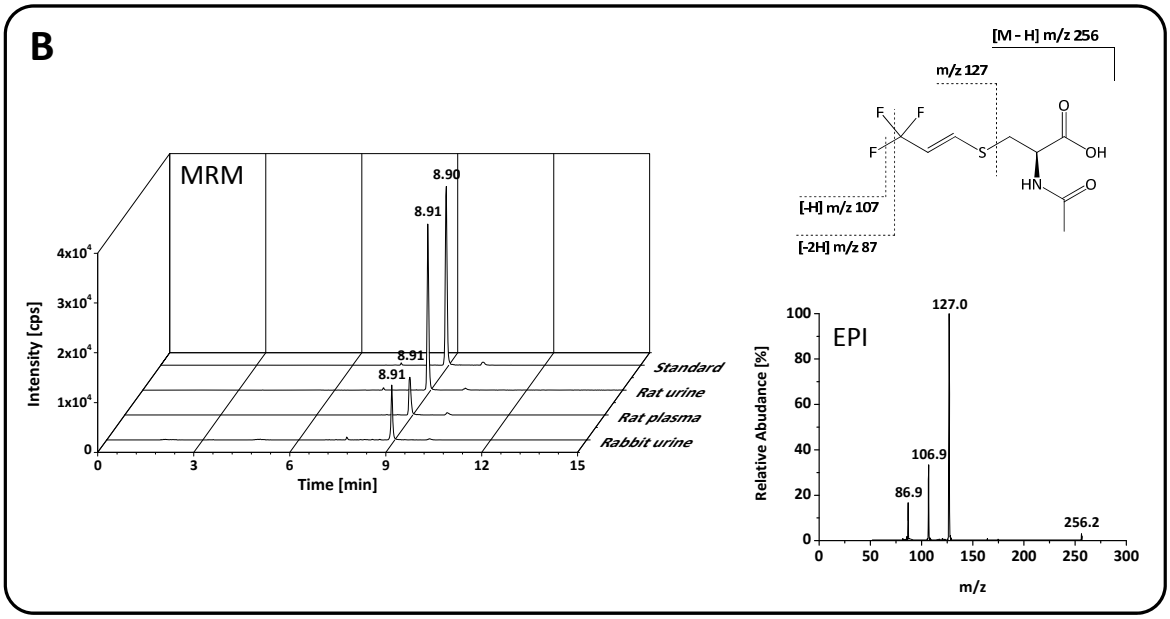
B
MRM
Intensity [cps]
Time [min]
8.90
8.91
8.91
8.91
Standard
Rat urine
Rat plasma
Rabbit urine
[M - H] m/z 256
m/z 127
[-H] m/z 107
[-2H] m/z 87
EPI
Relative Abudance [%]
m/z
127.0
106.9
86.9
256.2

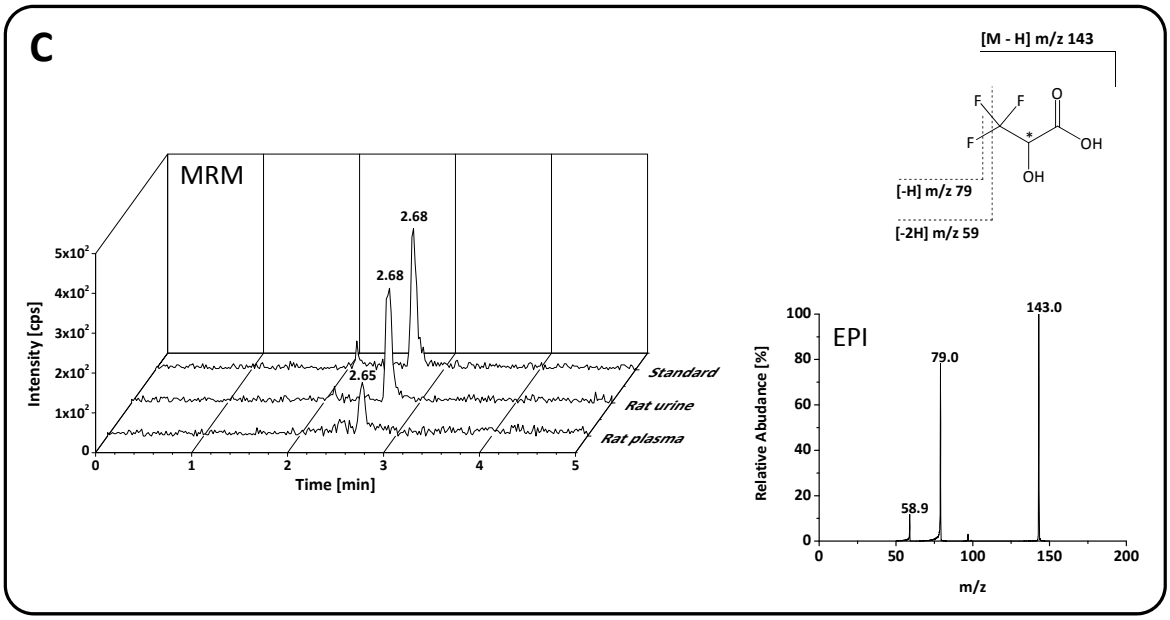
C
MRM
Intensity [cps]
Time [min]
2.68
2.68
2.65
Standard
Rat urine
Rat plasma
[M - H] m/z 143
[-H] m/z 79
[-2H] m/z 59
EPI
Relative Abudance [%]
m/z
143.0
79.0
58.9

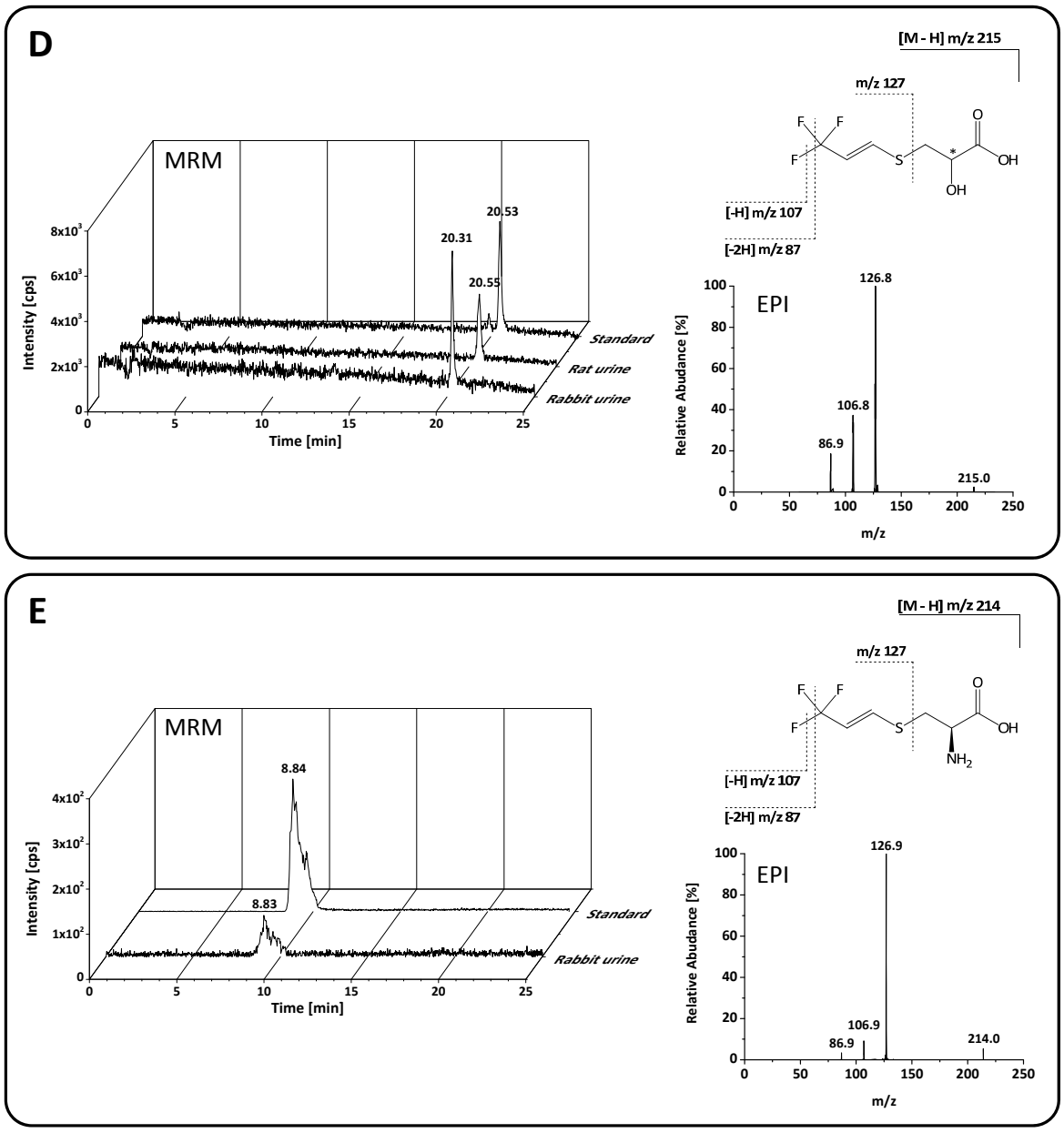

Fig. 33. LC-MS/MS (MRM-EPI operation mode with negative ionization) chromatograms and spectra of (**A**) *S*-(3,3,3-trifluoro-*trans*-propenyl)-glutathione (MRM: m/z 400-272), (**B**) *N*-acetyl-*S*-(3,3,3-trifluoro-*trans*-propenyl)-*L*-cysteine (MRM: m/z 256-127), (**C**) 3,3,3-trifluorolactic acid (MRM: m/z 143-79), (**D**) *S*-(3,3,3-trifluoro-*trans*-propenyl)-mercaptolactic acid (MRM: m/z 215-127) and (**E**) *S*-(3,3,3-trifluoro-*trans*-propenyl)-*L*-cysteine (MRM: m/z 214-127) in *in vitro* microsomal incubations (A: standard in water – 0.32 µg/mL, rat, rabbit and human subcellular liver cell fraction incubation supernatants) and *in vivo* specimen (B: standard in water – 19.5 ng/mL, rat urine – high dose/0-6 hour fraction, rat plasma – high dose/0 hour post-inhalation, rabbit urine – high dose/6-12 hour fraction; C: standard in water – 17.5 ng/mL, rat urine – high-dose/0-6 hour fraction, rat plasma – high dose/0 hour post-inhalation; D: standard in water, rat urine – high dose/0-6 hour fraction, rabbit urine – high dose/0-6 hour fraction; E: standard in conrol rabbit urine – 10 ng/mL, rabbit urine – high dose/0-6 hour fraction).

3.3.2.4 Determination of minor metabolites by LC-MS/MS

In order to identify further unknown metabolites observed in *in vitro* and *in vivo* ^{19}F-NMR spectra, LC-MS/MS experiments were performed in the CNL/EPI, EMS/EPI and MRM/EPI scan mode with negative ionization. Besides already known metabolites, one new structure was determined in rabbit urine. The obtained EPI spectrum was assigned to *N*-acetyl-*S*-(3,3,3-trifluoro-*trans*-propenyl)-*L*-cysteine sulfoxide (Fig. 34) showing the characteristic fragmentation pattern of *trans*-HCFO-1233zd conjugates with a loss of two molecules of hydrogen fluoride (CNL, 20 m/z) and the common CNL of mercapturic acids (129 m/z). The structure proposal was only based on mass spectra (EPI) and could not be confirmed by comparison with a synthesized standard. No additional biotransformation product could be determined in rat urine.

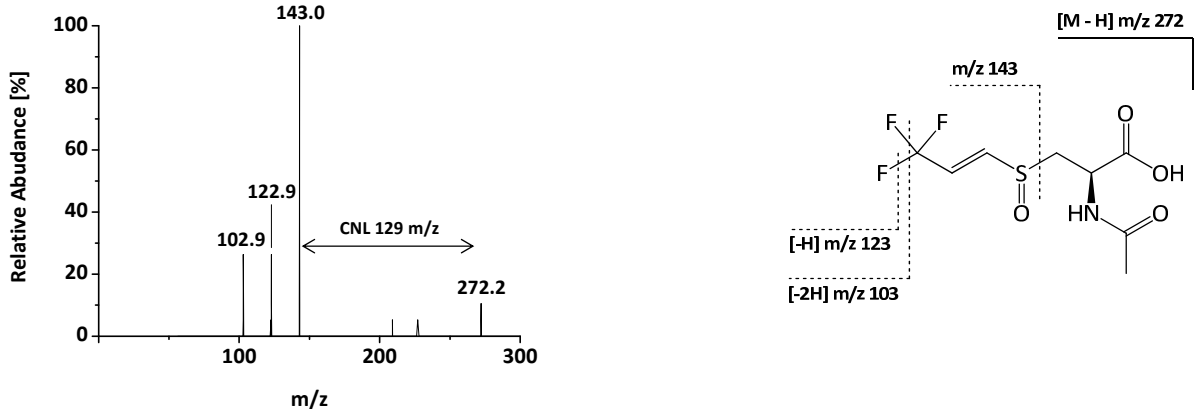

Fig. 34. LC/MS EPI spectrum of N-acetyl-S-(3,3,3-trifluoro-trans-propenyl)-L-cysteine sulfoxide in rabbit urine (R_t 12.8 min).

3.3.3 Quantitative analysis of *trans*-HCFO-1233zd metabolites

In vivo excretion kinetics were determined by LC-MS/MS quantification of *N*-acetyl-*S*-(3,3,3-trifluoro-*trans*-propenyl)-*L*-cysteine in rat and rabbit urine as well as of 3,3,3-trifluorolactic acid in rat urine (Fig. 35).

3.3.3.1 Determination of urinary *N*-acetyl-*S*-(3,3,3-trifluoro-*trans*-propenyl)-*L*-cysteine excretion kinetics

The excretion profiles of *N*-acetyl-*S*-(3,3,3-trifluoro-*trans*-propenyl)-*L*-cysteine (Fig. 35, A/B) showed a first order kinetics with peak excretion levels in the 0-6 hour post-inhalation fractions in rats and rabbits. Fast *N*-acetyl-*S*-(3,3,3-trifluoro-*trans*-propenyl)-*L*-cysteine excretion was indicated by high metabolite recoveries (compared to whole recovery within 48 hours – Table 23) within the first 24 hours after termination of the inhalation exposure:

98.2 ± 3.0% in rats and 97.1 ± 3.5% in rabbits. Urinary excretion half-life times were determined as 4.3 ± 4.4 hours in rats and 2.9 ± 2.1 hours in rabbits.

3.3.3.2 Determination of *N*-acetyl-*S*-(3,3,3-trifluoro-*trans*-propenyl)-*L*-cysteine excretion kinetics in rat plasma

In addition to urinary excretion, concentration levels of *N*-acetyl-*S*-(3,3,3-trifluoro-*trans*-propenyl)-*L*-cysteine were determined in rat plasma (Fig. 35, C). Mean peak levels were observed 0 hours after termination of the inhalation exposure in all three exposure groups. Concentrations then decreased, following a first order kinetics with a higher decline in the 2,000 and 5,000 ppm exposure groups compared to the 10,000 ppm exposure group. *N*-acetyl-*S*-(3,3,3-trifluoro-*trans*-propenyl)-*L*-cysteine was not detectable in the plasma samples taken after 48 hours post-exposure. In general, concentration levels were higher in the 10,000 ppm exposure group compared to the 5,000 and 2,000 ppm exposure groups, with the latter showing almost an equal concentration time course. Statistically, no difference between plasma concentrations could be determined between all groups at any time (one-way ANOVA, Tukey post-test, $p > 0.05$).

3.3.3.3 Determination of urinary 3,3,3-triflurorolactic acid excretion kinetics

The first order urinary excretion profiles of 3,3,3-trifluorolactic acid (Fig. 35, D) revealed peak excretion levels in the 6-12 hour post-inhalation fractions. Fast excretion was indicated by high metabolite recoveries (compared to whole recovery within 48 hours – Table 23) within the first 24 hours after termination of the inhalation exposure (87.2 ± 4.4%). Urinary excretion half-life time was determined as 5.6 ± 3.8 hours.

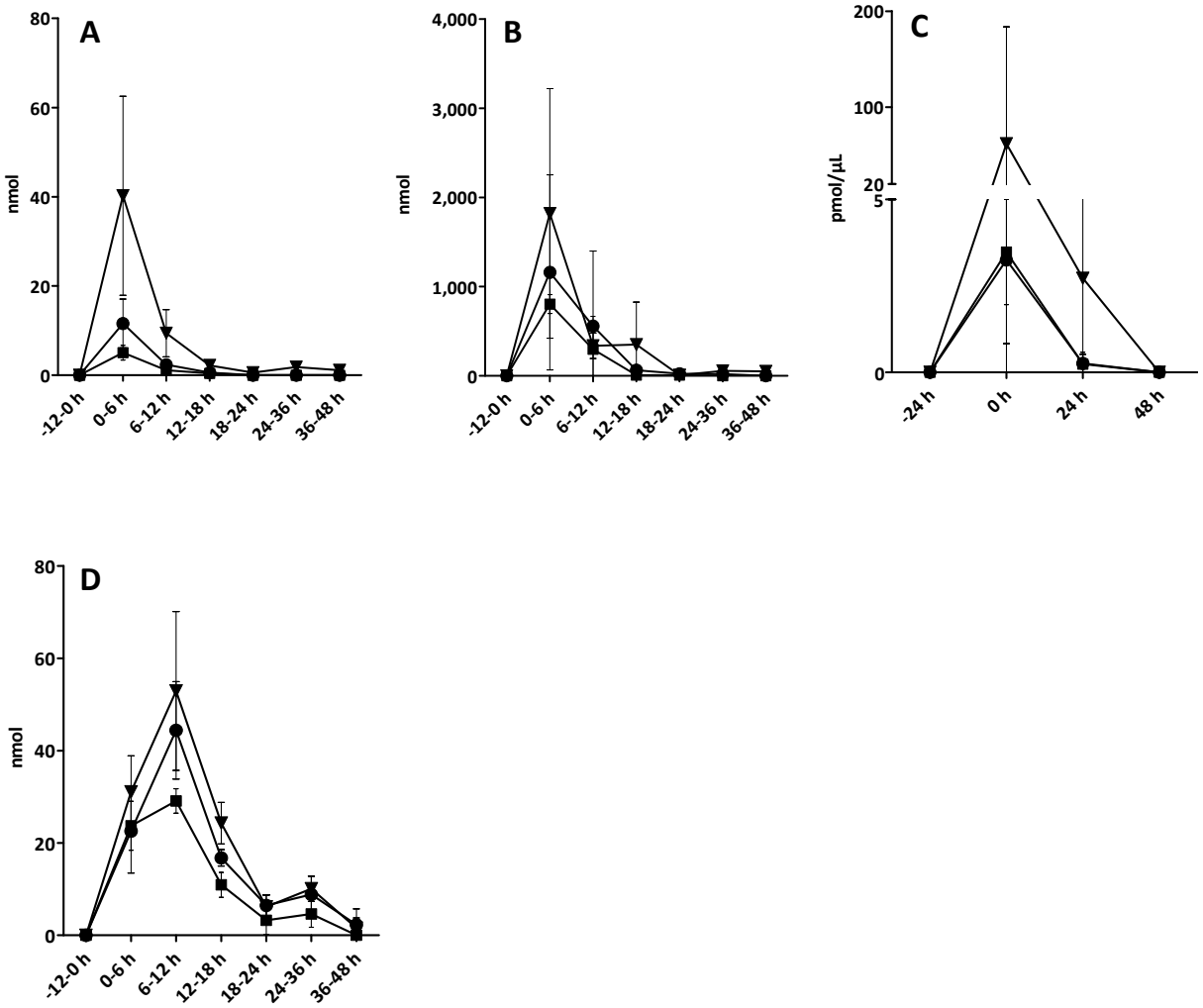

Fig. 35. Metabolite excretion in urine and metabolite plasma levels after whole-body inhalation of *trans*-HCFO-1233zd for 6 hours to 10,000 ppm (▼), 5,000 ppm (●) and 2,000 ppm (■): *N*-acetyl-*S*-(3,3,3-trifluoro-*trans*-propenyl)-*L*-cysteine in rat (**A**), rabbit urine (**B**) and in rat plasma (**C**); 3,3,3-trifluorolactic acid in rat urine (**D**).

Table 23. Metabolites of HFO-1233zd excreted in urine of male rats and female rabbits after a 6-hour whole-body inhalation exposure: *N*-acetyl-*S*-(3,3,3-trifluoro-*trans*-propenyl)-*L*-cysteine (MA) and 3,3,3-trifluorolactic acid (TFLA).

Fraction	Metabolite	Rabbit 10,000 ppm	Rabbit 5,000 ppm	Rabbit 2,000 ppm	Rat 10,000 ppm	Rat 5,000 ppm	Rat 2,000 ppm
0-6 h	**MA** [nmol] (cumulative excretion [%] of the total 48 h - excretion)	1,820.4 ± 1,399.1 (49.7 ± 43.8%)	1,160.4 ± 1,095.0 (84.5 ± 10.1%)	803.6 ± 105.6 (89.3 ± 10.5%)	40.3 ± 22.3 (71.1 ± 15.0%)	11.6 ± 5.5 (75.1 ± 20.5%)	5.1 ± 1.7 (76.9 ± 4.9%)
6-12 h		336.8 ± 143.6 (60.2 ± 52.4%)	556.4 ± 841.5 (91.6 ± 6.3%)	297.5 ± 368.4 (98.5 ± 1.2%)	9.4 ± 5.3 (89.2 ± 5.5%)	2.3 ± 0.9 (94.9 ± 5.2%)	1.1 ± 0.4 (95.1 ± 3.4%)
12-18 h		350.3 ± 477.4 (93.9 ± 3.1%)	63.4 ± 42.4 (96.2 ± 6.3%)	9.3 ± 3.2 (99.6 ± 0.7%)	2.2 ± 1.3 (93.6 ± 2.9%)	0.6 ± 0.3 (100%)	0.4 ± 0.2 (100%)
18-24 h		2.3 ± 3.9 (94.0 ± 3.2%)	7.6 ± 13.1 (97.7 ± 3.7%)	no urine	0.6 ± 0.3 (94.7 ± 2.7%)	< LOQ (100%)	< LOQ (100%)
24-36 h		55.8 ± 11.7 (96.1 ± 4.5%)	20.1 ± 18.0 (100%)	3.1 ± 5.3 (100%)	1.8 ± 0.6 (98.3 ± 1.7%)	< LOQ (100%)	< LOQ (100%)
36-48 h		50.1 ± 37.9 (100%)	< LOQ (100%)	< LOQ (100%)	1.1 ± 0.8 (100%)	< LOQ (100%)	< LOQ (100%)
0-48 h		1,878.0 ± 1,310.8 (100%)	1,414.3 ± 827.5 (100%)	845.6 ± 94.0 (100%)	55.2 ± 22.6 (100%)	14.5 ± 4.5 (100%)	6.5 ± 2.0 (100%)
0-6 h	**TFLA** [nmol] (cumulative excretion [%] of the total 48 h - excretion)	< LOD	< LOD	< LOD	29.4 ± 4.0 (23.2 ± 2.1%)	16.7 ± 6.6 (17.6 ± 6.7%)	21.2 ± 2.5 (29.3 ± 4.1%)
6-12 h		< LOD	< LOD	< LOD	46.0 ± 13.3 (58.5 ± 3.6%)	41.7 ± 5.6 (61.9 ± 3.9%)	27.9 ± 1.5 (68.1 ± 6.3%)
12-18 h		< LOD	< LOD	< LOD	24.9 ± 6.4 (77.9 ± 1.9%)	17.9 ± 5.2 (81.0 ± 7.5%)	11.5 ± 1.5 (83.9 ± 6.2%)
18-24 h		< LOD	< LOD	< LOD	8.6 ± 2.3 (84.6 ± 1.4%)	7.7 ± 3.4 (89.1 ± 5.4%)	2.9 ± 3.2 (87.9 ± 4.7%)
24-36 h		< LOD	< LOD	< LOD	12.5 ± 2.4 (94.4 ± 1.3%)	5.7 ± 3.9 (94.8 ± 3.8%)	6.6 ± 3.0 (96.8 ± 2.0%)
36-48 h		< LOD	< LOD	< LOD	7.3 ± 2.2 (100%)	5.0 ± 3.7 (100%)	2.3 ± 1.5 (100%)
0-48 h		< LOD	< LOD	< LOD	128.6 ± 25.9 (100%)	94.7 ± 14.1 (100%)	72.4 ± 4.1 (100%)

3.3.4 *In vitro* incubations with liver subcellular fractions

3.3.4.1 Metabolite identification by ^{19}F-NMR spectroscopy

Incubations of liver subcellular fractions with *trans*-HCFO-1233zd were performed both in the presence or absence of glutathione and/or NADPH regenerating system. The major signal observed in ^{19}F-NMR spectra (Fig. 36 and Table 24) of incubations with rat, rabbit and human subcellular liver fractions was allocated to *S*-(3,3,3-trifluoro-*trans*-propenyl)-glutathione (**23**, Fig. 36 A, B, C). Minor metabolites observed in incubations of *trans*-HCFO-1233zd in rat liver microsomes were identified as 3,3,3-trifluorolactic acid (**18**, Fig. 36 A), 3,3,3-trifluoro-1,2-propanediol (**17**, Fig. 36 A) and 3,3,3-trifluoro-1-hydroxyacetone (**16**, Fig. 36 A). ^{19}F-NMR spectra of rabbit microsomal incubations also showed several minor metabolites and three signals were attributed to 3,3,3-trifluorolactic acid (**18**, Fig. 36 B), 3,3,3-trifluoro-1,2-propanediol (**17**, Fig. 36 B) and 3,3,3-trifluoro-1-propanol (**28**, Fig. 36 B). The minor biotransformation products were present both in incubations containing a NADPH regenerating system and glutathione or only a NADPH regenerating system.

Table 24. ^{19}F-NMR signals observed in microsomal incubations (rat, rabbit and human) with liquefied *trans*-HCFO-1233zd.

Compound	Chemical shift [ppm]	Multiplicity	^{1}H - ^{19}F Coupling constants [Hz]
N-Acetyl-*S*-(3,3,3-trifluoro-*trans*-propenyl)-glutathione (20)	-62.0	dd	$^{3}J_{HF}$ = 6.5, $^{4}J_{HF}$ = 2.1
trans-HCFO-1233zd (3)	-63.2	dd	$^{3}J_{HF}$ = 6.6, $^{4}J_{HF}$ = 2.2
3,3,3-Trifluoro-1-propanol (28)	-64.3	t	$^{3}J_{HF}$ = 11.2
Unidentified metabolite	-73.5	d	$^{3}J_{HF}$ = 4.9
3,3,3-Trifluorolactic acid (18)	-75.4	d	$^{3}J_{HF}$ = 8.2
3,3,3-Trifluoro-1,2-propanediol (17)	-77.2	d	$^{3}J_{HF}$ = 7.3
Unidentified metabolite	-81.5	s	-
3,3,3-Trifluoro-1-hydroxyacetone (16)	-83.4	s	-
Unidentified metabolite	-84.8	d	$^{3}J_{HF}$ = 4.0

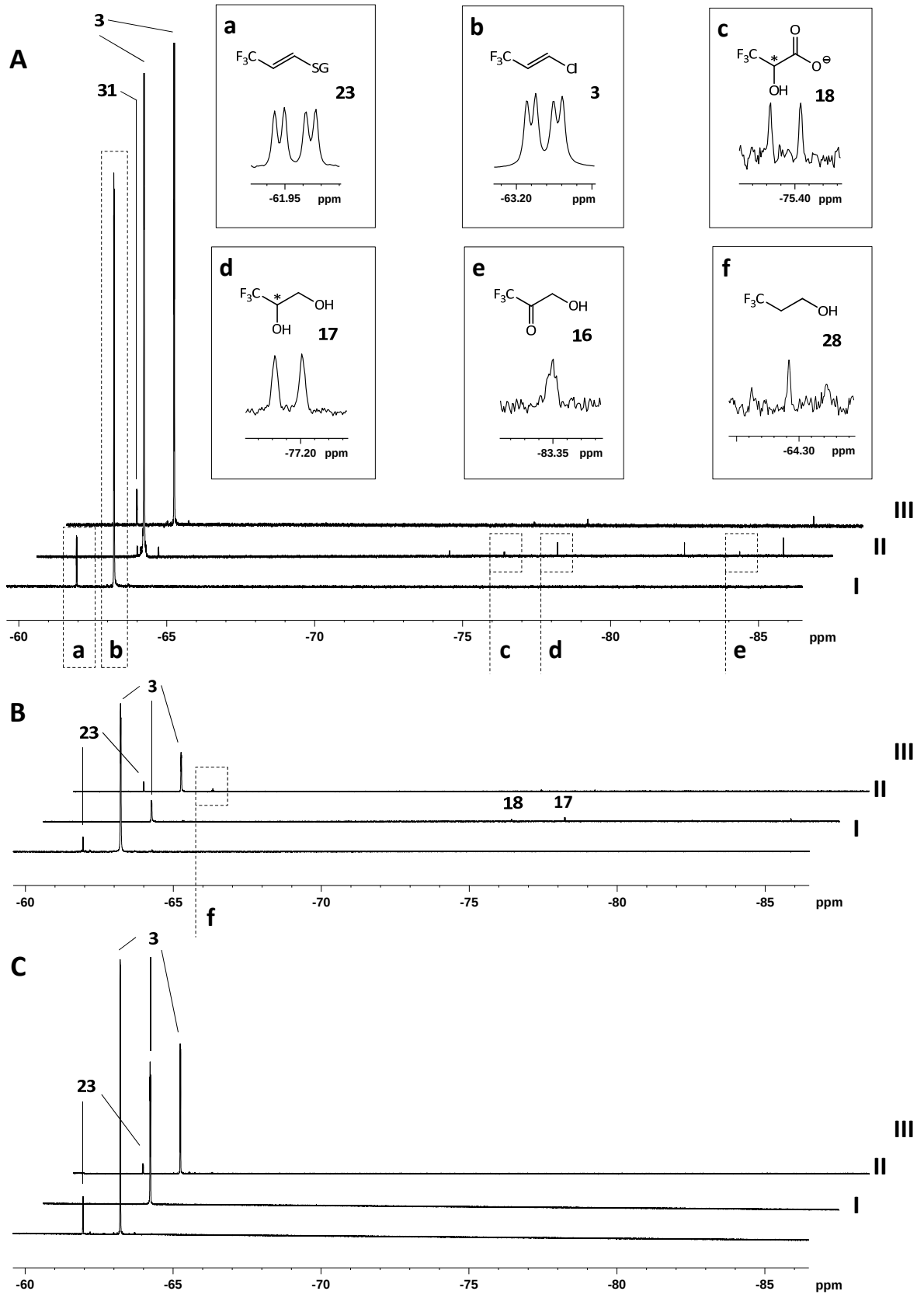

Fig. 36. ^{19}F-NMR spectra of supernatants from rat (**A**), rabbit (**B**) and human (**C**) liver microsomal incubations (3 mg protein/mL, 12-hour incubation , 20 µl liquefied *trans*-HCFO-1233zd); (**I**) 10 mM glutathione, (**II**) NADPH regenerating system, (**III**) 10 mM glutathione and NADPH regenerating system; GS, glutathione.

3.3.4.2 Metabolite identification by LC-MS/MS

In order to identify the additional signals in the ^{19}F-NMR spectra, LC-MS/MS experiments were performed in the CNL/EPI, EMS/EPI and MRM/EPI scan mode with negative ionization. Four minor metabolites were thus characterized in incubations in presence of glutathione.

All EPI spectra of rabbit, rat and human subcellular liver fraction incubation supernatants (incubation with 10 mM glutathione and a NADPH regenerating system) showed the characteristic fragmentation pattern of glutathione adducts (m/z 272, m/z 254 and m/z 179) (Farkas et al., 2007). Two of the EPI spectra suggest the presence of 1-*S*-(1-chloro-3,3,3-trifluoropropyl)-glutathione or 2-*S*-(1-chloro-3,3,3-trifluoropropyl)-glutathione (Fig. 37, A) and 2-*S*-(3,3,3-trifluoro-1,1-dihydroxypropanyl)-glutathione (Fig. 37, B). EPI spectra indicative for 2-*S*-(3,3,3-trifluoro-1-propanol)-glutathione (Fig. 37, C) and 2-*S*-(3,3,3-trifluoropropionic acid)-glutathione (Fig. 37, D) were only obtained in supernatants of incubations with cytochrome P-450 2E1 induced rat microsomes. The latter metabolites would appear as doublets in ^{19}F-NMR spectra and might therefore be assigned to the unidentified signals -73.5 and -84.8 ppm chemical shifts observed in the ^{19}F-NMR spectra of rat microsomal incubation supernatants. This has to be proven further by comparison with synthesized standard substances.

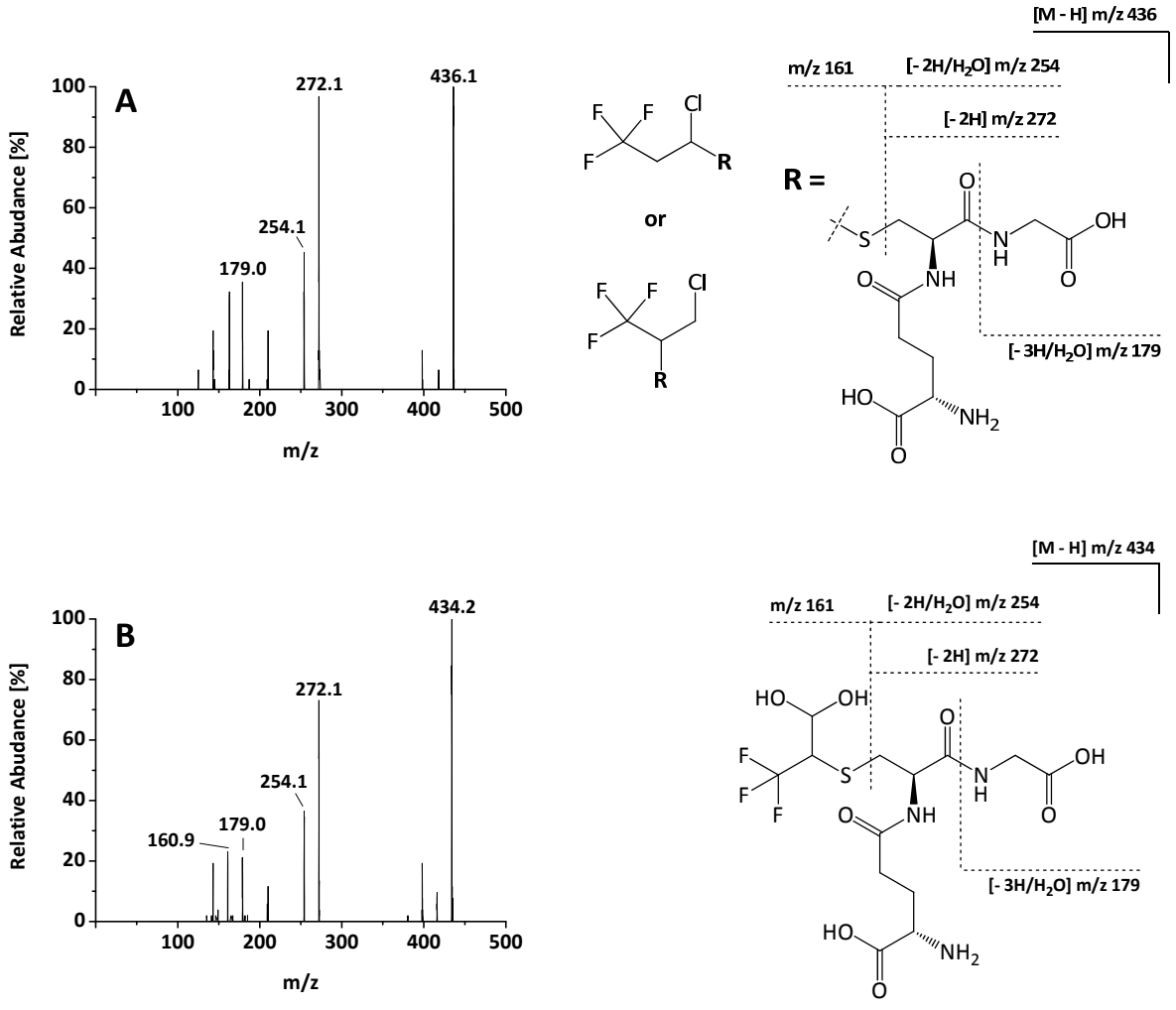

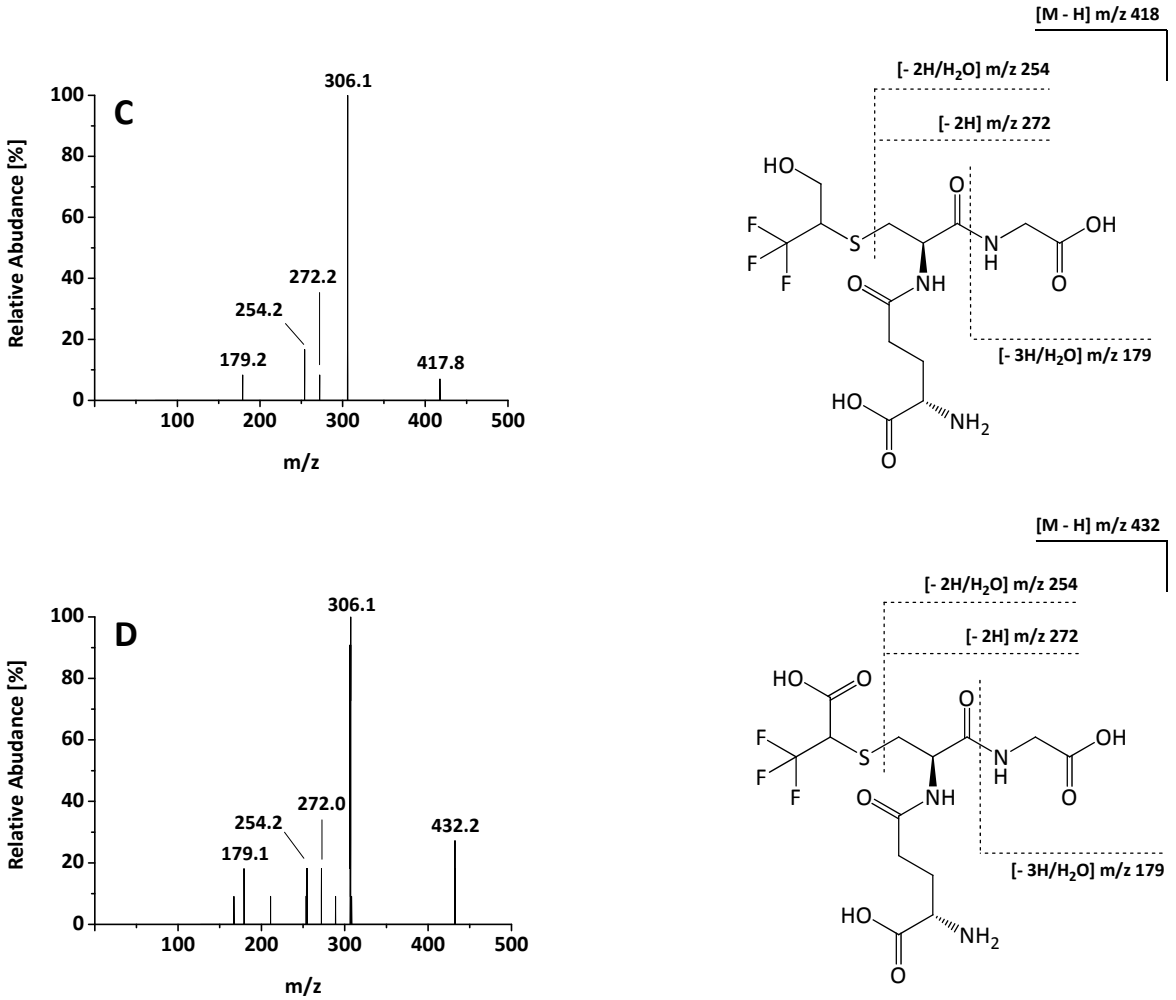

Fig. 37. LC-MS/MS EPI spectra of: (**A**) 1/2-*S*-(1-chloro-3,3,3-trifluoropropyl)-glutathione (R_t 18.3 min) and (**B**) 2-*S*-(3,3,3-trifluoro-1,1-dihydroxypropyl)-glutathione (R_t 18.4 min) in supernatants of rabbit, rat and human subcellular liver fraction incubation; (**C**) 2-*S*-(3,3,3-trifluoro-1-propanol)-glutathione (R_t 9.8 min) and (**D**) 2-*S*-(3,3,3-trifluoropropionic acid)-glutathione (R_t 11.2 min) in supernatants of CYP (cytochrome P-450) 2E1 induced rat liver microsomal incubations.

3.3.4.3 Kinetic formation of *S*-(3,3,3-trifluoro-*trans*-propenyl)-glutathione

The kinetics of the formation of *S*-(3,3,3-trifluoro-*trans*-propenyl)-glutathione, were characterized in rabbit, rat and human subcellular liver fractions (Fig. 38). Kinetic parameters K_m and V_{max} were determined by non-linear regression analysis as K_m – 249,600 ppm (rabbit), 213,400 ppm (rat) and 163,400 ppm (human) and V_{max} 21.8 [pmol/min x mg protein] (rabbit), 13.1 [pmol/min x mg protein] (rat), 5.0 [pmol/min x mg protein] (human). Kinetic analyses of the oxidative biotransformation of *trans*-HCFO-1233zd (3,3,3-trifluorolactic acid) in liver subcellular fractions could not be performed due to the low sensitivity of the quantitation procedures available for the highly polar products.

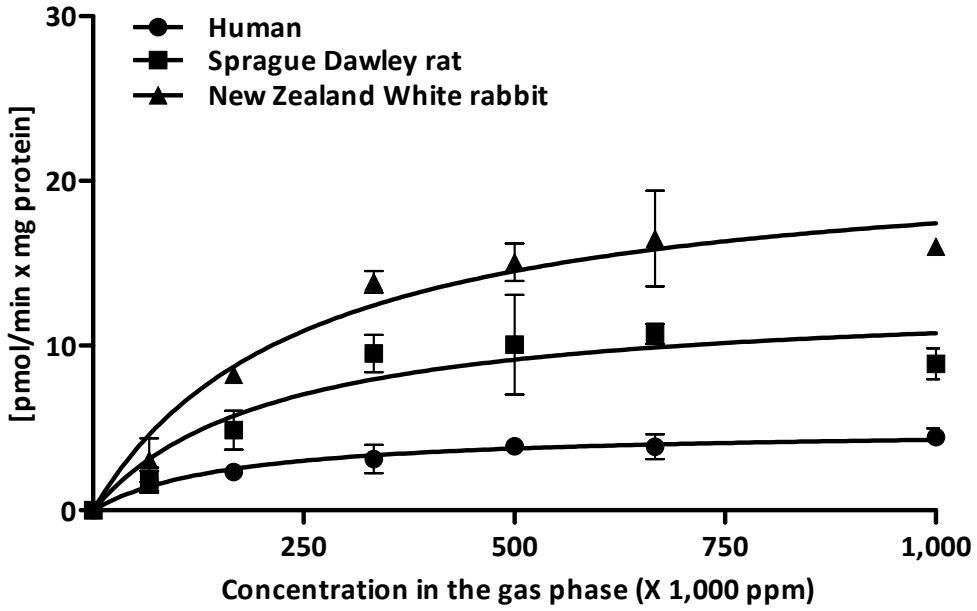

Fig. 38. Michaelis-Menten kinetics of *in vitro* *S*-(3,3,3-trifluoro-*trans*-propenyl)-glutathione formation.

4 Discussion

4.1 Biotransformation of HFO-1234yf in pregnant, non-pregnant female and male New Zealand White rabbits after single high dose inhalation exposure

Since maternal cardiotoxicity was observed in a HFO-1234yf developmental toxicity study in NZW rabbits (WIL, 2008), urinary metabolites of HFO-1234yf were analyzed in male and pregnant and non-pregnant female NZW rabbits. Regarding potentially changed metabolism during pregnancy, information on maternal hepatic enzyme activities of cytochrome P-450 2E1 or glutathione *S*-transferase in pregnant rabbits or humans (Anderson, 2005) is not available. These enzymes are involved in the biotransformation of HFO-1234yf. However, pregnant rats show decreased maternal capacity of cytochrome P-450 2E1 (Czekaj et al., 2005; He et al., 2005; Song and Cederbaum, 1996), and an increased detoxification of epoxides by glutathione *S*-transferase (Polidoro et al., 1981). Therefore, these changes in biotransformation capacities may influence the toxicity profile of HFO-1234yf in pregnant animals.

Biotransformation reactions for HFO-1234yf after single high dose inhalation exposure coincide with previous metabolic studies by Schuster et al. (2010) confirming biotransformation by cytochrome P-450 2E1 oxidation followed by conjugation of the intermediate epoxide with glutathione (Fig. 39). In contrast to previous studies in rabbits, the predominant metabolite in urine was *S*-(3,3,3-trifluoro-2-hydroxypropanyl)-mercaptolactic acid (**11**, Fig. 39) instead of *N*-acetyl-*S*-(3,3,3-trifluoro-2-hydroxypropanyl)-*L*-cysteine (**9**, Fig. 39). Both metabolites are formed by renal processing of *S*-(3,3,3-trifluoro-2-hydroxypropanyl)-*L*-cysteine, either by *N*-acetylation or by ß-oxidation. Possible explanations for the difference in renal processing could be the rabbit strain, housing conditions or diet. Besides this, the recorded ^{19}F-NMR spectra showed no major differences in metabolite patterns between non-pregnant and pregnant female animals (Fig. 16). Among the biotransformation products, metabolites suggesting changes in toxification pathways were not identified. Extensive LC-MS/MS analyses scanning for unknown metabolite structures revealed no potential toxic compounds. The highly nucleophilic 1,1,1-trifluoroacetone, determined previously in mice and rat urine, was not detected in rabbit urine neither by ^{19}F-NMR nor GC/MS analysis. The formation of glutathione *S*-conjugation metabolites (Anders and Dekant, 1998; Anders et al., 1992; Dekant, 1996), derived from HFO-1234yf, do not provide a conclusive explanation for myocardial inflammation (WIL, 2008) because the very small amounts of epoxide formed from HFO-1234yf in the liver are expected to be rapidly detoxified. Heart tissue only has very low cytochrome P-450 2E1 activity (Gottlieb, 2003; Thum and Borlak, 2000) and thus epoxide formation in the heart is presumably very limited. It is also considered unlikely that the low amounts of metabolites formed by ring-opening of the epoxide are involved in the cardiac effects induced by HFO-1234yf in rabbits, since they are highly polar, have little chemical reactivity, and are rapidly excreted.

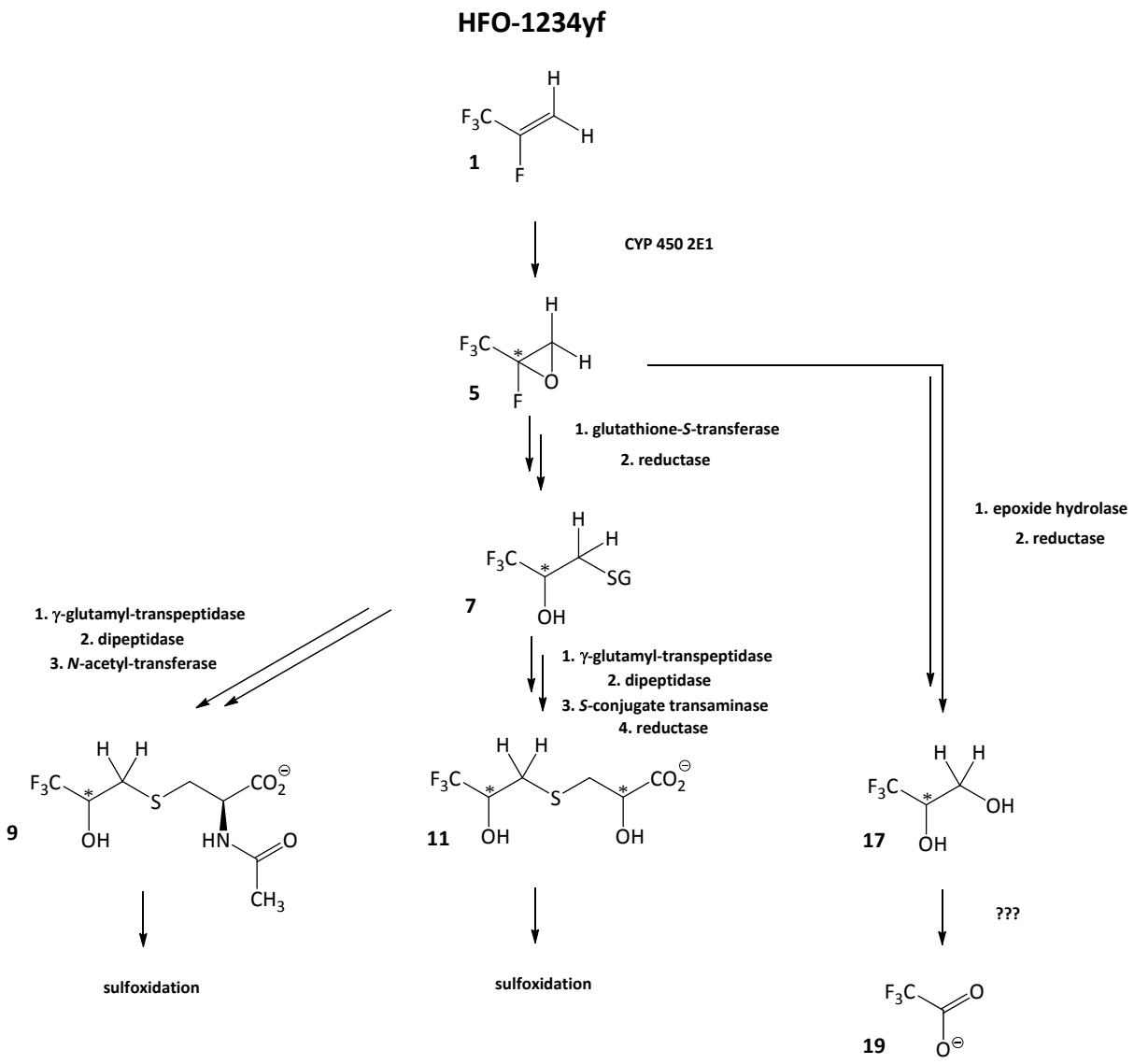

Fig. 39. Biotransformation of HFO-1234yf.

Based on urine recovery of *N*-acetyl-*S*-(3,3,3-trifluoro-2-hydroxypropanyl)-*L*-cysteine (Fig. 19, page 61 and Table 16, page 66), HFO-1234yf-metabolites are rapidly excreted in all study groups. More than 83% of the metabolite in male and more than 93% in non-pregnant female/pregnant female animals was excreted within 24 hours after inhalation exposure (50,000 ppm and 100,000 ppm exposures). However, pregnant females in the 100,000 ppm group eliminated approximately only half of the metabolite amount within the first 12 hours after exposure compared to non-pregnant females exposed to the same concentration of HFO-1234yf. On the other hand, total excretion of *N*-acetyl-*S*-(3,3,3-trifluoro-2-hydroxypropanyl)-*L*-cysteine (**9**, Fig. 39) within 48 hours was not significantly (Student's t-test, p = 0.6) different between non-pregnant female and pregnant female animals. Analysis of the inorganic fluoride kinetics of pregnant and non-pregnant female rabbits exposed to

100,000 ppm also showed the same characteristics with a rapid excretion of more than 70% of the whole excretion recovery determined within 48 hours in the first 24 hours and no significant excretion differences (Student's t-test, p = 0.2) within 48 hours after termination of inhalation exposure (Table 19, page 61 and Table 16, page 66). The calculated dosage of inorganic fluoride resulting from a one hour exposure lay between 0.9 and 1.7 mg/kg/KG. These levels were far below the NOAELs for inorganic fluoride regarding maternal (18 mg/kg/KG) and development toxicity NOAELs (29 mg/kg/KG) (Heindel et al., 1996).

The low fluoride excretion in comparison to the content of *N*-acetyl-*S*-(3,3,3-trifluoro-2-hydroxypropanyl)-*L*-cysteine (**9**, Fig. 39) in the rabbit urine samples is likely caused by the disposition of inorganic fluoride since only about 15% of fluoride intake is excreted in the urine (Hall et al., 1977). In addition, rabbit blood and urine is high in calcium (Redrobe, 2002) which may further reduce fluoride concentrations in urine due to formation of insoluble calcium fluoride.

Based on mean body weights of 3.0 kg in male, 3.3 kg in non-pregnant female and 3.4 kg in pregnant female rabbits, respiratory minute volume was calculated as 1.548 L/min, 1.663 L/min and 1.744 L/min respectively (Alexander et al., 2008). Therefore, the total dose of HFO-1234yf received within one hour of whole-body inhalation exposure was calculated as 386 mmol (male 100,000 ppm), 193 mmol (male 50,000 ppm), 415 mmol (non-pregnant female 100,000 ppm), 435 mmol (pregnant female 100,000 ppm) and 217 mmol (pregnant female 50,000 ppm) (Table 25).

The amount of HFO-1234yf metabolized was calculated to be less than 0.1% of the received dose in all groups confirming previous findings (0.05%) by Schuster et al. (2009, 2010). These results and the absence of clinical signs of toxicity suggest that lethality of HFO-1234yf in pregnant rabbits after inhalation exposure is unlikely due to changes in biotransformation patterns or capacity of pregnant rabbits.

Table 25. Biotransformation extent of HFO-1234yf in male (M), female (F) and pregnant female (P) rabbits after a 1-hour exposure.

Group	*N*-Acetyl-*S*-(3,3,3-trifluoro-2-hydroxypropanyl)-*L*-cysteine mean excretion within 48 hours [µmol]	*N*-Acetyl-*S*-(3,3,3-trifluoro-2-hydroxypropanyl)-*L*-cysteine mean fraction of the five main metabolites [%] *	Total fluoro metabolites excretion [µmol]	Amount of HFO-1234yf inhaled [µmol]**	Metabolized amount [%]
M 50,000 ppm	75.24 ± 15.67	35.83	209.99	192,976	0.11
P 50,000 ppm	60.97 ± 13.11	37.27	163.59	217,415	0.08
M 100,000 ppm	86.40 ± 38.68	32.70	264.22	385,952	0.07
P 100,000 ppm	50.47 ± 19.72	31.33	161.09	434,830	0.04
F 100,000 ppm	43.10 ± 22.35	29.10	148.11	414,755	0.04

* based on the metabolic pattern of one rabbit per group

** molar volume of HFO-1234yf was calculated to be 24.06 L/mol under standard conditions (293.15 K, 1013.25 hPa)

4.2 Biotransformation of HFO-1234yf in female and male New Zealand White rabbits after multiple inhalation exposure (28 days)

Since the metabolism of HFO-1234yf in male, pregnant and non-pregnant female NZW rabbits after single high dose exposures (50,000 and 100,000 ppm) revealed no differences in biotransformation and no potential toxic metabolite of HFO-1234yf could be observed (Huntingdon, 2011), a 28-day inhalation toxicity study in male and female NZW rabbits was designed. The aim of this study was to investigate whether there is a gender-based difference in toxic response and biotransformation of HFO-1234yf in rabbits after multiple exposures. A second objective was to investigate whether monofluoroacetate, a known heart toxicant in rabbits (Sherley, 2004), might be formed by HFO-1234yf biotransformation and accumulate as previously reported (Rowley, 1963).

Monofluoroacetate might be formed by defluorination of trifluoroacetate (**19**, Fig. 39), that was observed in rabbit urine after a HCFO-1234yf single high dose exposure. However, the C-F bond is the most stable chemical bond with its stability even increasing by degree of substitution (Lemal, 2004). As trifluoroacetate (**19**, Fig. 39) is not metabolized in mammalian systems to any great extent (Ema et al., 2010), formation of monofluoroacetate may have no obvious origin. Furthermore, the formation of the previously detected metabolite trifluoroacetate is not explicable with the current knowledge of biotransformation pathways of halogenated hydrocarbons and might be an artifact.

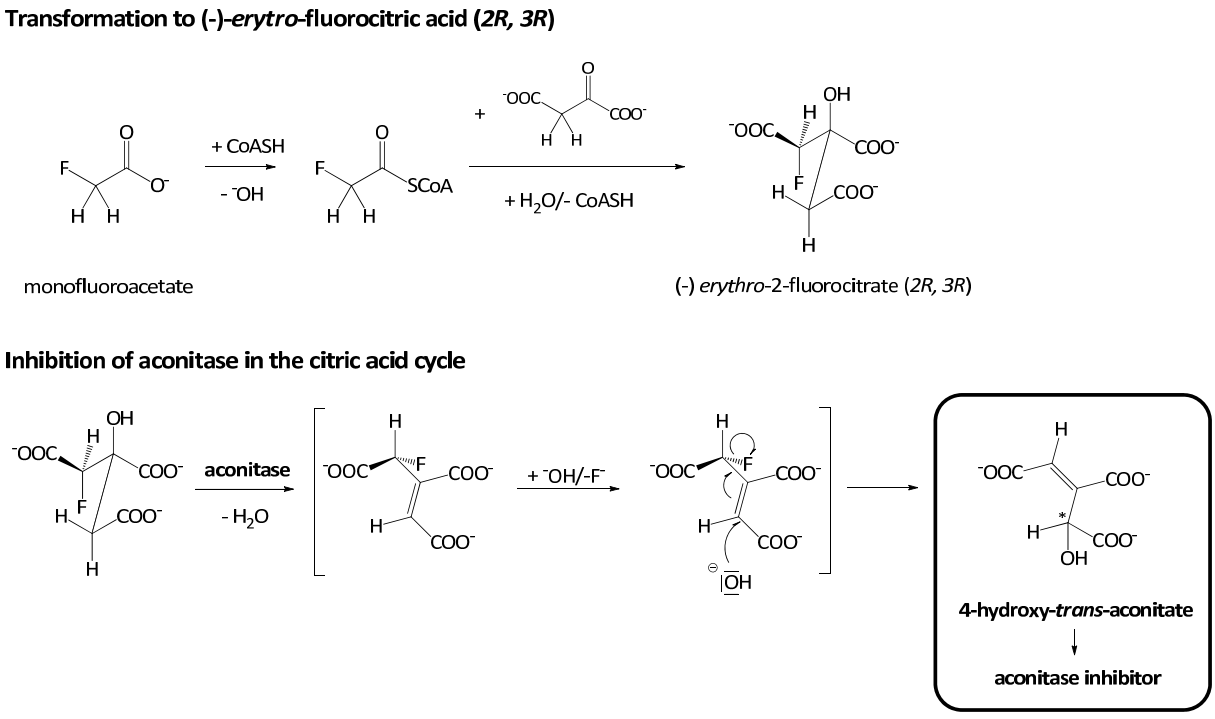

Fig. 40. Toxicity mechanism of monofluoroacetate (modified from Lauble et al., 1996).

The toxicity of monofluoroacetate, that is converted to (-)erythro-2-fluorocitrate (*2R, 3R*) acid *in vivo*, is based on its inhibitory effect of the enzyme aconitase (Beinert and Kennedy, 1993; Gooneratne et al., 1995). This citric acid cycle enzyme catalyzes the stereo-specific isomerization of citrate to *cis*-aconitase in a non-redox-active process. According to Goncharov et al., the transformation of (-)-erythro-2-fluorocitrate (*2R, 3R*) acid to 4-hydroxy-*trans*-aconitate is responsible for the aconitase inhibition by its formation of a very tight but not covalent binding with 4-hydroxy-*trans*-aconitate (Fig. 40) (Goncharov et al., 2006; Lauble et al., 1996). This enzyme inhibition leads to a depression of cellular respiration (decreased ATP production). Toxicity observed in rabbits after oral monofluoroacetate application was primarily found in the heart (ventricular fibrillation) but also in the nervous system (e.g. muscle weakness, ataxia, hypersensitivity to noise or disturbance and tonic-clonic seizures) (Sherley, 2004). Although signs of tissue inflammation were not explicitly reported, this could be an expected consequence of necrotic tissue damage and is likely to be caused by cardiac arrhythmia or seizures.

Biotransformation products of HFO-1234yf, identified in the multiple exposure study, support the results of earlier metabolic studies with this compound (Huntingdon, 2011; Schmidt et al., 2012; Schuster et al., 2010), showing a biotransformation of the fluoro-olefine by cytochrome P-450 2E1 oxidation and further conjugation of the epoxide (**5**, Fig. 39) with glutathione. The predominant metabolites were determined as *S*-(3,3,3-trifluoro-2-hydroxypropanyl)-mercaptolactic acid (**11**, Fig. 39) and *N*-acetyl-*S*-(3,3,3-trifluoro-2-hydroxypropanyl)-*L*-cysteine (**9**, Fig. 39) together representing 86.4 ± 5.9% of the total ^{19}F-NMR signal intensity. In detail, relative intensities of *S*-(3,3,3-trifluoro-2-hydroxypropanyl)-mercaptolactic acid (**11**, Fig. 39) were slightly higher in all analyzed samples compared to *N*-acetyl-*S*-(3,3,3-trifluoro-2-hydroxypropanyl)-*L*-cysteine (**9**, Fig. 39) except in urine of high dose male rabbits (Fig. 21, page 64). The signals of the two unknown metabolites (24 and 25, Fig. 21) were less intense but also detectable in samples of all three different exposure durations (7, 14, 28 days). The minor metabolites trifluoroacetic acid (**19**, Fig. 39), 3,3,3-trifluoro-1,2-propanediol (**17**, Fig. 39), 3,3,3-trifluoro-2-propanol (**14**, Fig. 8, page 16) and *S*-(3,3,3-trifluoro-2-hydroxypropanyl)-*L*-cysteine (**8**, Fig. 8, page 16), could only be detected in spectra of rabbits exposed for 14 or 28 days. No fluoro-containing metabolites were determined in ^{19}F-NMR spectra of urine samples of the 28 days recovery group, or in any of the extracts of heart tissues. Monofluoroacetate determination also showed no positive results in the tissue extracts analyzed by LC-MS/MS (LOD, 0.01 ppm). Since the achieved LOD was below reported mean heart tissue levels in NZW rabbits that received a sublethal single dose of monofluoroacetate (Gooneratne et al., 1995), it can be assumed that observed cardiotoxicity is unlikely to be related to monofluoroacetate accumulation. Besides the minor urinary excretion of the hepatotoxic trifluoroacetic acid (**19**, Fig. 39) (Rosenberg and Wahlstrom, 1971; Stier et al., 1972), already observed in rabbit urine after a single high dose exposure to HFO-1234yf, no potentially toxic metabolite could be identified.

The mean recovery of the major HFO-1234yf metabolite *N*-acetyl-*S*-(3,3,3-trifluoro-2-hydroxypropanyl)-*L*-cysteine (**9**, Fig. 39) showed no significant differences between male and female rabbits (Student's t-test, $p > 0.05$) except for male and female rabbits exposed to 500 ppm for 7 days (Student's t-test, $p = 0.03$). To compare the biotransformation extent of HFO-1234yf after multiple exposure with the transformation amount observed after a single inhalation, 18-hour urinary recoveries of all 1,000/1,500 ppm exposures were compared with the 60-hour urinary recoveries already determined by Schuster et al. (2010) (exposure level 2,000 ppm for 6 hours – mean recovery = 35 ± 11 µmol within 60 hours after inhalation exposure). No significant difference was observed (Student's t-test, $p> 0.05$) indicating a stable biotransformation capacity with no detectable increase in cytochrome P-450 2E1 activity. The low recoveries of *N*-acetyl-*S*-(3,3,3-trifluoro-2-hydroxypropanyl)-*L*-cysteine (**9**, Fig. 39) in urine of male and female rabbits of the high dose 7-day exposure groups compared to the other exposure levels could be explained by the halted inhalation exposure on day 7 and the fast urinary elimination of the mercapturic acid (> 83% within the 24 hours) (Schmidt et al., 2012; Schuster et al., 2010). The fast metabolism of HFO-1234yf is also responsible for a sudden steady state of metabolite levels in blood and urine. Therefore, no significant difference in *N*-acetyl-*S*-(3,3,3-trifluoro-2-hydroxypropanyl)-*L*-cysteine-excretion could be observed in the different dose groups for different inhalation exposure durations.

This was also observed for determined inorganic fluoride levels in serum and urinary inorganic fluoride excretion. Low inorganic fluoride levels determined for the 7-day high dose exposures could also be explained by the fast metabolism of HFO-1234yf reported previously (Schmidt et al., 2012; Schuster et al., 2010). Dose-dependent urinary excretion could be determined in some subgroups of male (7-, 14-, 28-day exposures) and female (28-day exposure) rabbits but increases were mostly not significant. Inorganic serum levels showed no dose-dependency. Only female and male high dose rabbits had a highly significant increase in inorganic serum fluoride levels. In addition to that, two serum levels (0.6 ppm and 0.5 ppm) of the 28-day high dose female exposure group exceeded the reported NOAEL serum fluoride level for maternal toxicity of 0.39 ± 0.14 ppm (Heindel et al., 1996). Nevertheless, these two female rabbits survived the inhalations but showed mild inflammation of the myocardium and increased clinical parameters (CK-MM,CK-MB, MYG and FABP) (Honeywell, 2012). Differences in urinary fluoride excretion and serum levels between male and female rabbits were observed in the 7-day high dose exposure groups, but were not confirmed after longer exposition durations. Measured control serum levels were consistent with levels reported by Heindel et al. (Heindel et al., 1996).

Effects of multiple HFO-1234yf exposure on liver enzyme activity of cytochrome P-450 3A4 and 2E1 showed no remarkable changes as already expected from the quantitation of *N*-acetyl-*S*-(3,3,3-trifluoro-2-hydroxypropanyl)-*L*-cysteine. Only minor enzyme induction was observed in male rabbits exposure to 4,500 ppm for 28 days (Student's t-test, $p = 0.03$) and female rabbits exposed to 5,500 ppm of HFO-1234yf for 7 days (Student's t-test, $p = 0.03$)

compared to control. Moreover, cytochrome P-450 2E1 induction was not seen in the high dose groups of female rabbits exposed for longer than 7 days.

Although no differences in HFO-1234yf biotransformation pattern or capacity could be observed after multiple exposures for up to 28 consecutive days, three rabbits died during the study (one male and one female rabbit of the high dose 7-day exposure group and one female of the high dose 28-day exposure group). While the male rabbit showed no clinical symptoms, the two females showed signs of debilitation for 1-2 days prior to death. Despite multifocal cardiac inflammation being seen in several animals of the mid and high dose exposure groups, no HFO-1234yf-related lesions were observed in the low dose exposure groups. As halogenated hydrocarbons are known for their arrhythmic and cardio depressant effects by various potential interactions with cellular structures or membrane potentials (e.g. impairment of Ca^{2+} flux across membranes, inhibition of gap junction intercellular communication) (Himmel, 2008; Hoffmann et al., 1994), further investigations should consider potential negative effects of HFO-1234yf on the heart rhythm of rabbits or its capability to interact with specific receptor affecting the rabbit cardiovascular system. A possible correlation with the observed cardiac inflammations might be relevant.

4.3 Toxicity assessment of HFO-1234yf including new biotransformation analysis studies

HFO-1234yf metabolic analysis after a single high dose inhalation exposure in pregnant and non-pregnant female and male NZW rabbits as well as a subchronic inhalation exposure study for 28 days in female and male NZW rabbits revealed no major changes in biotransformation products or capacity compared to previous results of a 6-hour single HFO-1234yf inhalation exposure study (Schuster et al., 2010). Concerning potential formation of a cardiotoxic metabolite, neither the pregnancy status, nor the gender or exposure duration might be relevant. No differences were observed in the biotransformation pattern and extent of HFO-1234yf between pregnant and non-pregnant females and males after a single high dose inhalation exposure. The biotransformation of HFO-1234yf in male and female rabbits after multiple exposures also appeared to be similar. Regarding potential monofluoroacetate formation as a cause for heart toxicity seen after multiple exposures, no accumulation of monofluoroacetate could be observed in heart tissue of any analyzed animal showing major clinical or pathological heart effects. If HFO-1234yf is metabolized to monofluoroacetate the results rather confirm previous analysis revealing a rapid elimination from tissue within approximately 6 hours after dosage (Gooneratne et al., 1995). Analysis of inorganic fluoride, a known cardiotoxic compound (Tylenda et al., 2003) formed as a consequence of the biotransformation of HFO-1234yf, revealed no significant gender-related differences in serum levels and urinary excretions. Only in two female rabbits the published NOEAL of 0.39 ± 0.14 ppm (Heindel et al., 1996) was exceeded and cardiotoxic effects could be seen. The observed minimal increase in cytochrome P-450 2E1 activity rather has no biological relevance, as the overall metabolite excretion did not significantly increase over

time (based on the *N*-acetyl-*S*-(3,3,3-trifluoro-2-hydroxypropanyl)-*L*-cysteine determination). These results suggest that the lethality of HFO-1234yf in female and male rabbits after multiple inhalation exposure is unlikely due to changes in biotransformation patterns or capacity. Because of potential negative effects of the parent compound HFO-1234yf on specific receptors, cellular structures or the energy supply of the heart, further studies have to be conducted. It can also be assumed that the observed lethality is related to stress caused by the multiple exposure treatment itself enhanced by the slight odor of the compound.

4.4 Biotransformation of *trans*-HCFO-1233zd in male Sprague Dawley rats and female New Zealand White rabbits after single inhalation exposure

In analogy to published data for *trans*-1,1,1,3-tetrafluoropropene (Schuster et al., 2009), *trans*-HCFO-1233zd is metabolized by both a direct glutathione conjugation and by oxidative metabolism by cytochrome P-450 2E1 (Fig. 41, Fig. 42, Fig. 43). This data is consistent with the information available on the biotransformation of structurally related compounds and the formation of all identified *trans*-HCFO-1233zd biotransformation products can readily be explained by these two pathways. The identified metabolites in intact animals show that a number of downstream processing reactions result in a complex metabolite pattern.

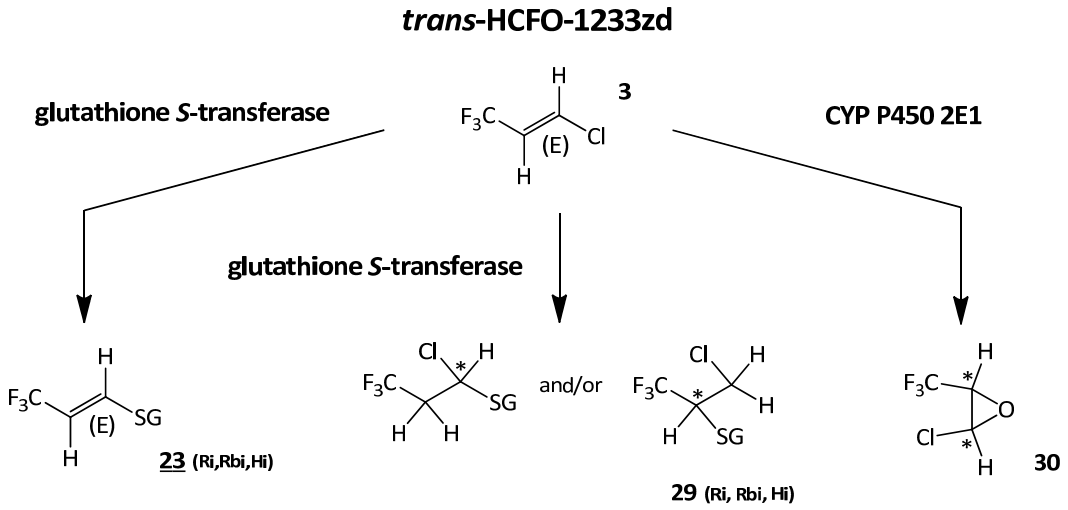

Fig. 41. Primary steps of biotransformation of *trans*-HCFO-1233zd by glutathione S-transferase and CYP P-450 2E1. Compounds conclusively identified by standard substances are underlined - rat *in vitro* (Ri), rabbit *in vitro* (Rbi), human *in vitro* (Hi), rat *in vivo* (R) and rabbit *in vivo* (Rb).

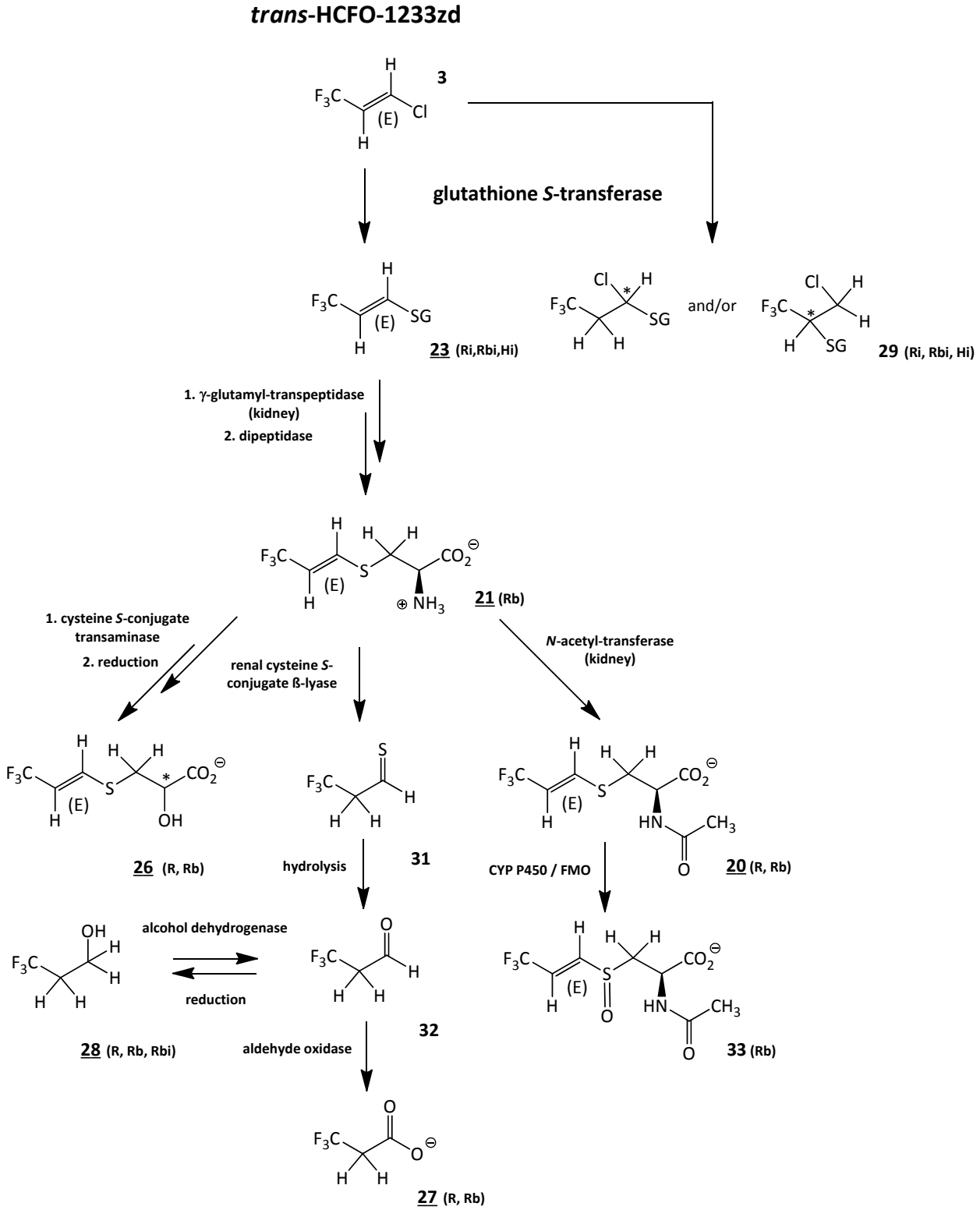

Fig. 42. Glutathione *S*-transferase dependent biotransformation of *trans*-HCFO-1233zd. Compounds conclusively identified by standard substances are underlined - rat *in vitro* (Ri), rabbit *in vitro* (Rbi), human *in vitro* (Hi), rat *in vivo* (R) and rabbit *in vivo* (Rb).

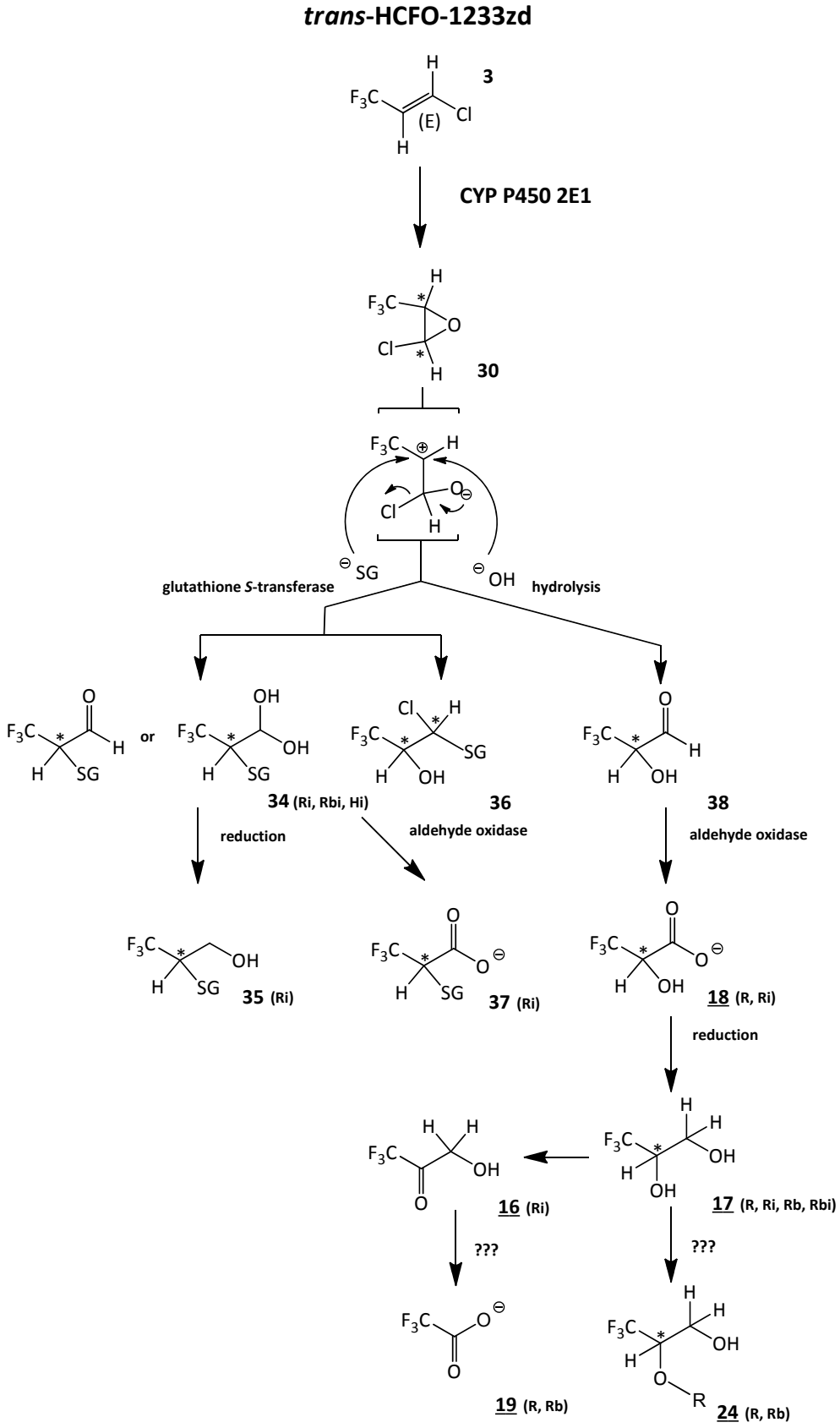

Fig. 43. Cytochrome P-450 2E1 dependent biotransformation of *trans*-HCFO-1233zd. Compounds conclusively identified by standard substances are underlined - rat *in vitro* (Ri), rabbit *in vitro* (Rbi), human *in vitro* (Hi), rat *in vivo* (R) and rabbit *in vivo* (Rb).

The biotransformation of *trans*-HCFO-1233zd mediated by glutathione *S*-transferase catalyzed addition-elimination reaction of glutathione with *trans*-HCFO-1233zd leads to the formation of *N*-acetyl-*S*-(3,3,3-trifluoro-*trans*-propenyl)-*L*-cysteine (**20**, Fig. 42). Consistent with this observation, *S*-(3,3,3-trifluoro-*trans*-propenyl)-glutathione (**23**, Fig. 41 and Fig. 42) is the major metabolite formed in liver subcellular fractions. Renal processing of *S*-(3,3,3-trifluoro-*trans*-propenyl)-glutathione (**23**, Fig. 41 and Fig. 42) by γ-glutamyl-transpeptidase and dipeptidases (Anders and Dekant, 1998) results in *S*-(3,3,3-trifluoro-*trans*-propenyl)-*L*-cysteine (**21**, Fig. 42). This cysteine S-conjugate is processed further by three different pathways. i) cysteine *S*-conjugate transaminase to *S*-(3,3,3-trifluoro-*trans*-propenyl)-mercaptopyruvic acid followed by reduction to *S*-(3,3,3-trifluoro-*trans*-propenyl)-mercaptolactic acid (**26**, Fig. 42); ii) renal cysteine *S*-conjugate β-lyase dependent biotransformation (Anders et al., 1992; Monks et al., 1990) to finally give 3,3,3-trifluoropropionic acid (**27**, Fig. 42) and 3,3,3-trifluoro-1-propanol (**28**, Fig. 42); and iii) *N*-acetyl-transferase to form *N*-acetyl-*S*-(3,3,3-trifluoro-*trans*-propenyl)-*L*-cysteine (**20**, Fig. 42) that is further oxidized to *N*-acetyl-*S*-(3,3,3-trifluoro-*trans*-propenyl)-*L*-cysteine sulfoxide (**33**, Fig. 42).

The second metabolic pathway for *trans*-HCFO-1233zd is catalyzed by cytochrome P-450 representing 51 ± 17% and 25 ± 9% of total ^{19}F-NMR signal intensities in spectra of rat respectively rabbit urine (0-48 hours after 10,000 ppm exposure). The initial biotransformation step results in the formation of 1-chloro-3,3,3-trifluoro-1,2-epoxypropane (**30**, Fig. 41 and Fig. 43). This epoxide can be further hydrolyzed to the intermediate 3,3,3-trifluoro-2-hydroxypropanal (**38**, Fig. 43) which may be oxidized to 3,3,3-trifluorolactic acid (**18**, Fig. 43) or reduced to 3,3,3-trifluoro-1,2-propanediol (**17**, Fig. 43). The latter may be subject to further phase two reactions such as conjugation to sulfate or glucuronic acid (**24**, Fig. 43). Alternatively, ring opening may be due to a reaction with glutathione to give 2-*S*-(3,3,3-trifluoropropanal)-glutathione respectively its hydrate (**34**, Fig. 43), which may be further oxidized to 2-*S*-(3,3,3-trifluoropropionic acid)-glutathione (**37**, Fig. 43) or reduced to 2-*S*-(3,3,3-trifluoro-1-propanol)-glutathione (**35**, Fig. 43). The formed glutathione *S*-conjugates might be subject to further processing by enzymes of the mercapturic acid pathway or the renal ß-lyase but could not be detected.

The structures of the minor metabolites proposed to be formed in the liver subcellular fractions are consistent with the reaction schemes developed. Tentative minor *in vitro* metabolites detected by LC-MS/MS in all species were the glutathione conjugate 1-*S*-(1-chloro-3,3,3-trifluoro-propyl)-glutathione or 2-*S*-(1-chloro-3,3,3-trifluoro-propyl)-glutathione (**29**, Fig. 41 and Fig. 42) and 2-*S*-(3,3,3-trifluoropropanal)-glutathione respectively its hydrate (**34**, Fig. 43). The addition of glutathione to double bonds may not necessarily be followed by elimination of HCl to give haloalkenyl glutathione *S*-conjugates and simple addition reactions of glutathione to the haloalkene have been described in the biotransformation of other haloalkenes (1-chloro-1,2,2-trifluoroethene and perfluoropropene) (Dekant, 2003). 2-*S*-(3,3,3-trifluoropropionic acid)-glutathione (**37**, Fig. 43) and 2-*S*-(3,3,3-trifluoro-1-propanol)-

glutathione (**35**, Fig. 41), products of the glutathione-mediated ring opening of the epoxide (**30**, Fig. 41 and Fig. 43) were only detected in supernatants of rat microsomes. Both, **35** and **37** (Fig. 43) are formed by oxidation or reduction of the intermediate product 2-S-(3,3,3-trifluoropropanal)-glutathione (**34**, Fig. 43) and were only detected using highly sensitive LC-MS/MS methods. Related ^{19}F-NMR signals were not observed, likely concentrations were below the much higher limit of detection of the ^{19}F-NMR method.

The ^{19}F-NMR spectra of rat (Fig. 30, page 76) and rabbit urine (Fig. 31, page 78) indicated the presence of several unidentified metabolites. The signal (δ = -61.5 ppm) close to the major metabolite *N*-acetyl-*S*-(3,3,3-trifluoro-*trans*-propenyl)-*L*-cysteine (**20**, Fig. 42) is most likely a derivative of *S*-(3,3,3-trifluoro-*trans*-propenyl)-glutathione pathway because of its similar multiplicity, ^{19}F-chemical shift and coupling constants. The unidentified doublets observed at ^{19}F-chemical shifts below -71 ppm possibly have a hydroxyl group in alpha position to the trifluoromethyl group, also indicated by their similar ^{19}F-chemical shift, multiplicity and coupling constants compared to the identified substances 3,3,3-trifluorolactic acid (**18**, Fig. 43), 3,3,3-trifluoro-1,2-propanediol (**17**, Fig. 43). Traces of *N*-acetyl-*S*-(3,3,3-trifluoro-*trans*-propenyl)-*L*-cysteine sulfoxide (**33**, Fig. 42), observed by LC-MS/MS analysis in rabbit urine, were below the limit of detection of the ^{19}F-NMR method and were not assigned to any signal.

Whereas 3,3,3-trifluorolactic acid (**18**, Fig. 43) turned out to be the main urinary metabolite in the rat, *N*-acetyl-*S*-(3,3,3-trifluoro-*trans*-propenyl)-*L*-cysteine (**20**, Fig. 42) was the main urinary biotransformation product in the rabbit. Quantification of the major metabolites 3,3,3-trifluorolactic acid (**18**, Fig. 43) and *N*-acetyl-*S*-(3,3,3-trifluoro-*trans*-propenyl)-*L*-cysteine (**20**, Fig. 42) revealed rapid excretions, with elimination half-life times of less than 6 hours for both substances in both species. Calculations based on total urinary recoveries for *N*-acetyl-*S*-(3,3,3-trifluoro-*trans*-propenyl)-*L*-cysteine (**20**, Fig. 42) or 3,3,3-trifluorolactic acid (**18**, Fig. 43) and estimations of *trans*-HCFO-1233zd uptake, revealed very low overall biotransformation amounts (Table 26). Compared to findings for *trans*-1,1,1,3-tetrafluoropropene in rats by Schuster, 2009 (approximately 0.007% biotransformation), rat biotransformation extent of *trans*-HCFO-1233zd was within the same order of magnitude. *In vitro* enzyme kinetics confirmed the low *in vivo* biotransformation amount and showed a lower glutathione *S*-transferase affinity to *trans*-HCFO-1233zd in humans compared to rodents.

Table 26. Quantitation of biotransformation extent of HFO-1233zd in male rats and female rabbits after a 6-hour whole-body exposure based on total excretion of *N*-acetyl-*S*-(3,3,3-trifluoro-*trans*-propenyl)-*L*-cysteine (MA) or 3,3,3-trifluorolactic acid (TFLA).

Group		Mean metabolite recovery within 48 h [µmol]		Fraction of total ^{19}F NMR signal intensity [%] *		Total fluoro metabolites excretion [µmol]		Received dose [µmol]**	% of received dose recovered as metabolites	
		MA	TFLA	MA	TFLA	MA	TFLA		MA	TFLA
Rat	2,000 ppm	0.01 ± 0.002	0.07 ± 0.01	7.92	52.10	0.08	0.14	5,241.98	0.002	0.003
	5,000 ppm	0.02 ± 0.01	0.10 ± 0.01			0.18	0.20	12,607.81	0.001	0.002
	10,000 ppm	0.06 ± 0.02	0.13 ± 0.03			0.70	0.24	26,757.34	0.003	0.001
Rabbit	2,000 ppm	0.85 ± 0.10	-	11.69	-	7.23	-	43,744.06	0.02	-
	5,000 ppm	1.41 ± 0.83	-			12.09	-	102,668.63	0.01	-
	10,000 ppm	1.88 ± 1.31	-			16.05	-	212,047.12	0.01	-

* based on the metabolic pattern of one animal per group

** molar volume of HFO-1233zd was calculated to be 24.06 L/ mol under standard conditions (273.15 K, 1013.25 hPa)

The two pathways of *trans*-HCFO-1233zd biotransformation may be competitive. Rat urinary metabolite quantification revealed an increase of *N*-acetyl-*S*-(3,3,3-trifluoro-*trans*-propenyl)-*L*-cysteine (**20**, Fig. 42) excretion compared to 3,3,3-trifluorolactic acid (**18**, Fig. 43) with increasing *trans*-HCFO-1233zd exposure concentrations (excretion amount of *N*-acetyl-*S*-(3,3,3-trifluoro-*trans*-propenyl)-*L*-cysteine/3,3,3-trifluorolactic acid: 2,000 ppm – 0.09, 5,000 ppm – 0.15, 10,000 ppm – 0.43; based on LC-MS/MS metabolite quantification). This increase of metabolism by the glutathione *S*-transferase might also explain that the oxidation of *trans*-HCFO-1233zd in *in vitro* incubations (high *trans*-HCFO-1233zd concentrations) was only a minor pathway. Signal intensities attributed to oxidative metabolites represented only about 16% to 19% of the total fluorine related ^{19}F-NMR signal intensity (incubations with glutathione and an NADPH regenerating system).

The metabolite structures suggest *trans*-HCFO-1233zd undergoes both oxidative biotransformation by cytochrome P-450 and direct glutathione conjugation with different intensities. Observed species differences were the lack of the major *trans*-HCFO-1233zd urinary rat metabolite 3,3,3-trifluorolactic acid (**18**, Fig. 43) in rabbit urine and the absence of the *trans*-HCFO-1233zd urinary rabbit trace metabolite 3,3,3-trifluoro-1-propanol (**28**, Fig. 42) in rat urine. *In vitro* incubation experiments with *trans*-HCFO-1233zd in rat, rabbit and human liver cell fractions, revealed *S*-(3,3,3-trifluoro-*trans*-propenyl)-glutathione (**23**, Fig. 41 and Fig. 42) as major metabolite in all three species. Excluding the still unidentified metabolites, no potent toxic *in vivo* and *in vitro* biotransformation products could be identified. The potential reactive metabolite 1-chloro-3,3,3-trifluoro-1,2-epoxypropane (**30**, Fig. 41 and Fig. 43) formed by cytochrome P-450 is possibly formed only in very low amounts due to low overall *in vivo* biotransformation extent (< 0.02% of received dose) and is apparently rapidly detoxified by epoxide hydrolase. It is therefore likely that covalent binding with tissue nucleophiles may be efficiently prevented by hydrolysis or also by glutathione conjugation. Formation of reactive metabolites (thioketenes or thioacylhalodies) by glutathione *S*-transferase and renal ß-lyase pathway observed for other halogenated carbons and hydrogcarbons (e.g. perfluoropropene, 1,1,2-trichloro-3,3,3-trifluoropropene, tetrachloroethene) is unlikely for *trans*-HCFO-1233zd due to the lack of multiple halogen leaving groups (Dekant et al., 1990; Monks et al., 1990; Vamvakas et al., 1989; Volkel et al., 1998). The low potential for glutathione *S*-transferase dependent toxicity of *trans*-HCFO-1233zd is further underlined by the very low formation of metabolites of this pathway (*N*-acetyl-*S*-(3,3,3-trifluoro-*trans*-propenyl)-*L*-cysteine [**20**, Fig. 42], *S*-(3,3,3-trifluoro-*trans*-propenyl)-mercaptolactic acid [**26**, Fig. 42] and 3,3,3-trifluoropropionic acid [**27**, Fig. 42]; cumulative urinary excretion within 48 hours after inhalation exposure to 10.000 ppm for 6 hours; < 0.1 µmol). In comparison, excretion of glutathione *S*-transferase mediated metabolites of known nephrotoxic compounds such as tetrachloroethene (male Wistar rat: *N*-acetyl-*S*-(trichlorovinyl)-*L*-cysteine, dichloroacetic acid; cumulative urinary excretion within 60 hours after inhalation exposure to the carcinogenic concentration of 400 ppm for 6 hours; < 1.5 µmol) (Volkel et al., 1998) or trichloroethene (male and female Wistar rats: of *N*-

acetyl-*S*-(1,2-dichlorovinyl)-*L*-cysteine and *N*-acetyl-*S*-(2,2-dichlorovinyl)-*L*-cysteine in urine within 48 hours after inhalation exposure to 160 ppm for 6 hours; < 0.01 µmol) (Bernauer et al., 1996) is considerably higher.

4.5 Toxicity potential of *trans*-HCFO-1233zd

Excluding the still unidentified metabolites, no potent toxic *in vivo* and *in vitro* biotransformation products could be identified. The hepatotoxic trifluoroacetic acid (**19**, Fig. 43) and the toxic 3,3,3-trifluoropropionic acid (**27**, Fig. 42) (observed in the rat) were only determined in very low rather nontoxic amounts (Bayer, 2005; Boutonnet et al., 1999; Stier et al., 1972). Due to the very low blood/air partition coefficients (0.6, human; 0.9, rabbit; 1.5, rat) of *trans*-HCFO-1233zd, its lipophilicity (log *P* = 2.2) and high vapor pressure (152 kPa at 30 °C) it can be assumed that most of the inhaled gas is not taken up into the blood extensively but rather suddenly exhaled almost completely (Gargas et al., 1989). Therefore the quantification of the predominant metabolites revealed an expected low overall *in vivo* biotransformation extent (< 0.02%, based on urinary metabolite recover) with a rapid urinary excretion for both major metabolites *N*-acetyl-*S*-(3,3,3-trifluoro-*trans*-propenyl)-*L*-cysteine (**20**, Fig. 42) and 3,3,3-trifluorolactic acid (**18**, Fig. 43) (only rat) in the rabbit and the rat. This low biotransformation potential was also observed in *in vitro* incubation experiments with rat, rabbit and human subcellular liver tissue fractions. Only very high concentrations of *trans*-HCFO-1233zd and long incubation times led to fluoro metabolite-related signals in ^{19}F-NMR spectra. Determination of *in vitro* enzyme kinetics further showed a lower glutathione *S*-transferase affinity to *trans*-HCFO-1233zd in humans compared to rodents and rabbits. Thus, it might be predicted that human biotransformation of *trans*-HCFO-1233zd is even lower than in most other mammals (rodents and non-rodents). The metabolite structures suggest *trans*-HCFO-1233zd undergoes both oxidative biotransformation by cytochrome P-450 and direct glutathione conjugation with different intensities. Whereas 3,3,3-trifluorolactic acid (**18**, Fig. 43) was the main urinary metabolite in the rat and was not observed in rabbit urine, *N*-acetyl-*S*-(3,3,3-trifluoro-*trans*-propenyl)-*L*-cysteine (**20**, Fig. 42) was the main urinary biotransformation product in the rabbit. It can be concluded that *trans*-HCFO-1233zd shows biotransformation reactions typical of other halogenated hydrocarbons and is very similar to the metabolism of *trans*-1,1,1,3-tetrafluoropropene (HFO-1234ze) analyzed by Schuster et al. (2009). The data on metabolism and toxicokinetics support prior studies indicating that *trans*-HCFO-1233zd has a low potential for toxicity in mammals and is not expected to be toxic or carcinogenic in humans.

5 Summary

The novel refrigerant 2,3,3,3-tetrafluoropropene (HFO-1234yf) as well as the novel foam blowing and precision cleaning agent *trans*-1-chloro-3,3,3-trifluoropropene (*trans*-HCFO-1233zd) are both chlorofluorocarbon replacements with low GWPs and a short atmospheric life time. Whereas the hydrofluoroolefin HFO-1234yf has no negative effect on stratospheric ozone due to the lack of chlorine in its structure, the hydrochlorofluoroolefine *trans*-HCFO-1233zd exhibits a very low potential for ozone depletion (ODP). This is approximately 100 times lower than the ozone depletion potential of precursor compounds such as 1,1,2-trichloro-1,2,2-trifluoroethane (CFC-113).

Principle aims of this thesis were to investigate the unknown metabolism of the new solvent *trans*-HCFO-1233zd and to further investigate a possible biotransformation based toxicity of HFO-1234yf observed in rabbits. Therefore study specimens of different *in vitro* and *in vivo* studies with *trans*-HCFO-1233zd and HFO-1234yf were analyzed for metabolites using ^{19}F-NMR spectroscopy, LC-MS/MS spectrometry and GC/MS spectrometry. Metabolites were identified by comparison with purchased or synthesized standard substances. Excretion kinetics of the predominant metabolites were determined by LC-MS/MS quantification, inorganic fluoride was determined by potentiometry. Moreover cytochrome P-450 2E1 and 3A4 liver enzyme activities were measured in a multi-exposure study with HFO-1234yf.

The biotransformation of HFO-1234yf was previously determined by Schuster et al. (2008, 2009, 2010) showing that HFO-1234yf is metabolized in a very low overall amount (< 1% in mice, rat and rabbit) by cytochrome P-450 and glutathione *S*-transferase. In female NZW rabbits, male SD rats and male B6C3F1 mice, the predominant metabolites of HFO-1234yf were *S*-(3,3,3-trifluoro-2-hydroxypropanyl)-mercaptolactic acid and *N*-acetyl-*S*-(3,3,3-trifluoro-2-hydroxypropanyl)-*L*-cysteine. The only species differences observed were the absence of the cytochrome P-450 mediated trace metabolites 3,3,3-trifluorolactic acid, trifluoroacetic acid, 3,3,3-trifluoro-1-hydroxyacetone and 1,1,1-trifluoroacetone in rabbit and 3,3,3-trifluoro-2-propanol in rat urine. Several *in vitro* and *in vivo* toxicity studies indicated no potential toxicity for HFO-1234yf, nevertheless developmental toxicity studies with HFO-1234yf showed mortality in pregnant female NZW rabbits.

Since the lethality in pregnant animals may be due to altered biotransformation of HFO-1234yf, it was evaluated whether the formation of toxic metabolites or a change in the biotransformation capacity might be relevant. A second aim was to determine if there are potential gender-related differences in the metabolism of HFO-1234yf. Therefore male, female and pregnant female rabbits were exposed to 50,000 ppm and 100,000 ppm for one hour and urine was collected for 48 hours after the inhalation exposure. The biotransformation analysis after this single high-dose exposure revealed no major differences in urinary metabolite pattern between the exposure groups. Moreover, no major

deviations were observed by comparison to previous results by Schuster et al. (2010). The only difference was that *N*-acetyl-*S*-(3,3,3-trifluoro-2-hydroxypropanyl)-mercaptolactic acid was determined as predominant metabolite in ^{19}F-NMR spectra of all analyzed urine samples instead of *N*-acetyl-*S*-(3,3,3-trifluoro-2-hydroxypropanyl)-*L*-cysteine as described by Schuster et al. (2010). Possible explanations for the difference in renal processing could be the rabbit strain, housing conditions or diet. Quantification of urinary *N*-acetyl-*S*-(3,3,3-trifluoro-2-hydroxypropanyl)-*L*-cysteine excretion confirmed a fast metabolite excretion of more than 83% in male and more than 93% in non-pregnant female/pregnant female animals (of total recovery of *N*-acetyl-*S*-(3,3,3-trifluoro-2-hydroxypropanyl)-*L*-cysteine within 48 hours) within 24 hours after inhalation exposure. The overall biotransformation amount was less than 0.1% in all groups and no significant differences in recovery of *N*-acetyl-*S*-(3,3,3-trifluoro-2-hydroxypropanyl)-*L*-cysteine between non-pregnant (43.10 ± 22.35 µmol) and pregnant female (50.47 ± 19.72 µmol) rabbits were observed (male rabbits exposed to 100,000 ppm for one hour excreted 86.40 ± 38.87 µmol). Urinary excretion of inorganic fluoride within 48 hours also showed no significant differences between pregnant (3.03 ± 1.76 µmol) and non-pregnant (4.44 ± 1.65 µmol) rabbits. As lethality and clinical signs of toxicity were not observed in any of the exposure groups, the results suggest that the lethality of HFO-1234yf in pregnant rabbits unlikely is due to changes in biotransformation patterns or capacity in pregnant rabbits. Moreover the study revealed no gender-related differences in the metabolism of HFO-1234yf.

Since an acute single high dose inhalation exposure revealed no differences in biotransformation and no potential toxic metabolite of HFO-1234yf could be observed, a second study was initiated to investigate whether multiple exposures may lead to toxic metabolites in male or female NZW rabbits. Therefore a 28-day inhalation study with a 28-day recovery period was performed and male and female rabbits were exposed 6 hours a day, 7 days a week for up to 7, 14 or 28 consecutive days. A recovery group, also exposed for 28 days, was observed for additional 28 days after the last exposure. Exposure levels were 0 (control), 500 (low dose), 1,000/1,500 (mid dose) and 4,500/5,500 (high dose) ppm of HFO-1234yf. Urine was collected for 18 hours after termination of each exposure. Tissue (liver and heart) and plasma samples were obtained at each necropsy.

In all analyzed urine samples, the predominant metabolites were again *S*-(3,3,3-trifluoro-2-hydroxypropanyl)-mercaptolactic acid and *N*-acetyl-*S*-(3,3,3-trifluoro-2-hydroxypropanyl)-*L*-cysteine. ^{19}F-NMR analysis of aqueous heart extracts, of animals with high clinical heart toxicity parameters, did not show any fluoro-related signal. The hypothetical formation and accumulation of monofluoroacetate in the heart was also not confirmed by LC-MS/MS analysis. Since no major differences in urinary metabolite pattern were observed between the groups, only the *N*-acetyl-*S*-(3,3,3-trifluoro-2-hydroxypropanyl)-*L*-cysteine excretion was quantified. No significant differences in recovery of *N*-acetyl-*S*-(3,3,3-trifluoro-2-hydroxypropanyl)-*L*-cysteine was seen in male and female rabbits. Inorganic fluoride levels in serum and urine were also unremarkable with no significant gender-related differences.

Effects of multiple HFO-1234yf exposure on liver enzyme activity of cytochrome P-450 3A4 and 2E1 showed no remarkable changes as well. Only minor enzyme induction was observed for high dose 28-day exposures in male (Student's t-test compared to control, $p = 0.03$) and high dose 7-day exposures in female rabbits (Student's t-test compared to control, $p = 0.03$) regarding cytochrome P-450 2E1 activity. In conclusion, it is rather unlikely that the observed lethality in rabbits in this multiple exposure-study and previous developmental toxicity studies is caused by the formation of toxic metabolites of HFO-1234yf. Further, no major differences in metabolite pattern and biotransformation extent were found between male and female NZW rabbits and in comparison with previous results of the biotransformation analysis in rabbit single exposure studies.

A second aim of this thesis was to determine the so far unknown metabolic fate of *trans*-HCFO-1233zd. For toxicological characterization and for evaluation of potential human health risks of *trans*-HCFO-1233zd, the biotransformation and kinetics of metabolite excretion were analyzed in *in vivo* test species and *in vitro* in subcellular liver fractions. Therefore liver microsomes from rats, rabbits and humans were incubated with *trans*-HCFO-1233zd both in the presence or absence of glutathione and/or a NADPH regenerating system for up to 12 hours. For *in vivo* studies, male SD rats and female NZW rabbits were exposed by whole-body inhalation to 2,000, 5,000 and 10,000 ppm of *trans*-HCFO-1233zd for 6 hours and urine was collected for 48 hours after the end of the exposures. Blood samples were taken 0, 24 and 48 hours after termination of the inhalations (only rat).

In vitro biotransformation of *trans*-HCFO-1233zd revealed *S*-(3,3,3-trifluoro-*trans*-propenyl)-glutathione as the predominant metabolite of *trans*-HCFO-1233zd in rat, rabbit and human liver microsomes in the presence of glutathione. Products of the oxidative biotransformation of *trans*-HCFO-1233zd were only minor metabolites when glutathione was present. In rats, both 3,3,3-trifluorolactic acid and *N*-acetyl-(3,3,3-trifluoro-*trans*-propenyl)-L-cysteine were observed as major urinary metabolites representing 40% respectively 32% of total ^{19}F-NMR fluorine signal intensity. While 3,3,3-trifluorolactic acid was not found in the urine of rabbits exposed to *trans*-HCFO-1233zd, the predominant metabolite was *N*-acetyl-(3,3,3-trifluoro-*trans*-propenyl)-*L*-cysteine (46% of total ^{19}F-NMR fluorine signal intensity). Quantification showed rapid excretions of both major metabolites, with elimination half-life times of less than 6 hours in both species. Based on metabolite recovery in urine and estimations of doses of *trans*-HCFO-1233zd received by inhalation, the extent of biotransformation of *trans*-HCFO-1233zd was determined as approximately 0.01% of received dose in rabbits and approximately 0.002% in rats. The metabolite structures suggest *trans*-HCFO-1233zd undergoes both oxidative biotransformation by cytochrome P-450 and direct glutathione conjugation with different intensities at very low rates. Observed species differences were the lack of the major *trans*-HCFO-1233zd urinary rat metabolite 3,3,3-trifluorolactic acid in rabbit urine and the absence of the *trans*-HCFO-1233zd urinary rabbit trace metabolite 3,3,3-trifluoro-1-propanol in rat urine. Excluding the still unidentified metabolites, toxic *in vivo* and *in vitro* biotransformation products could not be determined to any great extent.

The hepatotoxic trifluoroacetic acid and the highly toxic 3,3,3-trifluoropropionic acid with its feasible negative effects on the heart were only detected in traces. The reactive metabolite 1-chloro-3,3,3-trifluoro-1,2-epoxypropane formed by cytochrome P-450 is likely to be formed only in very low amounts and is apparently rapidly detoxified by epoxide hydrolase or by glutathione conjugation. Therefore possible covalent binding with tissue nucleophiles may be efficiently prevented. Formation of reactive metabolites by glutathione *S*-transferase and renal ß-lyase pathway as observed for other halogenated carbons and hydrogcarbons (e.g. prefluorpropen, 1,1,2-trichloro-3,3,3-trifluoropropene, tetrachloroethene) is unlikely for *trans*-HCFO-1233zd due to the lack of multiple halogen leaving groups. Furthermore, quantification of the glutathione *S*-transferase dependent metabolites revealed a very low overall formation compared to the extent excreted after exposition to potent nephrotoxic compounds (trichloroethene, tetrachloroethene). The low biotransformation amount and the rapid excretion of metabolites as well as the absence of potent toxic biotransformation products in both species, support the result of prior studies that *trans*-HCFO-1233zd has only a low potential for toxicity in mammals. The data on metabolism and toxicokinetics of *trans*-HCFO-1233zd are in good agreement with previously published data for the related nontoxic compound *trans*-1,3,3,3-tetrafluoropropene by Schuster et al. (2009). In conclusion, the results of this biotransformation analysis of *trans*-HCFO-1233zd suggest rather a low potential for mammalian toxicity and are in good agreement with other conducted toxicity studies of this compound.

6 Zusammenfassung

Das neue Kühlmittel 2,3,3,3-Tetrafluoropropen (HFO-1234yf) und das neue Treib- und Reinigungsmittel *trans*-1-Chlor-3,3,3-trifluorpropen (*trans*-HCFO-1233zd) sind Chlorfluorkohlenstoff-Ersatzstoffe mit sehr geringem Treibhauspotenzial und kurzer atmosphärischer Lebensdauer. Während HFO-1234yf keinerlei negative Auswirkungen auf den Abbau der Ozonschicht hat, schädigt *trans*-HCFO-1233zd diese aufgrund eines Chloratoms in seiner Struktur. Durch die erhöhte Abbaurate von *trans*-HCFO-1233zd in niedrigeren Luftschichten, wird im Vergleich zu seinen Vorgängersubstanzen (z.B. 1,1,2-Trichlor-1,2,2-trifluorethan, CFC-113) jedoch ein weitaus geringerer Ozonabbau in der Stratosphäre gewährleistet.

Im Rahmen dieser Arbeit wurde der Metabolismus von HFO-1234yf und *trans*-HCFO-1233zd in *In-vitro*- und *In-vivo*-Versuchen charakterisiert. Hierfür wurde das gewonnene Probenmaterial mittels ^{19}F-NMR-Spektroskopie, LC-MS/MS-Spektrometrie und GC/MS-Spektrometrie auf Fluor-Metabolite untersucht und diese durch Vergleichsmessungen mit Standardsubstanzen identifiziert. Die Quantifizierung der Hauptmetabolite und des anorganischen Fluorids in Urin und Plasma erfolgte mittels LC-MS/MS-Analyse bzw. mittels Potentiometrie. In einer Mehrfachexpositionsstudie mit HFO-1234yf wurde zudem die Aktivität der Cytochrom-P450-Enzyme 3A4 und 2E1 in gewonnenem Leber- und Herzgewebe ermittelt.

Der Metabolismus von HFO-1234yf wurde bereits in früheren Arbeiten von Schuster et al. (2008, 2009, 2010) charakterisiert. Es konnte gezeigt werden, dass HFO-1234yf nur in sehr geringem Maße mittels Cytochrom-P450 und Glutathion-*S*-Transferase verstoffwechselt wird (< 1% in der Maus, der Ratte und im Kaninchen). *S*-(3,3,3-Trifluor-2-hydroxypropanyl)-Mercaptomilchsäure und *N*-Acetyl-(3,3,3-trifluor-2-hydroxypropanyl)-*L*-Cystein konnten als Hauptmetabolite in männlichen B6C3F1 Mäusen, männlichen SD-Ratten sowie weiblichen NZW-Kaninchen identifiziert werden. Im Gegensatz zur Ratte fehlten im Kaninchenurin die Spurenmetabolite 3,3,3-Trifluormichsäure, Trifluoressigsäure und 3,3,3-Trifluor-1-hydroxyaceton. In diversen Tierstudien und *In-vitro*-Experimenten zeigte HFO-1234yf keinerlei Anzeichen für Toxizität. Dennoch kam es in Entwicklungstoxizitätsstudien mit NZW-Kaninchen zu Todesfällen bei trächtigen Tieren.

Im Rahmen dieser Arbeit sollte näher untersucht werden, ob die erhöhte Empfindlichkeit trächtiger Kaninchen gegenüber HFO-1234yf möglicherweise durch einen veränderten Metabolismus von HFO-1234yf begründet werden kann. Von Interesse war hierbei vor allem die eventuelle Bildung toxischer Biotransformationsprodukte oder Veränderungen in der Stoffwechselkapazität bei trächtigen NZW-Kaninchen. Ein weiteres Ziel dieser Arbeit war es mögliche geschlechtsspezifische Unterschiede im Metabolismus von HFO-1234yf zu untersuchen. Zur Beantwortung dieser Fragen wurde zunächst eine Hochdosis-

Inhalationsstudie (einmalige Exposition) mit männlichen, weiblichen und trächtigen weiblichen NZW-Kaninchen durchgeführt. Hierfür wurden die Tiere für eine Stunde einer HFO-1234yf-Konzentrationen von 50,000 bzw. 100.000 ppm ausgesetzt und anschließend der Tierurin für 48 Stunden gesammelt. Die Urinuntersuchungen konnten zeigen, dass die Metabolismusmuster der einzelnen Expositionsgruppen keine grundsätzlichen Unterschiede aufwiesen. Die einzige Abweichung zum bereits bekannten HFO-1234yf-Metabolismus war die Identifizierung von *S*-(3,3,3-Trifluor-2-hydroxypropanly)-Mercaptomilchsäure als Hauptmetabolit anstatt von *N*-Acetyl-*S*-(3,3,3-trifluor-2-hydroxypropanyl)-*L*-Cystein (Schuster et al., 2010). Mögliche Erklärungen für diese Abweichung sind die Verwendung eines anderen Kaninchenstamms, veränderte Haltungsbedingungen oder anderes Futter. Die Quantifizierung von *N*-Acetyl-*S*-(3,3,3-trifluor-2-hydroxypropanyl)-*L*-Cystein konnte zudem eine schnelle Metabolitenausscheidung bestätigten. So schieden die männlichen Kaninchen innerhalb der ersten 24 Stunden nach Ende der Inhalation bereits mehr als 83%, die nicht trächtigen und trächtigen Weibchen mehr als 93% der insgesamt in 48 Stunden ausgeschiedenen Menge an *N*-Acetyl-*S*-(3,3,3-trifluor-2-hydroxypropanyl)-*L*-Cystein aus. Die Gesamtbiotransformation in allen Gruppen betrug weniger als 0.1% der aufgenommenen HFO-1234yf-Menge, wobei es keine signifikanten Unterschiede in der gesamten Ausscheidungsmenge von *N*-Acetyl-*S*-(3,3,3-trifluor-2-hydroxypropanyl)-*L*-Cystein zwischen trächtigen (43,10 ± 22,35 µmol; 100.000 ppm Exposition) und nicht trächtigen Weibchen (50,47 ± 19,73 µmol; 100.000 ppm Exposition) gab. Die Ausscheidung der Männchen war im Vergleich zu den Weibchen mit 86,40 ± 38,87 µmol (100.000 ppm Exposition) innerhalb von 48 Stunden signifikant höher. Die Bestimmung der anorganischen Fluorid-Ausscheidung zeigte ebenfalls keinen signifikanten Unterschied zwischen trächtigen (3,03 ± 1,76 µmol) und nicht trächtigen (4,44 ± 1,65 µmol) Tieren. Da weder Todesfälle noch klinische Anzeichen einer toxischen Wirkung von HFO-1234yf in einer der Expositionsgruppen auftraten, kann davon ausgegangen werden, dass die beobachtete Toxizität in trächtigen Weibchen weder durch eine Veränderung der Biotransformationswege noch durch eine veränderte Stoffwechselkapazität bedingt ist. Geschlechtsspezifische Unterschiede im HFO-1234yf Metabolismus konnten ebenfalls nicht festgestellt werden.

Aufgrund der geringen Biotransformationsveränderungen nach einmaliger Hochdosis-Inhalation mit HFO-1234yf, wurde der Metabolismus in einer zweiten Studie auf mögliche Veränderungen nach mehrfacher Exposition untersucht. Für diese Fragestellung wurden weibliche und männliche NZW-Kaninchen 6 Stunden am Tag für 7, 14 oder 28 Tage gegenüber HFO-1234yf exponiert. Eine weitere Gruppe wurde 28 Tage exponiert und darauffolgend für weitere 28 Tage ohne Exposition beobachtet. Als Expositionskonzentrationen wurden 0 (Kontrolle), 500 (niedrige Dosis), 1.000/1.500 (mittlere Dosis) und 4.500/5.500 ppm (hohe Dosis) gewählt. Nach Beendigung der Inhalationen bzw. der 28-tägigen Beobachtungsphase wurde der Tierurin für 18 Stunden gesammelt. Anschließend wurden Herz-/Lebergewebe und Blutproben gewonnen.

Auch in dieser Studie konnten in allen Kaninchenurinen *N*-Acetyl-*S*-(3,3,3-trifluor-2-hydroxypropanyl)-*L*-Cystein und *S*-(3,3,3-Trifluor-2-hydroxypropanyl)-Mercaptomilchsäure als die beiden Hauptausscheidungs-produkte von HFO-1234yf identifiziert werden. Im Gegensatz zu den Ergebnissen von Schuster et al. (2010) war bei dieser Messung wiederum *S*-(3,3,3-Trifluor-2-hydroxypropanyl)-Mercaptomilchsäure der Metabolit mit der höchsten ^{19}F-NMR Signalintensität. Untersuchungen wässriger Herzmuskelextrakte von Kaninchen mit erhöhten klinischen Herzparametern bzw. positiven Herzpathologiebefunden auf das Vorhandensein von Fluormetaboliten lieferten keinerlei ^{19}F-NMR-Signale. Die Hypothese zur Bildung und Akkumulation der kardiotoxischen Monofluoressigsäure im Herzgewebe konnte durch LC-MS/MS-Untersuchungen nicht bestätigt werden. Erneut konnten auch in dieser Studie keine Unterschiede in den Metabolismusmustern der einzelnen Expositionsgruppen gefunden werden. Die Quantifizierung von *N*-Acetyl-*S*-(3,3,3-trifluor-2-hydroxypropanyl)-*L*-Cystein und des anorganischen Fluorids im 18-Stunden-Sammelurin ergab ebenfalls keine nennenswerten Unterschiede zwischen weiblichen und männlichen Tieren. Gleiches kann zur Bestimmung der anorganischen Fluoridkonzentrationen im Kaninchenplasma festgehalten werden. Ein eindeutiger Effekt auf die Cytochrom-P-450 3A4- und 2E1-Aktivitäten durch Mehrfachexposition mit HFO-1234yf wurde nicht festgestellt. Die geringe Induktion von Cytochrom-P450 2E1 in Lebermikrosomen von männlichen (28 Tage Exposition; t-Test im Vergleich zur Kontrolle, $p = 0,03$) und weiblichen (7 Tage Exposition; t-Test im Vergleich zur Kontrolle, $p = 0,03$) Hochdosis-Tieren sind von keiner biologischen Relevanz.

Zusammenfassend kann festgehalten werden, dass die beobachteten Todesfälle in dieser Mehrfachexpositionsstudie und den zuvor durchgeführten Entwicklungstoxizitätsstudien kaum auf einen potentiell toxischen Metaboliten von HFO-1234yf zurückzuführen sind. Die Ergebnisse bestätigen den bereits bekannten Metabolismus von HFO-1234yf im NZW-Kaninchen auch nach einmaliger Hochdosisexposition sowie Mehrfachexposition für bis zu 28 Tage. Die Untersuchung auf geschlechtsspezifische Biotransformationsunterschiede lieferte in beiden Studien keine relevante Abweichung zwischen den Geschlechtern. Ebenso konnte für trächtige Tiere kein Unterschied in der Biotransformation von HFO-1234yf festgestellt werden.

Das zweite Ziel der vorliegenden Arbeit war die Charakterisierung des bislang unbekannten Metabolismus von *trans*-HCFO-1233zd. Zur Bewertung des toxischen Potentials und einer möglichen Gefährdung für den Menschen durch *trans*-HCFO-1233zd, wurde die Biotransformation von *trans*-HCFO-1233zd in Ratten und Kaninchen sowie durch Inkubationen von Leberzellfraktionen *in vitro* untersucht. Zunächst wurden Lebermikrosomen von Kaninchen, Mensch und Ratte mit *trans*-HCFO-1233zd in Gegenwart bzw. Abwesenheit von Glutathion und/oder eines NADPH regenerierenden Systems inkubiert. Für die *In-vivo*-Versuche wurden männliche SD-Ratten und weibliche NZW-Kaninchen gegenüber 0, 2.000, 5.000 und 10.000 ppm *trans*-HCFO-1233zd für 6 Stunden

exponiert. Anschließend wurden die Tierurine für 48 Stunden gesammelt und zusätzlich 0, 24 und 48 Stunden nach Beendigung der Inhalation Blutproben genommen (nur Ratte).

Die *In-vitro*-Experimente mit Lebermikrosomen und *trans*-HCFO-1233zd zeigten, dass *S*-(3,3,3-Trifluor-*trans*-propenyl)-Glutathion der Hauptmetabolit in allen drei Spezies war. Oxidative Metabolite spielten dabei eine untergeordnete Rolle und wurden nur in Spuren nachgewiesen. In der Ratte waren 3,3,3-Trifluormilchsäure (40% des ^{19}F-NMR Gesamtintegrals) und *N*-Acetyl-(3,3,3-trifluor-*trans*-propenyl)-*L*-Cystein (32% des ^{19}F-NMR Gesamtintegrals) die Metabolite mit den größten Signalintensitäten in den ^{19}F-NMR-Spektren der Urinproben. Im Kaninchenurin konnte *N*-Acetyl-(3,3,3-trifluor-*trans*-propenyl)-*L*-Cystein (46% des ^{19}F-NMR Gesamtintegrals) als Hauptmetabolit identifiziert werden. 3,3,3-Trifluormilchsäure war dagegen nicht nachweisbar. Die Quantifizierung der Hauptmetabolite zeigte eine schnelle Exkretion mit Halbwertszeiten < 6 Stunden für beide Spezies. Auf Grundlage der errechneten *trans*-HCFO-1233zd-Aufnahme und der wiedergefunden Metabolitenmengen im Urin von Ratte und Kaninchen kann von einer sehr geringen Biotransformation von *trans*-HCFO-1233zd in beiden Spezies ausgegangen werden (Ratte – ca. 0.002%; Kaninchen – ca. 0.01%). Die Metabolitenstrukturen wiesen auf zwei Hauptstoffwechselwege hin: Zum einen auf den oxidativen Metabolismus von *trans*-HCFO-1233zd via Cytochrom-P-450 und zum anderen auf die Konjugation von Glutathion mittels Glutathion-*S*-Transferase. Beide Wege waren in ihrem Ausmaß von der Expositionskonzentration abhängig. So überwog der oxidative Metabolismus bei geringen, die Konjugation mit Glutathion bei höheren *trans*-HCFO-1233zd-Konzentrationen. Speziesunterschiede zwischen Ratte und Kaninchen zeigten sich durch das Fehlen von 3,3,3-Trifluormilchsäure im Kaninchen- und das Fehlen von 3,3,3-Trifluor-1-propanol im Rattenurin. Abgesehen von den noch unbekannten Fluorverbindungen in Ratten- und Kaninchenurin konnten keine potentiell toxischen Verbindungen in hohen Mengen festgestellt werden. Dennoch können sich zwei in geringen Mengen nachgewiesene Substanzen auf Organfunktionen auswirken: Für die Trifluoressigsäure sind Einflüsse auf den Leberstoffwechsel (Glykolyse/Gluconeogenese) und das Lebergewicht bekannt, für die toxische 3,3,3-Trifluorpropionsäure gibt es Anzeichen, dass sie sich auf die Herzfunktion von Ratten negativ auswirkt. Beide Metabolite konnten allerdings nur in Spuren nachgewiesen werden. Der reaktive Metabolit 1-Chlor-3,3,3-trifluor-1,2-epoxypropan wird offensichtlich nur in sehr geringem Ausmaß von Cytochrom-P-450 gebildet und vollständig durch Hydrolyse bzw. Glutathionkonjugation entgiftet. Es kann davon ausgegangen werden, dass es nicht zur Ausbildung von kovalenten Bindungen mit Gewebebestandteilen kommt. Eine Aktivierung von *trans*-HCFO-1233zd durch die Glutathion-*S*-Transferase und die renale ß-Lyase, wie es für andere halogenierte Kohlenstoff- und Kohlenwasserstoffverbindungen gezeigt werden konnte (z.B. Perfluorpropen, 1,1,2-Trichlor-3,3,3-trifluorpropen, Tetrachlorethen), ist aufgrund des Mangels mehrerer Abgangsgruppen unwahrscheinlich. Zudem ist im Vergleich zu nephrotoxischen Verbindungen, wie etwa Trichlorethen oder Tetrachlorethen, die gesamte Ausscheidung an Glutathion-*S*-Transferase-abhängigen Stoffwechselprodukten bei *trans*-HCFO-1233zd um ein Vielfaches niedriger.

Abschließend kann festgehalten werden, dass die geringe Biotransformation sowie die schnelle Metabolitenausscheidung und das Fehlen toxischer Metabolite in relevanten Mengen die Ergebnisse vorheriger toxikologischer Studien bestätigen. Zudem stimmen die gewonnen Metabolismus- und Toxikokinetikdaten mit Studienergebnissen der chemisch verwandten Substanz *trans*-1,3,3,3-Tetrafluorpropen überein, für die ebenfalls eine sehr geringe Biotransformation und keinerlei toxische Metabolite nachgewiesen werden konnten. Die Annahme aus vorhergehenden Toxizitätsstudien, dass durch *trans*-HCFO-1233zd nur ein sehr geringes Gefährdungspotential für Säugetiere ausgeht, kann durch die Ergebnisse dieser Arbeit bestätigt werden.

7 References

ALEXANDER, D. J., COLLINS, C. J., COOMBS, D. W., GILKISON, I. S., HARDY, C. J., HEALEY, G., KARANTABIAS, G., JOHNSON, N., KARLSSON, A., KILGOUR, J. D. & MCDONALD, P. 2008. Association of Inhalation Toxicologists (AIT) Working Party Recommendation for Standard Delivered Dose Calculation and Expression in Non-Clinical Aerosol Inhalation Toxicology Studies with Pharmaceuticals. *Inhalation Toxicology,* 20**,** 1179-1189.

ANDERS, M. W. 1991. Metabolism and toxicity of hydrochlorofluorocarbons: current knowledge and needs for the future. *Environmental Health Perspectives,* 96**,** 185-91.

ANDERS, M. W. & DEKANT, W. 1998. Glutathione-dependent bioactivation of haloalkenes. *Annual Review of Pharmacology and Toxicology,* 38**,** 501-537.

ANDERS, M. W., DEKANT, W. & VAMVAKAS, S. 1992. Glutathione-dependent toxicity. *Xenobiotica,* 22**,** 1135-45.

ANDERSEN, M. P. S., NILSSON, E. J. K., NIELSEN, O. J., JOHNSON, M. S., HURLEY, M. D. & WALLINGTON, T. J. 2008. Atmospheric chemistry of trans-CF(3)CH = CHCl: Kinetics of the gas-phase reactions with Cl atoms, OH radicals, and O(3). *Journal of Photochemistry and Photobiology a-Chemistry,* 199**,** 92-97.

ANDERSON, G. D. 2005. Pregnancy-induced changes in pharmacokinetics: a mechanistic-based approach. *Clinical Pharmacokinetics,* 44**,** 989-1008.

ANDERSON, J. G., TOOHEY, D. W. & BRUNE, W. H. 1991. Free-Radicals within the Antarctic Vortex - the Role of Cfcs in Antarctic Ozone Loss. *Science,* 251**,** 39-46.

BACK, K. C. & VAN STEE, W. 1977. Toxicology of haloalkane propellants and fire extinguishants. *Annual Review of Pharmacology and Toxicology,* 17**,** 83-95.

BAYER, T. 2005. *Toxicity and Biotransformation of 1,1,1,3,3-Pentafluoropropane, 3,3,3-Trifluoropropionic acid and 1,1,1,3-Tetrachloropropane.* Unpublished thesis, Department of Pharmacology and Toxicology of the Julius-Maximilians-University of Wuerzburg.

BEINERT, H. & KENNEDY, M. C. 1993. Aconitase, a two-faced protein: enzyme and iron regulatory factor. *The FASEB Journal,* 7**,** 1442-9.

BENOIT, E., CRESTEIL, T., RIVIERE, J. L. & DELATOUR, P. 1992. Specific and enantioselective sulfoxidation of an aryl-trifluoromethyl sulfide by rat liver cytochromes P-450. *Drug Metabolism and Disposition,* 20**,** 877-81.

BERNAUER, U., BIRNER, G., DEKANT, W. & HENSCHLER, D. 1996. Biotransformation of trichloroethene: Dose dependent excretion of 2,2,2-trichloro-metabolites and mercapturic acids in rats and humans after inhalation. *Archives of Toxicology,* 70**,** 338-346.

BIRNER, G., RICHLING, C., HENSCHLER, D., ANDERS, M. W. & DEKANT, W. 1994. Metabolism of Tetrachloroethene in Rats - Identification of N-Epsilon-(Dichloroacetyl)-L-Lysine and N-Epsilon-(Trichloroacetyl)-L-Lysine as Protein Adducts. *Chemical Research in Toxicology,* 7**,** 724-732.

BOUTONNET, J. C., BINGHAM, P., CALAMARI, D., DE ROOIJ, C., FRANKLIN, J., KAWANO, T., LIBRE, J. M., MCCULLOCH, A., MALINVERNO, G., ODOM, J. M., RUSCH, G. M., SMYTHE, K., SOBOLEV, I., THOMPSON, R. & TIEDJE, J. M. 1999. Environmental risk assessment of trifluoroacetic acid. *Human and Ecological Risk Assessment,* 5**,** 59-124.

BRUNING, T., VAMVAKAS, S., MAKROPOULOS, V. & BIRNER, G. 1998. Acute intoxication with trichloroethene: Clinical symptoms, toxicokinetics, metabolism, and development of biochemical parameters for renal damage. *Toxicological Sciences,* 41**,** 157-165.

CHAPMAN, S. 1930. A theory of upper atmosperic ozone. *Memoirs of the Royal Meterological Society,* 3**,** 103-125.

CHEN, Q., JONES, T. W., BROWN, P. C. & STEVENS, J. L. 1990. The Mechanism of Cysteine Conjugate Cytotoxicity in Renal Epithelial-Cells - Covalent Binding Leads to Thiol Depletion and Lipid-Peroxidation. *Journal of Biological Chemistry,* 265**,** 21603-21611.

CLAYTON, J. W. 1977. Toxicology of Fluoroalkenes - Review and Research Needs. *Environmental Health Perspectives,* 21**,** 255-267.

COMMANDEUR, J. N. M., STIJNTJES, G. J. & VERMEULEN, N. P. E. 1995. Enzymes and Transport-Systems Involved in the Formation and Disposition of Glutathione S-Conjugates - Role in Bioactivation and Detoxication Mechanisms of Xenobiotics. *Pharmacological Reviews,* 47**,** 271-330.

CONSTAN, A. A., SPRANKLE, C. S., PETERS, J. M., KEDDERIS, G. L., EVERITT, J. I., WONG, B. A., GONZALEZ, F. L. & BUTTERWORTH, B. E. 1999. Metabolism of chloroform by cytochrome P450 2E1 is required for induction of toxicity in the liver, kidney, and nose of male mice. *Toxicology and Applied Pharmacology,* 160**,** 120-126.

CUMMINGS, C. C. & MCIVOR, M. E. 1988. Fluoride-induced hyperkalemia: the role of Ca2+-dependent K+ channels. *The American Journal of Emergency Medicine,* 6**,** 1-3.

CZEKAJ, P., WIADERKIEWICZ, A., FLOREK, E. & WIADERKIEWICZ, R. 2005. Tobacco smoke-dependent changes in cytochrome P450 1A1, 1A2, and 2E1 protein expressions in fetuses, newborns, pregnant rats, and human placenta. *Archives of Toxicology,* 79**,** 13-24.

DAMANI, L. A. & HOUDI, A. A. 1988. Cytochrome P-450 and FAD-monooxygenase mediated S- and N-oxygenations. *Drug Metabolism and Drug Interactions,* 6**,** 235-44.

DAVIS, F. A., JENKINS, L. A. & BILLMERS, R. L. 1986. Chemistry of Sulfenic Acids .7. Reason for the High Reactivity of Sulfenic Acids - Stabilization by Intramolecular Hydrogen-Bonding and Electronegativity Effects. *Journal of Organic Chemistry,* 51**,** 1033-1040.

DEKANT, W. 1996. Toxicology of chlorofluorocarbon replacements. *Environmental Health Perspectives,* 104**,** 75-83.

DEKANT, W. 2003. Biosynthesis of toxic glutathione conjugates from halogenated alkenes. *Toxicology Letters,* 144**,** 49-54.

DEKANT, W., SCHULZ, A., METZLER, M. & HENSCHLER, D. 1986. Absorption, Elimination and Metabolism of Trichloroethylene - a Quantitative Comparison between Rats and Mice. *Xenobiotica,* 16**,** 143-152.

DEKANT, W., URBAN, G., GORSMANN, C. & ANDERS, M. W. 1991. Thioketene Formation from Alpha-Haloalkenyl 2-Nitrophenyl Disulfides - Models for Biological Reactive Intermediates of Cytotoxic S-Conjugates. *Journal of the American Chemical Society,* 113**,** 5120-5122.

DEKANT, W., VAMVAKAS, S., KOOB, M., KOCHLING, A., KANHAI, W., MULLER, D. & HENSCHLER, D. 1990. A Mechanism of Haloalkene-Induced Renal Carcinogenesis. *Environmental Health Perspectives,* 88**,** 107-110.

DUPONT 2008. In Vitro Partition Coefficients in Human Blood and Rat and Rabbit Blood, Muscle, Liver and Fat, Project ID DuPont-25456. E.I. du Pont de Nemours and Company, DuPont Haskell Global Centres for Health and Environmental Sciences, P.O. Box 50, Newark, Delawar 19714.

EMA, M., NAYA, M., YOSHIDA, K. & NAGAOSA, R. 2010. Reproductive and developmental toxicity of hydrofluorocarbons used as refrigerants. *Reproductive Toxicology,* 29**,** 125-31.

EP 2006. DIRECTIVE 2006/40/EC. THE EUROPEAN PARLIAMENT AND THE COUNCIL OF THE EUROPEAN UNION.

EPA 2007. Achievments in Stratosperic Ozone Protection. Progress Report.

FARKAS, M., BERRY, J. O. & AGA, D. S. 2007. Determination of enzyme kinetics and glutathione conjugates of chlortetracycline and chloroacetanilides using liquid chromatography-mass spectrometry. *Analyst,* 132**,** 664-671.

FRANKLIN, J. 1993. The Atmospheric Degradation and Impact of 1,1,1,2-Tetrafluoroethane (Hydrofluorocarbon 134a). *Chemosphere,* 27**,** 1565-1601.

GARGAS, M. L., BURGESS, R. J., VOISARD, D. E., CASON, G. H. & ANDERSEN, M. E. 1989. Partition-Coefficients of Low-Molecular-Weight Volatile Chemicals in Various Liquids and Tissues. *Toxicology and Applied Pharmacology,* 98**,** 87-99.

GONCHAROV, N. V., JENKINS, R. O. & RADILOV, A. S. 2006. Toxicology of fluoroacetate: a review, with possible directions for therapy research. *Journal of Applied Toxicology,* 26**,** 148-161.

GOONERATNE, S. R., EASON, C. T., DICKSON, C. J., FITZGERALD, H. & WRIGHT, G. 1995. Persistence of Sodium Monofluoroacetate in Rabbits and Risk to Nontarget Species. *Human & Experimental Toxicology,* 14**,** 212-216.

GOTTLIEB, R. A. 2003. Cytochrome P450: major player in reperfusion injury. *Archives of Biochemistry and Biophysics,* 420**,** 262-267.

GUENGERICH, F. P. 2001. Common and uncommon cytochrome P450 reactions related to metabolism and chemical toxicity. *Chemical Research in Toxicology,* 14**,** 611-650.

GUENGERICH, F. P., CRAWFORD, W. M. & WATANABE, P. G. 1979. Activation of Vinyl-Chloride to Covalently Bound Metabolites - Roles of 2-Chloroethylene Oxide and 2-Chloroacetaldehyde. *Biochemistry,* 18**,** 5177-5182.

GUENGERICH, F. P., MASON, P. S., STOTT, W. T., FOX, T. R. & WATANABE, P. G. 1981. Roles of 2-Haloethylene Oxides and 2-Haloacetaldehydes Derived from Vinyl Bromide and Vinyl-Chloride in Irreversible Binding to Protein and DNA. *Cancer Research,* 41**,** 4391-4398.

HALL, L. L., KILPPER, R. W., SMITH, F. A., MORKEN, D. A. & HODGE, H. C. 1977. Kinetic model of fluoride metabolism in the rabbit. *Environmental Research,* 13**,** 285-302.

HAMNER 2007. Toxicogenomic assessment of the carcinogenic potential of 2,3,3,3-tetrafluoropropene, Report No. 06014, conducted for Honeywell International. Hamner Institute for Health Sciences, 6 Davis Drive, PO Box 12137, Research Triangle Park, NC 27709.

HAYES, J. D., FLANAGAN, J. U. & JOWSEY, I. R. 2005. Glutathione transferases. *Annual Review of Pharmacology and Toxicology,* 45**,** 51-88.

HE, X. J., EJIRI, N., NAKAYAMA, H. & DOI, K. 2005. Effects of pregnancy on CYPs protein expression in rat liver. *Experimental and Molecular Pathology,* 78**,** 64-70.

HEINDEL, J. J., BATES, H. K., PRICE, C. J., MARR, M. C., MYERS, C. B. & SCHWETZ, B. A. 1996. Developmental toxicity evaluation of sodium fluoride administered to rats and rabbits in drinking water. *Fundamental and Applied Toxicology,* 30**,** 162-77.

HERBST, J., KOSTER, U., KERSSEBAUM, R. & DEKANT, W. 1994. Role of P4502e1 in the Metabolism of 1,1,2,2-Tetrafluoro-1-(2,2,2-Trifluoroethoxy)-Ethane. *Xenobiotica,* 24**,** 507-516.

HIMMEL, H. M. 2008. Mechanisms involved in cardiac sensitization by volatile anesthetics: general applicability to halogenated hydrocarbons? *Critical Reviews in Toxicology,* 38**,** 773-803.

HINCHMAN, C. A. & BALLATORI, N. 1990. Glutathione-degrading capacities of liver and kidney in different species. *Biochemical Pharmacology,* 40**,** 1131-5.

HINCHMAN, C. A. & BALLATORI, N. 1994. Glutathione Conjugation and Conversion to Mercapturic Acids Can Occur as an Intrahepatic Process. *Journal of Toxicology and Environmental Health,* 41**,** 387-409.

HOFFMANN, P., HEINROTH, K., RICHARDS, D., PLEWS, P. & TORAASON, M. 1994. Depression of calcium dynamics in cardiac myocytes--a common mechanism of halogenated hydrocarbon anesthetics and solvents. *Journal of Molecular and Cellular Cardiology,* 26**,** 579-89.

HONEYWELL 2007. Material Safety Data Sheet, 2,3,3,3-tetrafluoropropene. Honeywell, 101 Columbia Road, Morristown, NJ 07962-1139.

HONEYWELL 2008. Material Safety Data Sheet, *trans*-1-chloro-3,3,3-trifluoropropene. Honeywell, 101 Columbia Road, Morristown, NJ 07962-1139.

HONEYWELL 2011. trans-1-Chloro-3,3,3-Trifluoropropylene: Toxicology Summary. Honeywell, 101 Columbia Road, Morristown, NJ 07962-1139.

HONEYWELL 2012. Clinical Pathology Draft Report - 2012. Honeywell, 101 Columbia Road, Morristown, NJ 07962-1139.

HOPFGARTNER, G., VARESIO, E., TSCHAPPAT, V., GRIVET, C., BOURGOGNE, E. & LEUTHOLD, L. A. 2004. Triple quadrupole linear ion trap mass spectrometer for the analysis of small molecules and macromolecules. *Journal of Mass Spectrometry,* 39**,** 845-55.

HOUGHTON, J. T., CALLANDER, B. A. AND VARNEY, S. K 1992. Climate Change 1992: The supplementary Report to the IPCC Scientific assessment. IPCC.

HUNTINGDON 2004. HFO-1234yf An Acute (4-hour) Inhalation Toxicity Range finding Study in the mouse via whole-body exposure, HLS Study No. 03-5479C, conducted for Honeywell International,. Huntingdon Life Sciences, 100 Mettlers Road East Millstone, New Jersey 08875-2360.

HUNTINGDON 2011. A 2-PHASE INHALATION SCREENING STUDY AND SINGLE EXPOSURE STUDY IN RABBITS VIA WHOLE-BODY INHALATION EXPOSURE, HLS Study No. 10-2226, conducted for Honeywell. Huntingdon Life Sciences, 100 Mettlers Road East Millstone, New Jersey 08875-2360.

JAKOBY, W. B. 1978. Glutathione Transferases in Detoxification. *Hoppe-Seylers Zeitschrift für Physiologische Chemie,* 359**,** 1038-1038.

KO, M., SHIA, R. L., SZE, N. D., MAGID, H. & BRAY, R. G. 1999. Atmospheric lifetime and global warming potential of HFC-245fa. *Journal of Geophysical Research-Atmospheres,* 104**,** 8173-8181.

KOOP, D. R. 1992. Oxidative and Reductive Metabolism by Cytochrome-P450-2e1. *The Faseb Journal,* 6**,** 724-730.

KOSTER, U., SPEERSCHNEIDER, P., KERSSEBAUM, R., WITTMANN, H. & DEKANT, W. 1994. Role of Cytochrome-P450 2e1 in the Metabolism of 1,1,2,3,3,3-Hexafluoropropyl Methyl-Ether. *Drug Metabolism and Disposition,* 22**,** 667-672.

LASH, L. H., SAUSEN, P. J., DUESCHER, R. J., COOLEY, A. J. & ELFARRA, A. A. 1994. Roles of Cysteine Conjugate Beta-Lyase and S-Oxidase in Nephrotoxicity - Studies with S-(1,2-Dichlorovinyl)-L-Cysteine and S-(1,2-Dichlorovinyl)-L-Cysteine Sulfoxide. *Journal of Pharmacology and Experimental Therapeutics,* 269**,** 374-383.

LASHOF, D. A. & AHUJA, D. R. 1990. Relative Contributions of Greenhouse Gas Emissions to Global Warming. *Nature,* 344**,** 529-531.

LAUBLE, H., KENNEDY, M. C., EMPTAGE, M. H., BEINERT, H. & STOUT, C. D. 1996. The reaction of fluorocitrate with aconitase and the crystal structure of the enzyme-inhibitor complex. *Proceedings of the National Academy of Sciences of the United States of America,* 93**,** 13699-13703.

LEITERER, M. 2008. Validierung von Untersuchungsmethoden in der analytischen Praxis. Thüringer Landesanstalt für Landwirtschaft, .

LEMAL, D. M. 2004. Perspective on fluorocarbon chemistry. *Journal of Organic Chemistry,* 69**,** 1-11.

LENZ, E. M., BRIGHT, J., KNIGHT, R., WESTWOOD, F. R., DAVIES, D., MAJOR, H. & WILSON, I. D. 2005. Metabonomics with H-1-NMR spectroscopy and liquid chromatography-mass spectrometry applied to the investigation of metabolic changes caused by gentamicin-induced nephrotoxicity in the rat. *Biomarkers,* 10**,** 173-187.

LOOS, R. & BARCELO, D. 2001. Determination of haloacetic acids in aqueous environments by solid-phase extraction followed by ion-pair liquid chromatography-electrospray ionization mass spectrometric detection. *Journal of Chromatography A,* 938**,** 45-55.

LOWRY, O. H., ROSEBROUGH, N. J., FARR, A. L. & RANDALL, R. J. 1951. Protein Measurement with the Folin Phenol Reagent. *Journal of Biological Chemistry,* 193**,** 265-275.

MACDONALD, T. L. 1983. Chemical Mechanisms of Halocarbon Metabolism. *Critical Reviews in Toxicology,* 11**,** 85-120.

MANZER, L. E. 1990. The Cfc-Ozone Issue - Progress on the Development of Alternatives to Cfcs. *Science,* 249**,** 31-35.

MCCULLOCH, A. 1999. CFC and Halon replacements in the environment. *Journal of Fluorine Chemistry,* 100**,** 163-173.

MCIVOR, M. E., CUMMINGS, C. E., MOWER, M. M., WENK, R. E., LUSTGARTEN, J. A., BALTAZAR, R. F. & SALOMON, J. 1987. Sudden cardiac death from acute fluoride intoxication: the role of potassium. *Annals of Emergency Medicine,* 16**,** 777-81.

MCKINNEY, L. L., ELDRIDGE, A. C. & COWAN, J. C. 1959a. Cysteine Thioethers from Chloroethylenes. *Journal of the American Chemical Society,* 81**,** 1423-1427.

MCKINNEY, L. L., PICKEN, J. C., WEAKLEY, F. B., ELDRIDGE, A. C., CAMPBELL, R. E., COWAN, J. C. & BIESTER, H. E. 1959b. Possible Toxic Factor of Trichloroethylene-Extracted Soybean Oil Meal. *Journal of the American Chemical Society,* 81**,** 909-915.

MCLEAN, A. E. M. 1977. Chlorofluorocarbons - in Can, in Man and in Atmosphere. *British Journal of Clinical Pharmacology,* 4**,** 663-666.

MENNICKE, W. H., GORLER, K. & KRUMBIEGEL, G. 1983. Metabolism of Some Naturally-Occurring Isothiocyanates in the Rat. *Xenobiotica,* 13**,** 203-207.

MINOR, B. H., HERRMANN, D. & GRAVEL, R. 2010. Flammability characteristics of HFO-1234yf. *Process Safety Progress,* 29**,** 150-154.

MITOMA, C., STEEGER, T., JACKSON, S. E., WHEELER, K. P., ROGERS, J. H. & MILMAN, H. A. 1985. Metabolic Disposition Study of Chlorinated Hydrocarbons in Rats and Mice. *Drug and Chemical Toxicology,* 8**,** 183-194.

MOLINA, M. J. & ROWLAND, F. S. 1974. Stratospheric Sink for Chlorofluoromethanes - Chlorine Atomic-Catalysed Destruction of Ozone. *Nature,* 249**,** 810-812.

MONKS, T. J., ANDERS, M. W., DEKANT, W., STEVENS, J. L., LAU, S. S. & VAN BLADEREN, P. J. 1990. Glutathione conjugate mediated toxicities. *Toxicology and Applied Pharmacology,* 106**,** 1-19.

MUTLIB, A., LAM, W., ATHERTON, J., CHEN, H., GALATSIS, P. & STOLLE, W. 2005. Application of stable isotope labeled glutathione and rapid scanning mass spectrometers in detecting and characterizing reactive metabolites. *Rapid Communications in Mass Spectrometry,* 19**,** 3482-92.

NIELSEN, O. J., JAVADI, M. S., ANDERSEN, M. P. S., HURLEY, M. D., WALLINGTON, T. J. & SINGH, R. 2007. Atmospheric chemistry of CF3CF=CH2: Kinetics and mechanisms of gas-phase reactions with Cl atoms, OH radicals, and O-3. *Chemical Physics Letters,* 439**,** 18-22.

ORKIN, V. L., HUIE, R. E. & KURYLO, M. J. 1996. Atmospheric lifetimes of HFC-143a and HFC-245fa: Flash photolysis resonance fluorescence measurements of the OH reaction rate constants. *Journal of Physical Chemistry,* 100**,** 8907-8912.

ORRENIUS, S., ORMSTAD, K., THOR, H. & JEWELL, S. A. 1983. Turnover and Functions of Glutathione Studied with Isolated Hepatic and Renal-Cells. *Federation Proceedings,* 42**,** 3177-3188.

POLIDORO, G., DIILIO, C., ARDUINI, A. & FEDERICI, G. 1981. Effect of Pregnancy on Hepatic Glutathione S-Transferase Activities in the Rat. *Biochemical Pharmacology,* 30**,** 1859-1860.

RAMANATHAN, V. 1975. Greenhouse Effect Due to Chlorofluorocarbons - Climatic Implications. *Science,* 190**,** 50-51.

RAUCY, J. L., KRANER, J. C. & LASKER, J. M. 1993. Bioactivation of Halogenated Hydrocarbons by Cytochrome-P4502e1. *Critical Reviews in Toxicology,* 23**,** 1-20.

REDROBE, S. 2002. Calcium metabolism in rabbits. *Seminars in Avian and Exotic Pet Medicine,* 11**,** 94-101.

ROSENBERG, P. H. & WAHLSTROM, T. 1971. Hepatotoxicity of halothane metabolites in vivo and inhibition of fibroblast growth in vitro. *Acta Pharmacologica et Toxicologica,* 29**,** 9-19.

ROWLEY 1963. The effect on rabbits of repeated subleathal doses of Sodium Fluoroacetate. *Wildlife Research,* 8**,** 52 - 55.

SAUSEN, P. J. & ELFARRA, A. A. 1990. Cysteine conjugate S-oxidase. Characterization of a novel enzymatic activity in rat hepatic and renal microsomes. *The Journal of Biological Chemistry,* 265**,** 6139-45.

SAUSEN, P. J. & ELFARRA, A. A. 1991. Reactivity of Cysteine S-Conjugate Sulfoxides - Formation of S-[1-Chloro-2-(S-Glutathionyl)Vinyl]-L-Cysteine Sulfoxide by the Reaction of S-(1,2-Dichlorovinyl)-L-Cysteine Sulfoxide with Glutathione. *Chemical Research in Toxicology,* 4**,** 655-660.

SCHAUMANN, E. 1988. The Chemistry of Thioketens. *Tetrahedron,* 44**,** 1827-1871.

SCHMIDT, J., KRAMELL, R. & SCHNEIDER, G. 1995. Liquid chromatography electrospray tandem mass spectrometry of amino acid conjugates of jasmonic acid under positive and negative ionisation. *European Mass Spectrometry,* 1**,** 573-581.

SCHMIDT, T., BERTERMANN, R., RUSCH, G. M., HOFFMAN, G. M. & DEKANT, W. 2012. Biotransformation of 2,3,3,3-tetrafluoropropene (HFO-1234yf) in male, pregnant and non-pregnant female rabbits after single high dose inhalation exposure. *Toxicology and Applied Pharmacology*.

SCHUSTER, P. 2009. *Biotransformation of trans-1,1,1,3-tetrafluoropropene, 2,3,3,3-tetrafluoropropene and 1,2,3,3,3-pentafluoropropene.* Unpublished thesis, Department of Pharmacology and Toxicology of the Julius-Maximilians-University of Wuerzburg.

SCHUSTER, P., BERTERMANN, R., SNOW, T. A., HAN, X., RUSCH, G. M., JEPSON, G. W. & DEKANT, W. 2008. Biotransformation of 2,3,3,3-tetrafluoropropene (HFO-1234yf). *Toxicology and Applied Pharmacology,* 233**,** 323-32.

SCHUSTER, P., RUSCH, G. M. & DEKANT, W. 2009. Biotransformation of trans-1,1,1,3-tetrafluoropropene (HFO-1234ze). *Toxicology and Applied Pharmacology,* 239**,** 215-23.

SCHUSTER, P., RUSCH, G. M. & DEKANT, W. 2010. Biotransformation of 2,3,3,3-tetrafluoropropene (HFO-1234yf) in rabbits. *Toxicology and Applied Pharmacology,* 244**,** 247-53.

SHERLEY, M. 2004. The traditional categories of fluoroacetate poisoning signs and symptoms belie substantial underlying similarities. *Toxicology Letters,* 151**,** 399-406.

SONG, B. J. & CEDERBAUM, A. I. 1996. Ethanol-inducible cytochrome P450 (CYP2E1): Biochemistry, molecular biology and clinical relevance: 1996 update. *Alcoholism-Clinical and Experimental Research,* 20**,** A138-A146.

STEVENS, J. L., ROBBINS, J. D. & BYRD, R. A. 1986. A purified cysteine conjugate beta-lyase from rat kidney cytosol. Requirement for an alpha-keto acid or an amino acid oxidase for activity and identity with soluble glutamine transaminase K. *The Journal of Biological Chemistry,* 261**,** 15529-37.

STIER, A., KUNZ, H. W., WALLI, A. K. & SCHIMASSEK, H. 1972. Effects on growth and metabolism of rat liver by halothane and its metabolite trifluoroacetate. *Biochemical Pharmacology,* 21**,** 2181-92.

STOLL, A. & SEEBECK, E. 1948. *Allium-Substanzen .1. Uber Alliin, Die Genuine Muttersubstanz Des Knoblauchols. *Helvetica Chimica Acta,* 31**,** 189-210.

THOMPSON, M., ELLISON, S. L. R. & WOOD, R. 2002. Harmonized guidelines for single-laboratory validation of methods of analysis - (IUPAC technical report). *Pure and Applied Chemistry,* 74**,** 835-855.

THUM, T. & BORLAK, J. 2000. Gene expression in distinct regions of the heart. *Lancet,* 355**,** 979-983.

TNO 2005a. Chromosome Aberration Test with HFO-1234yf in Cultured Human Lymphocytes (conducted for Honeywell International). TNO Quality of Life, Toxicology and Applied Pharmacology, Zeist, Utrechtseweg 48, P.O. Box 36011, 3700 AJ, Zeist, The Netherland.

TNO 2005b. Micronucleus Test in Bone Marrow Cells of Mice Treated with HFO-1234yf Administered by Inhalation (conducted for Honeywell International). TNO Quality of Life, Toxicology and Applied Pharmacology, Zeist, Utrechtseweg 48, P.O. Box 36011, 3700 AJ, Zeist, The Netherland.

TNO 2006a. Acute Inhalation Toxicity Study with HFO-1234yf in rats (conducted for Honeywell International). TNO Quality of Life, Toxicology and Applied Pharmacology, Zeist, Utrechtseweg 48, P.O. Box 36011, 3700 AJ, Zeist, The Netherland.

TNO 2006b. Subacute (2-week) Inhalation toxicity Study with HFO-1234yf in rats (conducted for Honeywell International). TNO Quality of Life, Toxicology and Applied Pharmacology, Zeist, Utrechtseweg 48, P.O. Box 36011, 3700 AJ, Zeist, The Netherland.

TNO 2006c. Subacute (4-week) Inhalation toxicity Study including Unscheduled DNA Synthesis and Micronucleus test) with 2-week recovery period, with HFO-1234yf in rats (conducted for Honeywell International). TNO Quality of Life, Toxicology and Applied Pharmacology, Zeist, Utrechtseweg 48, P.O. Box 36011, 3700 AJ, Zeist, The Netherland.

TNO 2007. Bacterial Reverse Mutation Test with HFO-1234yf (conducted for Honeywell International). TNO Quality of Life, Toxicology and Applied Pharmacology, Zeist, Utrechtseweg 48, P.O. Box 36011, 3700 AJ, Zeist, The Netherland.

TOMISAWA, H., HAYASHI, M., FUKUSHIMA, M., IIDA, S., UDA, F., HATTORI, K. & TATEISHI, M. 1993. A Novel Pathway for Formation of Thiol Metabolites and Cysteine Conjugates from Cysteine Conjugate Sulfoxides. *Biochemical Pharmacology,* 46**,** 1113-1117.

TROCHIMOWICZ, H. J. 1993. Industrial-Research on Alternative Fluorocarbons. *Toxicology Letters,* 68**,** 25-30.

TYLENDA, C. A., JONES, D., INGERMAN, L., SAGE, G. & CHAPPELL, L. 2003. TOXICOLOGICAL PROFILE FOR FLUORIDES, HYDROGEN FLUORIDE, AND FLUORINE. U.S. DEPARTMENT OF HEALTH AND HUMAN SERVICES, Public Health Service, Agency for Toxic Substances and Disease Registry.

UNEP 2009. vital ozone graphics 2.0 climate link.

URBAN, G., SPEERSCHNEIDER, P. & DEKANT, W. 1994. Metabolism of the Chlorofluorocarbon Substitute 1,1-Dichloro-2,2,2-Trifluoroethane by Rat and Human Liver-Microsomes - the Role of Cytochrome-P450 2e1. *Chemical Research in Toxicology,* 7**,** 170-176.

VAMVAKAS, S., DEKANT, W., BERTHOLD, K., SCHMIDT, S., WILD, D. & HENSCHLER, D. 1987. Enzymatic transformation of mercapturic acids derived from halogenated alkenes to reactive and mutagenic intermediates. *Biochemical Pharmacology,* 36**,** 2741-8.

VAMVAKAS, S., ELFARRA, A. A., DEKANT, W., HENSCHLER, D. & ANDERS, M. W. 1988. Mutagenicity of Amino-Acid and Glutathione S-Conjugates in the Ames Test. *Mutation Research,* 206**,** 83-90.

VAMVAKAS, S., KREMLING, E. & DEKANT, W. 1989. Metabolic-Activation of the Nephrotoxic Haloalkene 1,1,2-Trichloro-3,3,3-Trifluoro-1-Propene by Glutathione Conjugation. *Biochemical Pharmacology,* 38**,** 2297-2304.

VOLKEL, W., FRIEDEWALD, M., LEDERER, E., PAHLER, A., PARKER, J. & DEKANT, W. 1998. Biotransformation of perchloroethene: Dose-dependent excretion of trichloroacetic acid, dichloroacetic acid, and N-acetyl-S-(trichlorovinyl)-L-cysteine in rats and humans after inhalation. *Toxicology and Applied Pharmacology,* 153**,** 20-27.

WAALKENS-BERENDSEN, D. H. 2011. Inhalatory two-generation reproduction toxicity study with HFO-1234yf in Wistar rats, study code V7931, conducted for Honeywell International. TNO, Utrechtseweg 48, P.O Box 360, 3700 AJ Zeist, The Netherlands.

WAGNER, S., SCHOLZ, K., DONEGAN, M., BURTON, L., WINGATE, J. & VOLKEL, W. 2006. Metabonomics and biomarker discovery: LC-MS metabolic profiling and constant neutral loss scanning combined with multivariate data analysis for mercapturic acid analysis. *Anal Chem,* 78**,** 1296-305.

WALLINGTON, T. J., SCHNEIDER, W. F., WORSNOP, D. R., NIELSEN, O. J., SEHESTED, J., DEBRUYN, W. J. & SHORTER, J. A. 1994. The Environmental-Impact of Cfc Replacements - Hfcs and Hcfcs. *Environmental Science & Technology,* 28**,** A320-A326.

WELLMITZ, J. & GLUSCHKE, M. 2005. Leitlinie zur Methodenvalidierung Umweltbundesamt, Berlin.

WERNER, M., BIRNER, G. & DEKANT, W. 1995. The Role of Cytochrome P4503a1/2 in the Sex-Specific Sulfoxidation of the Hexachlorobutadiene Metabolite, N-Acetyl-S-(Pentachlorobutadienyl)-L-Cysteine in Rats. *Drug Metabolism and Disposition,* 23**,** 861-868.

WERNER, M., BIRNER, G. & DEKANT, W. 1996. Sulfoxidation of mercapturic acids derived from tri- and tetrachloroethene by cytochromes P450 3A: a bioactivation reaction in addition to deacetylation and cysteine conjugate beta-lyase mediated cleavage. *Chemical Research in Toxicology,* 9**,** 41-9.

WHITE, I. N. H. & DE MATTEIS, F. 2001. The role of CYP forms in the metabolism and metabolic activation of HCFCs and other halocarbons. *Toxicology Letters,* 124**,** 121-128.

WIL 2006. Acute Cardiac Sensitization Study of HFO-1234yf in Dogs, conducted for Honeywell International. WIL Research Laboratories, LLC, 1407 George Road, Ashland, OH 44805-8946.

WIL 2008. An inhalation range-finding prenatal developmental toxicity study of HFO-1234yf (2,3,3,3-tetrafluoropropene) in rabbits, study No. WIL-447021, conducted for Honeywell International. WIL Research Laboratories, LLC, 1407 George Road, Ashland, OH 44805-8946.

WIL 2011. An inhalation prenatal developmental toxicity study of HFO-1234yf (2,3,3,3-tetrafluoropropene) in rabbits, revised final report, study No. WIL-447022, conducted for Honeywell International. WIL Research Laboratories, LLC, 1407 George Road, Ashland, OH 44805-8946.

XIA, Y.-Q., MILLER, J. D., BAKHTIAR, R., FRANKLIN, R. B. & LIU, D. Q. 2003. Use of a quadrupole linear ion trap mass spectrometer in metabolite identification and bioanalysis. *Rapide Communications in Mass Spectrometry,* 17**,** 1137-1145.

YLLNER, S. 1961. Urinary Metabolites of 14c-Tetrachloroethylene in Mice. *Nature,* 191**,** 820.